International Journal of Analytical Chemistry

Characterization of Food Structures and Functionalities

Lead Guest Editor: Xingxun Liu
Guest Editors: Ying Yang, Changmou Xu, and Jiajia Rao

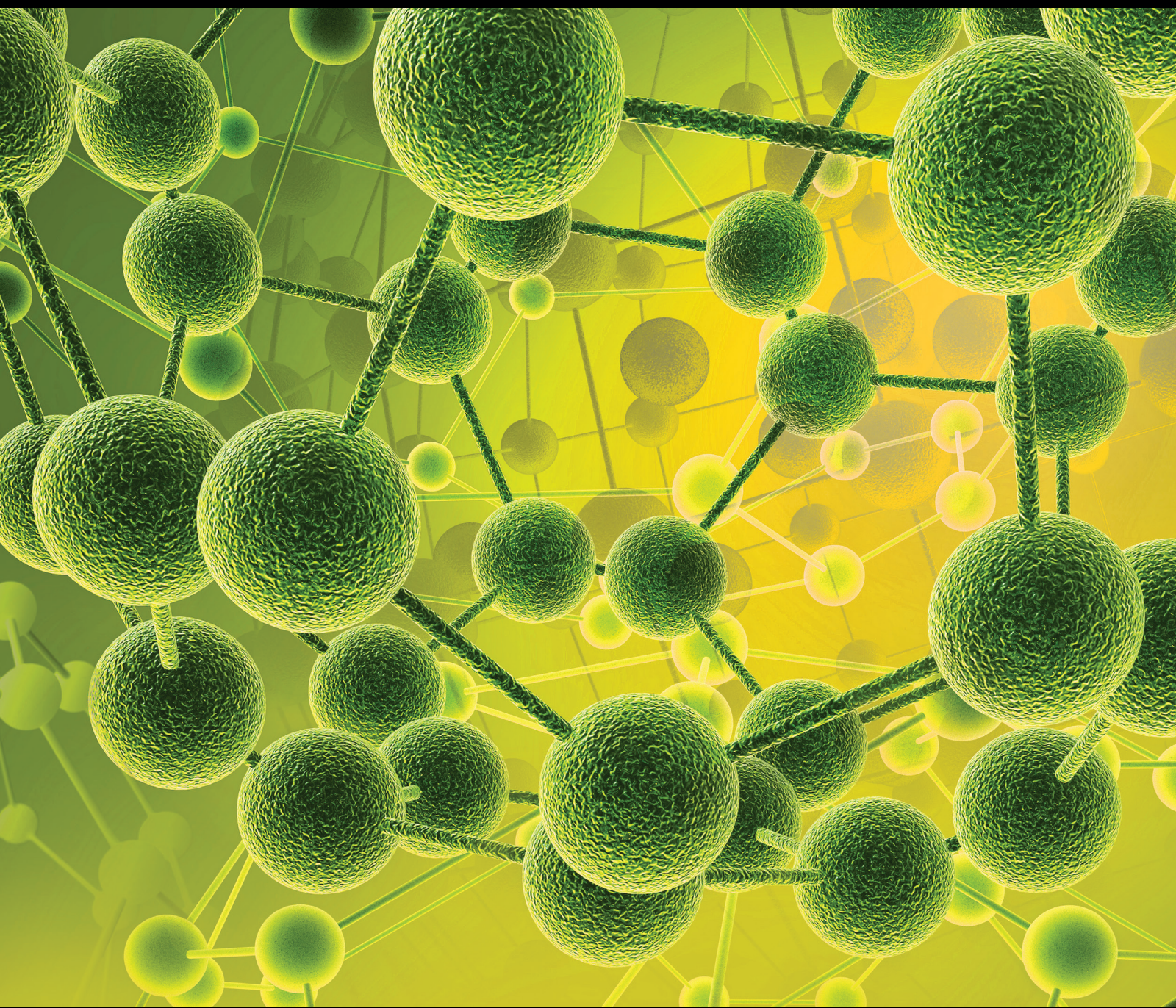

Characterization of Food Structures and Functionalities

International Journal of Analytical Chemistry

Characterization of Food Structures and Functionalities

Lead Guest Editor: Xingxun Liu
Guest Editors: Ying Yang, Changmou Xu, and Jiajia Rao

Editorial Board

Contents

Hindawi
International Journal of Analytical Chemistry
Volume 2018, Article ID 4818253, 2 pages
https://doi.org/10.1155/2018/4818253

Editorial

Characterization of Food Structures and Functionalities

Xingxun Liu,[1] **Ying Yang**,[1] **Changmou Xu**,[2] **and Jiajia Rao**[3]

[1]*Institute of Food Science and Technology (IFST), Chinese Academy of Agricultural Science (CAAS), Beijing, China*
[2]*Food Science and Technology Department, University of Nebraska–Lincoln, Lincoln, NE, USA*
[3]*Department of Plant Sciences, North Dakota State University, Fargo, ND, USA*

Correspondence should be addressed to Xingxun Liu; ytboy652@163.com

Received 14 March 2018; Accepted 14 March 2018; Published 19 April 2018

Some functional properties such as texture and nutrition are the most important attributes used by consumers to assess food qualities, which have been used for in nearly all kinds of food products, from beverage, yoghurt, and ice cream to bread and noodles. Nowadays, there is a desire to make foods healthier and at the same time not diminish sensory quality. This requires an understanding of key elements of food structure associated with texture and nutritional perception. In terms of taste perception, texture is perceived during oral processing of food.

Knowledge of structure-oral processing-texture interrelations could be utilized to develop or prevent specified textural attributes. Overall, the investigation of structure-oral processing-texture interrelations is just starting as a research focus preferentially. However, factors are as including nonuniversal and inconsistent sensory terminology, omission of consideration for structural changes incurred by oral processes, the imbalances between texture and nutrition occurring during food design, the confusions of the key elements of food structure to determine food texture or nutrition, and the lack of cross-disciplinary investigations hamper progress in this field. Consideration of these factors in future investigations on sensory texture and nutrition functionalities, as well as the development of the relevant analytical methods for studying the structural changes or evaluating texture and nutrition functionality changes, will increase the applicability of their findings and bring us closer to understanding the contribution of food structure to sensory texture while helping us to make a balance between food textures and food functionalities during food design.

Nowadays varieties of analysis methods based on spectral analysis and chromatographic analysis have been developed to identify and analyze food composition and food structure more quickly. Technologies such as dynamic light scattering, X-ray, neutron scattering, and various microscopy (optical and electron) techniques were applied to study the food structure from different scale level, while some other analysis technologies have been developed to mimic the oral chewing procedure and the digestion procedure for food textures and food functionalities study. All these developments will help us get a better overall understanding of the relationship between food structures and functionalities.

In recent years, varieties of analysis methods were used to characterize food structures and functionalities and have experienced a rapid development with the purpose of improving food systems. This special issue aims to provide an opportunity for researchers in the area of characterization of food structures and functionalities to share their state-of-the-art researches. These original researches uncovered the development of food characterization and specifically include the following: (i) advanced technologies of analyzing the structures of food; (ii) advanced technologies of analyzing the textures of food; (iii) advanced technologies of analyzing the nutrition and functionalities of food; (iv) investigation of the interrelations between food compositions/food structures and food textures/nutrition; (v) analytical model from food structures to food textures/nutrition.

We hope readers will benefit for the researches included in this special issue.

Acknowledgments

We would like to express our appreciation to all the authors for their informative contributions and the reviewers for their

support and constructive critiques in making this special issue possible.

Xingxun Liu
Ying Yang
Changmou Xu
Jiajia Rao

Hindawi
International Journal of Analytical Chemistry
Volume 2018, Article ID 1784073, 5 pages
https://doi.org/10.1155/2018/1784073

Research Article

Analyses of Essential Elements and Heavy Metals by Using ICP-MS in Maternal Breast Milk from Şanlıurfa, Turkey

Serap Kılıç Altun,[1] **Hikmet Dinç**,[2] **Füsun Karaçal Temamoğulları**,[2] **and Nilgün Paksoy**[3]

[1]*Department of Food Hygiene and Technology, Faculty of Veterinary Medicine, Harran University, 63200 Şanlıurfa, Turkey*
[2]*Department of Pharmacology and Toxicology, Faculty of Veterinary Medicine, Harran University, 63200 Şanlıurfa, Turkey*
[3]*Department of Biochemistry, Faculty of Veterinary Medicine, Harran University, 63200 Şanlıurfa, Turkey*

Correspondence should be addressed to Nilgün Paksoy; nilgun_uren@hotmail.com

Received 7 November 2017; Revised 21 February 2018; Accepted 1 March 2018; Published 4 April 2018

Academic Editor: Xingxun Liu

Maternal breast milk is a unique biological matrix that contains essential micronutrients. Potentially heavy metals may also affect infants' health and growth through maternal breast milk. The purpose of this study was to determine and compare the essential elements and heavy metals of maternal breast milk of nursery mothers residing in Şanlıurfa province, Turkey. Maternal breast milk concentrations of sodium, magnesium, phosphorus, potassium, calcium, iron, copper, zinc, arsenic, and lead were analyzed in a random sample of the first time in urban and suburban nursery Turkish mothers (n: 42). Eight essential elements and two heavy metals were analyzed using ICP-MS after microwave digestion. For bivariate analyses of variables, we use nonparametric Spearman's correlation coefficient test. The mean concentrations of essential elements and heavy metals were as follows: sodium 330 ± 417 mg/L, magnesium 32.6 ± 15.5 mg/L, phosphorus 156 ± 46.2 mg/L, potassium 488 ± 146 mg/L, calcium 193 ± 53.2 mg/L, iron 1.65 ± 1.43 mg/L, copper 0.54 ± 0.46 mg/L, zinc 2.89 ± 3.23 mg/L, arsenic < 1 μg/L, and lead < 1 μg/L. Concentrations of heavy metals in maternal breast milk may have the important implication that it is not affected by environmental pollution in this province. This study provides reliable information about maternal breast milk concentrations of nursery mothers residing in Şanlıurfa, Turkey, and also compares the relations between essential elements and socioeconomic conditions, residing areas, and using copper equipment for food preparation of which some have not previously been reported.

1. Introduction

Maternal breast milk (MBM) is a unique biological matrix of nutrition for infants. Breastfeeding is vital for optimal health, growth, and development with its macro- and micronutrients, including essential elements [1]. World Health Organization (WHO) declared that MBM provides ideal nutrition for the first six months of early life [2].

Essential elements in MBM are crucial for ideal growth and development of infants. There are a lot of benefits associated with MBM, such as decreasing the morbidity, mortality, and incidences of diseases [3]. The composition of MBM can be affected by various factors such as maternal diet, social-economic conditions, timing of delivery, period of lactation, and sampling time of day [4]. Essential element deficiencies are correlated with increased rates of infections and chronic diseases. Also, high amount of essential elements may also be harmful to human life [1]. Elements levels depend on host susceptibility which contains physiological conditions, genetic characteristics, age, and gender. Also, lactation is a period of life with increased risks for heavy metals [5] such as arsenic and lead. The concentrations of heavy metals may vary widely depending on exposures. The most common source of lead is the exhaust gases of vehicles [6, 7]. Researchers have shown that lead can pass by maternal way to fetus and by milk to infants. Arsenic is a heavy metal naturally found in the earth and taken up to metabolism by contaminated water and plants. Prolonged exposure to arsenic in the infants can lead to arsenic poisoning and cancer risk [6, 8].

Concentration data on some essential elements and heavy metals in MBM of nursery mothers from different countries analyzed with different techniques such as flame

Table 1: Data of nursery mother and the infants' status.

Parameter	Total number (n)	Percentage (%)	Min	Max	Mean ± SD
Age of infant (day)	42	100.0	3	520	162 ± 139
Age of mother (year)	42	100.0	17	44	28.3 ± 7.08
Income rate < minimum wage	21	50.0			
Income rate ≥ minimum wage	21	50.0			
Residing in urban area	25	59.5			
Residing in suburban area	17	40.4			
Using copper equipment	13	31.0			
Not using copper equipment	29	69.0			

photometry [9], ion chromatography [10], proton-induced X-ray emission, and instrumental neutron activation [11] have been reported. ICP-MS has been used to determine the level of essential elements and heavy metals in various matrices including biological samples and foods [12]. There is, however, no recent study of essential elements and heavy metals in MBM, particularly not from Turkish mothers.

The aim of this study is to provide and access the information of concentrations of essential elements in MBM from nursery mothers who are residing in Şanlıurfa province of Turkey using a sensitive method and also compare the relations between essential elements and socioeconomic conditions, residing areas, and using copper equipment for food preparation.

2. Materials and Methods

2.1. Breast Milk Sampling. Samples were collected from 42 nursery mothers with an average age of 28.3 ± 7.08 years delivered at full term (38–40 weeks) of gestation. All samples were obtained from nursery mothers' 3–520 lactation days postpartum during the hours of 08:00–11:30 a.m. MBM samples were manually expressed from the breast using a manual pump to sterile falcon tube after 3 mL was discarded and stored at −20°C until analyses. Based on self-reporting on the socioeconomic levels, residing areas, and using copper equipment for food preparation, participants were divided into groups (Table 1).

2.2. Chemical and Standard Solutions. Mixed calibration standards of sodium, magnesium, phosphorus, potassium, calcium, iron, copper, zinc, arsenic, and lead were prepared from dilutions of stock solutions (Agilent Japan (Lot Number: 10-160YPY2)). TraceSELECT grade of nitric acid (65.0% concentrated, Merck, Germany) and hydrogen peroxide (30.0% concentrated, Merck, Germany) were used for sample digestion.

Ultrapure water was provided in the laboratory (18.2 MΩ/cm at 25°C) by MES MP Mini pure, (Turkey) device. Every plastic and glassware were cleaned in acid bath (5% nitric acid (laboratory grade, Merck, Germany)) for 24 h and rinsed with ultrapure water and dried before use. The gas 99.9990% Argon was supplied by Linde Gases (Linde Group, Turkey). Whole solutions were prepared with ultrapure water.

2.3. Equipment and Accessories. Elements were analyzed on Agilent 7500 ce with an octopole reaction system inductively coupled plasma-mass spectrometer (Agilent Technologies, Japan) with an autosampler (Cetac ASX-520) and a nebulizer (Agilent Technologies, Japan).

2.4. Sample Preparation. MBM samples were analyzed by ICP-MS after microwave-assisted acid digestion. 1.0 mL of each sample and blank samples was digested with 4.0 mL of 65% (v/v) HNO_3, and 2.0 mL of 30% (v/v) H_2O_2 in PTFE vessels. Microwave acid digestion procedure was as follows: firstly up to 120°C for 15 min, for the second step constant for 10 min; up to 160°C in 20 min; and finally constant for 15 min; at the end a cooling stage (30 min) was done in room temperature and the samples and blanks were diluted to 50 mL with ultrapure water.

2.5. Isotopes. The isotopes $^{23}Na^+$, $^{24}Mg^+$, $^{26}Mg^+$, $^{31}P^+$, $^{39}K^+$, $^{44}Ca^+$, $^{56}Fe^+$, $^{63}Cu^+$, $^{66}Zn^+$, $^{75}As^+$, and $^{208}Pb^+$ were detected. All samples were analyzed in triplicate. These isotopes were preferred to maximize the sensitivity and minimize interferences.

2.6. Quality Control. Limit of quantification (LOQ) and limit of detection (LOD) were calculated for ten times and the recovery of 12 elements (Na, Mg, P, K, Ca, Fe, Cu, Zn, As, and Pb) in raw milk samples was between 92.4 and 124.1% as shown in Table 2. The standard deviation of the blank was relative to the slope of the analytical curve. LOQ and LOD were calculated separately. The digested MBM was used in the calculation of LOQ and LOD.

2.7. Recovery Experiments. With a view to impose the integrity of the analyses, the same concentrations of each element as in the original sample were added to a sample and performed in the same microwave digestion procedure as the samples.

2.8. Statistical Analyses. Statistical analyses were carried out using SPSS 11.00 (SPSS Inc., Chicago, IL, USA). For bivariate analyses of variables, nonparametric Spearman's correlation coefficient was used.

2.9. Ethical Committee. Ethics committee approval was obtained from Medical Faculty of Harran University

Table 2: Quantification and detection limits.

Element	LOQ	LOD	Concentration range of standard solution
Na (mg/L)	315	10.0	1–2000
Mg (mg/L)	48.6	4.60	1–100
P (mg/L)	562	35.0	10–1000
K (mg/L)	1413	100	10–1000
Ca (mg/L)	678	22.0	10–1000
Fe (mg/L)	2.53	0.40	0.1–1000
Cu (mg/L)	0.06	0.01	0.01–100
Zn (mg/L)	1.81	0.20	0.1–100
As (μg/L)	0.04	0.01	0.1–100
Pb (μg/L)	0.04	0.01	0.1–100

Table 3: Concentration of essential elements and heavy metals of MBM samples.

	Min	Max	Mean ± SD
Essential elements			
Na (mg/L)	44.7	1703	330 ± 417
Mg (mg/L)	12.7	85.9	32.6 ± 15.5
P (mg/L)	84.0	300	156 ± 46.3
K (mg/L)	161	903	488 ± 147
Ca (mg/L)	90.0	276	193 ± 53.2
Fe (mg/L)	0.45	5.11	1.65 ± 1.43
Cu (mg/L)	0.08	2.02	0.54 ± 0.46
Zn (mg/L)	0.45	15.8	2.89 ± 3.23
Heavy metals			
As (μg/L)	<1	<1	<1
Pb (μg/L)	<1	<1	<1

(74059997.050.01.04/65). Informed consents were obtained and signed by the participating nursery mothers to protect the participants' privacy, personal and clinical data, and MBM samples used only for this study purpose.

3. Results and Discussion

The nursery mothers included in this study were on the average age of 17–44 (28.3 ± 7.08) years at the time of lactation period average of 3–520 (163 ± 139) day. Table 3 shows the element levels in MBM samples. Na, Mg, P, K, Ca, Fe, Cu, and Zn were present in all MBM samples (positive rate 100.0%). As and Pb were not present in all MBM samples (negative rate 100.0%). K is the major essential element (488 ± 147 mg/L), followed by Na (330 ± 417 mg/L) > Ca (193 ± 53.2 mg/L) > P (156 ± 46.3 mg/L) > Mg (32.6 ± 15.5 mg/L) > Zn (2.89 ± 3.23 mg/L) > Fe (1.65 ± 1.43 mg/L) > Cu (0.54 ± 0.46 mg/L). The levels of heavy metals arsenic and lead were found below the limit of detection, which is also expected in MBM.

Sodium levels in MBM samples ranged between 44.7 and 1703 mg/L and significantly correlated with copper (r: 0.719; $P < 0.001$), iron (r: 0.516; $P < 0.001$), and magnesium concentrations (r: 0.558; $P < 0.001$). Magnesium concentrations in MBM were in a range of 12.7–85.9 mg/L with a mean level of 32.6 ± 15.5 mg/L. Magnesium and zinc levels were significantly correlated (r: 0.474; $P < 0.01$).

MBM phosphorus concentrations were between the level of 84–300 mg/L, with a mean level of 156 ± 46.3 mg/L. Phosphorus concentrations were negatively correlated with iron concentrations (r: −0.414; $P < 0.01$), lactation period (r: −0.436; $P < 0.01$), and positively correlated with nursery mothers' age (r: 0.434, $P < 0.01$).

Potassium concentrations of MBM varied between 161 and 903 mg/L. The content of potassium was positively correlated with zinc (r: 0.715; $P < 0.01$), sodium (r: 0.519; $P < 0.01$), magnesium (r: 0.451; $P < 0.01$), and copper (r: 0.719; $P < 0.001$).

Calcium concentrations of MBM were in the range of 90–276 mg/L with a mean level of 193 ± 53.2 mg/L. Calcium was positively correlated with the residing area (r: −0.315, $P < 0.05$). Also, calcium levels were significantly correlated with magnesium (r: 0.420; $P < 0.01$) and potassium (r: 0.525; $P < 0.01$). Concentrations of calcium in MBM from suburban nursery mothers were significantly lower than concentrations of calcium in urban nursery mothers.

The mean concentration of iron in MBM was 1.65 ± 1.43 mg/L. Copper concentration of MBM was positively correlated with sodium (r: 0.719; $P < 0.001$), magnesium

(r: 0.673; $P < 0.001$), and lactation period (r: 0.832; $P < 0.001$) and with using copper equipment in food preparation (r: 0.333; $P < 0.05$).

The zinc concentrations were positively correlated with sodium (r: 0.586; $P < 0.001$) and potassium (r: 0.715; $P < 0.001$) concentrations of MBM samples.

In this study, the results showed the differences in essential elements and heavy metals concentrations in MBM of nursery mothers residing in Şanlıurfa, Turkey. Specifically, nursery mothers from the suburban area (Eyyübiye) of Şanlıurfa tended to have lower intake concentrations of calcium assessed as compared with nursery mothers residing in urban areas (Haliliye and Karaköprü). As a result, MBM from nursery mothers residing in suburban area (Eyyübiye) were of poorer nutritional quality that has obvious implication for infants nutrition. Arising from this result, family population was crowded and socioeconomic levels of these families were low. The results of this study were parallel with Qian et al.s' [10] study who determined and compared the composition of MBM in urban and suburban areas in Shanghai, China.

Calcium is the principal element of skeleton system that improves bone mineral density in infants. Our findings show that maternal calcium intake was lower in suburban nursery mothers than other participants of this study. Qian et al. [10] reported that maternal calcium intake was low in both urban and suburban groups of nursery mothers. The concentrations of in MBM ranged from 90 to 276 mg/L in this study. In Sweden, Björklund et al. [12] reported 274–305 mg/L calcium levels in 60 MBM samples. Supposing a daily intake of 750 mL breast milk, infants should obtain 67.5–207 mg of calcium per day. For age 0–6 months, the concentration of calcium is lower daily intake that recommended amount of 210 mg [13].

There is evidence that sodium levels in infancy may have a long-term effect on blood pressure. The observation was that mean concentrations of sodium were higher than the previous studies [9, 14]. Mean sodium concentration of our study was 330 ± 417 mg/L. Our sodium concentrations were similar to MBM samples of the urban area of Shanghai but higher than the MBM samples from the suburban area of Shanghai [10]. And also our mean level of sodium was higher than the mean level of sodium (135 mg/L) from Japanese mothers' [15] and the rural Gambian mothers' MBM with a mean level of sodium (163 mg/L) [9]. The high sodium concentrations of this study may be due to dietary habits of Turkish women with a consumption of salt 14 g/day [16].

MBM samples seem to contain enough concentration of magnesium as there has not been a report of magnesium deficiency in breastfed infants [11]. The levels of magnesium in MBM samples were in the range of 12.7–85.9 mg/L with a mean level of 32.6 ± 15.5 mg/L which was in accordance with Yamawaki et al.s' study [15] (mean 27 ± 9 mg/L). Magnesium concentrations in MBM samples were with values similar to Swedish mothers with an average level of magnesium 28 mg/L [12].

We also found that phosphorus concentrations were in a negative correlation with lactation period. The measured phosphorus concentrations in MBM samples ranged within 84–300 mg/L with an average level of 156 ± 46.3 mg/L which was similar to Japan nursery mothers P levels with an average level of 150 ± 38 mg/L [15], Shanghai nursery mothers with a range of 139–163 mg/L phosphorus levels [8], and Swedish mothers with a range of 126–233 mg/L [12].

Potassium is an intracellular cation [11]. Average concentrations of potassium varied between 161 and 903 mg/L with a mean level of 488 ± 147 mg/L. Comparing our data with those of other studies in which MBM samples were gathered during lactation in, for example, Shanghai [10], Japan [15], and Sweden [12] shows similarity in concentrations of potassium.

There have been few reports about iron content in MBM [5, 15, 17]. Iron is an essential element for ideal growth under the case of oxidative stress [5]. Our mean data of iron was 1.65 ± 1.43 mg/L with levels that confirm the results reported in the literature [5, 18]. The concentration of iron was found to be higher than the Uppsala mothers with median level of 0.31 mg/L [9], and American mothers living in South Texas with a mean level of 0.4 mg/L [4], and lower than in Croatian nursery mothers with a mean level of 3.3 mg/L [5].

The mission of essential elements in biological functions makes them especially significant for nutrition of infant. It is noted that an infant is well protected so long as certain age by maternal homeostatic processes in the event of iron, copper, and zinc [19]. Infants are born with an adequate supply of iron and copper in the liver, owing to low concentrations of these elements situated in MBM [20].

Zinc and copper are essential elements which support development and represent significant levels in MBM [21]. We found that zinc levels were in the range of 0.45–15.8 mg/L with a mean level of 2.89 ± 3.23 mg/L. Assuming a daily intake of 750 mL, infants should obtain 2.16 mg of zinc per day. This concentration is suitable daily intake for age of 0–6 months that is recommended [22]. Zinc concentrations in MBM are regulated by the mammary glands [23]. Reported average concentration of zinc in MBM was between 1.24 and 20 mg/L [5, 10, 12, 17, 19].

It is presumed that the transition of copper from blood to milk regulated transfer by the mammary gland epithelium [19]. Consequently, there was not any correlation between the concentrations of copper in mother's blood and milk which was expected [19, 24]. The levels of copper in MBM in Croatia were 3.4 ± 0.7 mg/L. Our results of copper concentrations with a mean 0.54 ± 0.46 mg/L are lower than the reported study [5]. Mohd-Taufek et al. [18] reported a mean concentration of copper 0.22 ± 0.03 mg/L and also Yamawaki et al. reported [15] similar copper concentrations with a mean level of 0.35 ± 0.21 mg/L. The results of the present study (range 0.08–2.01 mg/L) were very similar to those found by Almeida et al. [19].

By detecting the concentrations of heavy metals (arsenic and lead) of MBM, we estimated that no influences from the maternal intake or environmental exposure to these elements by reason of the concentrations were below the detection limit. This result may be because the Şanlıurfa province is away from the industry. Compared with concentrations reported in the literature [5, 19] the arsenic and lead levels detected in this study were so much lower than most of the reported values.

We should be noted that MBM samples were obtained in one-time collection. Next research needed the composition of

MBM varying on a time to time basis. Serial analyses of MBM samples in repeated times should address the concentrations of essential elements and heavy metals of Turkish mothers.

4. Conclusion

In brief, our results agree on the whole with previous reports about the essential element composition of maternal breast milk but it was clearly understood that there is a large standard variation in the composition of essential elements such as Ca, Fe, and Zn. We confirmed that the composition of human milk is affected by various factors such as residing area and using copper equipment.

In conclusion, we found a significant correlation in MBM concentrations between nursery mothers from urban and suburban areas of Şanlıurfa. More researches at multiple-time compositional studies are warranted to detect the concentrations for identifying appropriate interventions to ensure healthy growth and development of breastfed infants.

Conflicts of Interest

The authors declare that there are no conflicts of interest regarding the publication of this paper.

References

[1] L. D. Klein, A. A. Breakey, B. Scelza, C. Valeggia, G. Jasienska, and K. Hinde, "Concentrations of trace elements in human milk: Comparisons among women in Argentina, Namibia, Poland, and the United States," *PLoS ONE*, vol. 12, no. 8, Article ID e0183367, 2017.

[2] World Health Organization, "Global Strategy for Infant and Young Child Feeding, 2003," http://whqlibdoc.who.int/publications/2003/9241562218.pdf.

[3] M. Besculides, K. Grigoryan, and F. Laraque, "Increasing breastfeeding rates in New York City, 1980-2000," *Journal of Urban Health*, vol. 82, no. 2, pp. 198–206, 2005.

[4] L. A. Nommsen, C. A. Lovelady, M. J. Heinig, B. Lönnerdal, and K. G. Dewey, "Determinants of energy, protein, lipid, and lactose concentrations in human milk during the first 12 mo of lactation: the darling study," *American Journal of Clinical Nutrition*, vol. 53, no. 2, pp. 457–465, 1991.

[5] J. G. Letinić, M. M. Sarić, M. Piasek et al., "Use of human milk in the assessment of toxic metal exposure and essential element status in breastfeeding women and their infants in coastal Croatia," *Journal of Trace Elements in Medicine and Biology*, vol. 38, pp. 117–125, 2016.

[6] H. Aysal and N. Atasoy, "Determination of Heavy Metal Ions (As, Pb, Cd) and Zinc Mineral (Zn) in Human's and Cow's Milk in Bitlis (Turkey)," *Revista De Chimie*, vol. 68, no. 5, pp. 962–966, 2017.

[7] R. L. Boeckx, "Lead poisoning in children," *Analytical Chemistry*, vol. 58, no. 2, pp. 274–287, 1986.

[8] H. J. Hapke, Hacettepe University, "Salt Consumption in Turkey, 2016," http://www.halksagligiens.hacettepe.edu.tr/dunyasaglikgunu/11.pdf.

[9] A. A. Richards, M. K. Darboe, K. Tilling, G. D. Smith, A. M. Prentice, and D. A. Lawlor, "Breast milk sodium content in rural Gambian women: Between- and within-women variation in the first 6 months after delivery," *Paediatric and Perinatal Epidemiology*, vol. 24, no. 3, pp. 255–261, 2010.

[10] J. Qian, T. Chen, W. Lu, S. Wu, and J. Zhu, "Breast milk macro- and micronutrient composition in lactating mothers from suburban and urban Shanghai," *Journal of Paediatrics and Child Health*, vol. 46, no. 3, pp. 115–120, 2010.

[11] O. A. Akanle, F. A. Balogun, J. A. Owa, and N. M. Spyrou, "Study of the nutritional status of maternal breast milk in preterm infants in Nigeria," *Journal of Radioanalytical and Nuclear Chemistry*, vol. 244, no. 1, pp. 231–235, 2000.

[12] K. L. Björklund, M. Vahter, B. Palm, M. Grandér, S. Lignell, and M. Berglund, "Metals and trace element concentrations in breast milk of first time healthy mothers: A biological monitoring study," *Environmental Health: A Global Access Science Source*, vol. 11, no. 1, article no. 92, 2012.

[13] A. Bhargava, "Modeling the effects of maternal nutritional status and socioeconomic variables on the anthropometric and psychological indicators of Kenyan infants from age 0-6 months," *Econometrics, Statistics, and Computational Approaches in Food and Health Sciences*, pp. 191–206, 2006.

[14] R. P. Wack, E. L. Lien, D. Taft, and J. D. Roscelli, "Electrolyte composition of human breast milk beyond the early postpartum period," *Nutrition Journal* , vol. 13, no. 9, pp. 774–777, 1997.

[15] N. Yamawaki, M. Yamada, T. Kan-no, T. Kojima, T. Kaneko, and A. Yonekubo, "Macronutrient, mineral and trace element composition of breast milk from Japanese women," *Journal of Trace Elements in Medicine and Biology*, vol. 19, no. 2-3, pp. 171–181, 2005.

[16] http://www.halksagligiens.hacettepe.edu.tr/dunyasaglikgunu/11.pdf, 2016.

[17] M. A. Hannan, B. Faraji, J. Tanguma, N. Longoria, and R. C. Rodriguez, "Maternal milk concentration of zinc, iron, selenium, and iodine and its relationship to dietary intakes," *Biological Trace Element Research*, vol. 127, no. 1, pp. 6–15, 2009.

[18] N. Mohd-Taufek, D. Cartwright, M. Davies et al., "The Simultaneous Analysis of Eight Essential Trace Elements in Human Milk by ICP-MS," *Food Analytical Methods*, vol. 9, no. 7, pp. 2068–2075, 2016.

[19] A. A. Almeida, C. M. P. V. Lopes, A. M. S. Silva, and E. Barrado, "Trace elements in human milk: Correlation with blood levels, inter-element correlations and changes in concentration during the first month of lactation," *Journal of Trace Elements in Medicine and Biology*, vol. 22, no. 3, pp. 196–205, 2008.

[20] J. G. Dorea, "Iron and copper in human milk," *Nutrition Journal*, vol. 16, no. 3, pp. 209–220, 2000.

[21] M. K. Georgieff, "Nutrition and the developing brain: nutrient priorities and measurement," *The American Journal of Clinical Nutrition*, vol. 85, no. 2, pp. 614S–620S, 2007.

[22] H. Robberecht, H. Benemariya, and H. Deelstra, "Daily dietary intake of copper, zinc, and selenium of exclusively breast-fed infants of middle-class women in Burundi, Africa," *Biological Trace Element Research*, vol. 49, no. 2-3, pp. 151–159, 1995.

[23] B. Lönnerdal, "Regulation of mineral and trace elements in human milk: Exogenous and endogenous factors," *Nutrition Reviews*, vol. 58, no. 8, pp. 223–229, 2000.

[24] M. Domellöf, B. Lönnerdal, K. G. Dewey, R. J. Cohen, and O. Hernell, "Iron, zinc, and copper concentrations in breast milk are independent of maternal mineral status," *American Journal of Clinical Nutrition*, vol. 79, no. 1, pp. 111–115, 2004.

Hindawi
International Journal of Analytical Chemistry
Volume 2018, Article ID 5081938, 12 pages
https://doi.org/10.1155/2018/5081938

Research Article

Rheological Behavior of Tomato Fiber Suspensions Produced by High Shear and High Pressure Homogenization and Their Application in Tomato Products

Yong Wang,[1,2] **Ping Sun**,[3] **He Li**,[1] **Benu P. Adhikari**,[4] **and Dong Li**[5]

[1]*Beijing Advanced Innovation Center for Food Nutrition and Human Health, Beijing Technology & Business University, 11 Fuchenglu, Beijing 100048, China*
[2]*Beijing Key Laboratory of Nutrition & Health and Food Safety, COFCO Nutrition & Health Research Institute, No. 4 Road, Future Science & Technology Park, Beijing 102209, China*
[3]*Processing Technology Research Center for Tomato, COFCO Tunhe, Changji, Xinjiang 831100, China*
[4]*School of Applied Sciences, RMIT University, City Campus, Melbourne, VIC 3001, Australia*
[5]*College of Engineering, China Agricultural University, P.O. Box 50, 17 Qinghua Donglu, Beijing 100083, China*

Correspondence should be addressed to He Li; lihe@btbu.edu.cn

Received 29 September 2017; Revised 29 December 2017; Accepted 22 January 2018; Published 18 March 2018

Academic Editor: Jiajia Rao

This study investigated the effects of high shear and high pressure homogenization on the rheological properties (steady shear viscosity, storage and loss modulus, and deformation) and homogeneity in tomato fiber suspensions. The tomato fiber suspensions at different concentrations (0.1%–1%, w/w) were subjected to high shear and high pressure homogenization and the morphology (distribution of fiber particles), rheological properties, and color parameters of the homogenized suspensions were measured. The homogenized suspensions were significantly more uniform compared to unhomogenized suspension. The homogenized suspensions were found to better resist the deformation caused by external stress (creep behavior). The apparent viscosity and storage and loss modulus of homogenized tomato fiber suspension are comparable with those of commercial tomato ketchup even at the fiber concentration as low as 0.5% (w/w), implying the possibility of using tomato fiber as thickener. The model tomato sauce produced using tomato fiber showed desirable consistency and color. These results indicate that the application of tomato fiber in tomato-based food products would be desirable and beneficial.

1. Introduction

Tomato (*Lycopersicon esculentum* Mill.) is one of the most popular fruits over the world because of its unique visual appeal, taste, and nutritional value as it contains ascorbic acid (vitamin C) and lycopene [1]. Processed tomato products such as purees and sauces are a primary source of tomatoes in contemporary diet. Considerable research has been undertaken in the past to quantify and elucidate the natural consistency and structure of tomato products [2].

From a structural point of view, most tomato products are aqueous dispersion containing aggregated or disintegrated cells and cell wall material dispersed in water soluble tomato components. The consistency of processed tomato products arises from the cell wall components such as cellulose, semicellulose, pectin, and interactions among these components [2]. Cellulose is major component of vegetable cell wall suspensions and it is also the main component that affects the rheology of processed tomato products. Pectins are embedded naturally within the cellulose backbone and they are also found in the serum phase. They are known to contribute to the structure of tomato products significantly depending on the processing conditions [3–6].

Homogenization is a key processing step in the production of ketchup, sauces, and other tomato products. The homogenization process decreases the mean particle size of

the tomato suspensions and imparts smoother texture and higher viscosity. It also alters the nature of the suspensions network and increases the viscosity of the suspensions [7, 8]. During homogenization, tomato pulp is subjected to very high turbulence, shear, cavitation, and impact when it is forced through the homogenizer [9]. The homogenization process was found to alter particle size distribution, pulp sedimentation behavior, serum cloudiness, color, and microstructure of tomato juice, by disrupting the suspended pulp particles [10]. High pressure homogenization was reported to decrease the particle size due to the disruption of matrix and increase tomato product's Bostwick consistency, probably due to the formation of fiber network [11]. The large discrete cells and cell fragments of tomato suspensions were easily degraded by homogenization which resulted into higher water-holding capacity [6, 7, 11]. The high pressure homogenization reduced the mean particle size and narrowed the particle size distribution thereby increasing the total surface area and the interaction among the particles [12]. Bengtsson et al. reported that the nonhomogenized tomato suspensions had swollen cell structure with relatively few cell aggregates; however, the homogenized suspensions contained large number of degraded cell fragments [13].

Tomato peel is a by-product of tomato industry and fiber is extracted from tomato peel using chemical method [14]. Tomato peel fiber contains about 80% of total dietary fiber (mainly water insoluble fiber) much higher than other vegetable by-products [15]. Due to its unique chemical composition and functional properties, tomato peel fiber can be used as a food supplement to improve physical, chemical, and nutritional properties of food products. However, the color and flavor of tomato peel fiber must be considered carefully to avoid their negative impact on the sensorial characteristics of the final products [16]. To date the tomato fiber has received very little research attention despite its ability to contribute to desirable food texture and good mouth feel.

To the best of our knowledge, there is no study on the effect of high shear and high pressure homogenization on the tomato fiber. Thus, this study aimed to study the effects of high shear and high pressure homogenization on the morphological and rheological properties of tomato fiber suspensions. We also compared the morphological, rheological, and color parameters of homogenized tomato fiber suspensions with those of commercial tomato ketchup and a model tomato sauce formulated for comparison. We believe that the findings presented in this paper will provide better understanding of the functional properties of tomato fiber and help broaden its application as an important thickening ingredient in food industry.

2. Materials and Methods

2.1. Materials. The tomato fiber sample was kindly provided by COFCO Tunhe Co. Ltd., Beijing, China. The solid content of this fiber sample was determined and found to be 4.80% (w/w). This fiber sample contained 2.11% (w/w) insoluble dietary fiber as tested following the AOAC Official Method 991.43 [17] and 1.12% (w/w) protein as tested using China's national food safety standards [18]. The tomato fiber was produced by concentrating and separating the solid part out of the tomato paste (without tomato peels or seeds), by using high speech rotary mechanical instrument.

The food grade tomato paste (29.0° Brix cold break), tomato ketchup, sugar, soybean fiber, and salt used in this study were provided by COFCO Tunhe Co. Ltd., Beijing, China. Deionized water was used to prepare samples.

2.2. Mechanical Treatments. The tomato fiber suspensions were prepared in four concentrations (0.1%, 0.25%, 0.5%, and 1%, w/w) by mixing raw tomato fiber with adequate amount of deionized water as calculated based on the moisture content of tomato fiber.

The shearing treatments were carried out using a laboratory disperser (IKA Ultra-Turrax T25, Germany). The tomato fiber suspensions were subjected to 3400 rpm, 5000 rpm, 8000 rpm, 10000 rpm, 12000 rpm, and 14000 rpm for 12 minutes each.

The above-mentioned sheared samples were homogenized using a high pressure homogenizer (ATS AH100D, Shanghai, China), which is a lab-scale homogenizer equipped with valve. The maximum pressure of this homogenizer is 140 MPa. The homogenization was carried out for 2 passes at 0 MPa, 5 passes at 5 MPa, and then another 5 passes at 10 MPa.

2.3. Determination of Morphology. Twenty milliliter of untreated, sheared, and homogenized suspensions were separately placed in colorimetric tubes. Images were captured with a digital camera in order to compare the appearance of these suspensions. The microscope images of all the above-mentioned samples were acquired. Very small drop of each sample was placed on a microscope slide and the pictures were taken using a microscope (Olympus CX31, Japan) at 100x and 400x magnification.

2.4. Rheological Measurements. Rheological measurements were performed using AR2000ex rheometer (TA Instruments Ltd., Crawley, UK). This is a controlled stress, direct strain, and controlled rate rheometer coming with torque range from 0.0001 to 200 mN·m and high stability normal force from 0.01 to 50 N. The parallel plate was used for all the tests. The temperature was controlled by a water bath connected to the Peltier system in the bottom plate. A thin layer of silicone oil was applied on the edges of samples in order to prevent evaporation. The linear viscoelastic region was determined for each sample through strain sweeps at 1 Hz (data not shown). Viscoelastic properties [storage (G'), loss (G'') modulus, and loss tangent (δ)] of samples were determined within the linear viscoelastic region. The samples were allowed to equilibrate for 2 min before each measurement.

The steady shear tests were performed at 25°C over the shear rate range of 0.01–100 s^{-1} to measure the apparent viscosity. A steel cone geometry (60 mm diameter, 59 μm gap) was chosen for these measurements, since cone geometry is more preferable for viscosity measurement.

The frequency sweep tests were performed at 25°C over the angular frequency range of 0.1–10 rad/s. The strain amplitude of these frequency sweep measurements was selected to be 1% according to the strain sweep results (data not

Table 1: Composition of tomato sauce prepared by using tomato paste and tomato fiber or soybean fiber.

Sample	Tomato paste	2.5% homogenized tomato fiber	Soybean fiber
P101	75 g	0	0
P102	76 g	8.33 g	0
P103	77 g	18.75 g	0
P104	78 g	32.14 g	0
P105	79 g	0	0.74 g
P106	80 g	0	1.48 g
P107	81 g	0	2.96 g

Table 2: The composition of tomato sauce prepared by using tomato fiber or soybean fiber, tomato paste, sugar, and salt.

Sample	Tomato paste (%)	2.5% tomato fiber homogenized (%)	Soybean fiber (%)	Sugar (%)	Salt (%)	Water (%)	Total
P110	80	--	2.5	6.2	0.9	10.4	100
P111	80	13	--	6.1	0.9	--	100
P112	75	16	--	8.1	0.9	--	100
P113	70	19	--	10.1	0.9	--	100

shown) in order to confine these tests within linear viscoelastic region. An aluminum parallel plate geometry (40 mm diameter, 1 mm gap) was chosen for these measurements.

Creep experiments were carried out at a fixed shear stress of 7.958 mPa at 25°C. The variation in shear strain in response to the applied stress was measured over a period of 2 min. An aluminum parallel plate geometry (40 mm diameter, 1 mm gap) was chosen for these creep measurements.

2.5. Preparation of Tomato Sauce. The formulation of tomato sauce samples used in the first round of tests is provided in Table 1. The tomato paste and homogenized tomato fiber or soybean fiber were mixed according to this formulation. Required amount of water was added to make the mass of the sample to be 110 g. The homogenized tomato fiber with 2.5% concentration was prepared as described in Section 2.2.

The formulation of tomato sauce for second round of tests is shown in Table 2. Two hundred grams of sauce was prepared for each formulation by measuring and mixing ingredients listed in Table 2. The mixture was then heated at 95°C for 10 min in a water bath with continuous stirring. The sauce container was covered during heating to minimize the evaporation of water. The sauce was finally cooled down to ambient temperature.

2.6. Analysis of Physicochemical Properties. Bostwick consistency was determined using a standard 24 cm Bostwick Consistometer with 48 × 0.5 cm graduations (Endecotts ZXCON-CON1, London, UK). Seventy-five mL of sample was used to perform these tests. As the fluid flows down the instrument, the measurements were carried out after 30 seconds.

Colorimetric tests were performed using a spectrophotometer (Hunter Lab UltraScan VIS, Reston, US) in transmission mode. The samples were filled into a 10 mL quartz transmission cell with 10 mm path length. The L, a, and b values were calculated by the averaging the data of triplicate runs. The suspensions were shaken to achieve uniformity in color immediately before measurement.

The pH and total acidity of samples were measured using an automatic acid analyzer (Metrohm 877 Titrino plus, Switzerland).

In order to measure the Bostwick consistency, color, pH, and total acidity of the tomato source samples, the total soluble solids content was adjusted to 12.5° Brix in order to keep the same test condition. A refractometer (Atogo RX-5000α, Japan) was used for this purpose.

2.7. Statistical Analysis. All of the above-mentioned tests were carried out in triplicate. The rheological data was obtained directly from the AR2000ex rheometer software (TA Instruments Ltd., Crawley, UK). The averaged value of triplicate runs was reported as the measured value along with the standard deviation.

3. Results and Discussion

3.1. Effect of Homogenization on Suspension Morphology. The effect of mechanical treatment on the appearance of tomato fiber suspensions at solid concentrations of 0.1–1.0% (w/w) is shown in Figure 1. The solid content was easily precipitated towards the bottom of the tube in all of the untreated samples irrespective of fiber concentration and the amount of sediment increased with increase in fiber concentration. The uniformity of suspensions greatly increased after shear homogenization or high pressure homogenization. The uniformity was relatively poor in shear homogenized samples at 0.1% and 0.25% (w/w) concentration compared with that of high pressure homogenized samples. The uniformity of suspensions produced by shear homogenization and high pressure homogenization was similar at 0.5% and 1.0% (w/w). It has been previously reported that the more stable

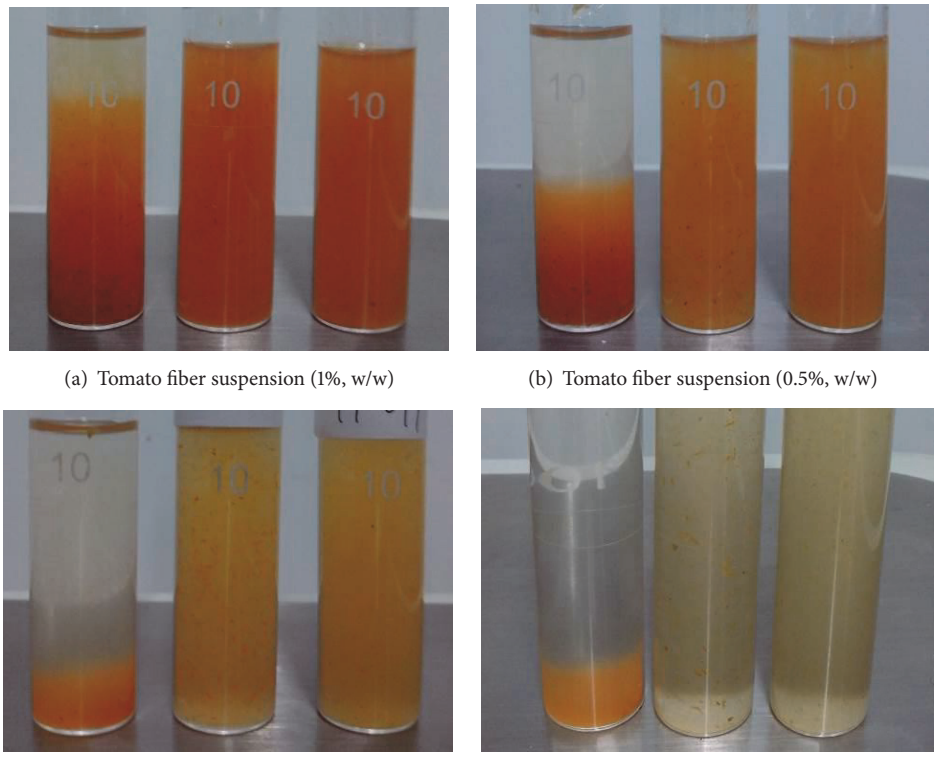

(a) Tomato fiber suspension (1%, w/w)

(b) Tomato fiber suspension (0.5%, w/w)

(c) Tomato fiber suspension (0.25%, w/w)

(d) Tomato fiber suspension (0.1%, w/w)

Figure 1: Photographs of tomato fiber suspensions at different concentration. In each photograph from left to right, untreated sample, high shear homogenized sample, and high pressure homogenized sample.

network structure can be formed in tomato fiber suspension when homogenized at 9 MPa [7]. It can be observed from photographs presented in Figure 1 that the shear homogenization affects only a part of the tomato fiber, most likely from tomato flesh. The fibers from tomato pericarp could only be fragmented under high pressure homogenization. The structural features of tomato fiber particles are drastically altered by the high pressure homogenization. It has been reported that the homogenized tomato fiber suspensions consisted of smashed cellular material which eventually formed fibrous-like network while the nonhomogenized suspensions consisted of a mixture of whole cells and dispersed cell wall materials [6].

The distribution of solids in tomato fiber suspensions is illustrated in Figure 2. Dark red discrete particles are observed in untreated and high shear homogenized samples at all concentrations, while the high pressure homogenized sample showed much better uniformity in solid distribution. The high pressure homogenized suspensions containing 0.5% or 1% (w/w) fiber began to exhibit water-holding properties, indicated by the increased height of tomato fiber sample on the glass (picture not shown). It was reported earlier that the homogenized tomato fiber suspensions showed higher water-holding capacity albeit at much higher solid concentrations (10% to 21.7%) [13]. This increased water-holding capacity would be a beneficial whenever the tomato fiber is used as an ingredient to impart desired texture in food products. The information presented in Figures 1 and 2 agree with the findings in an earlier study [19] that the unhomogenized tomato juice showed whole cells with intact membranes and characteristic lycopene crystals while the homogenized samples showed large number of small particles composed of cell walls and internal constituents suspended in the juice serum.

The values of colorimetric parameters (L, a, and b) of unhomogenized tomato fiber suspensions at different concentration are presented in Table 3. The L and b values decreased with increase in fiber concentration while the a value showed substantial increase. The a/b value, which is of vital importance in the tomato processing industry, significantly ($p < 0.05$) increased with the increase in concentration. The a/b value of 2% (w/w) tomato fiber suspension suggested that this formulation has desirable color for potential application in tomato sauces. It has also been reported in an earlier study that the values for L^*, a^*, and b^* increased with the increase in homogenization pressure indicating that the tomato fiber suspensions became more saturated in red and yellow color [10].

The effects of high shear and high pressure homogenization on the 1% (w/w) tomato fiber suspension are shown in Figure 3. None of the L, a, or b parameters was significantly ($p > 0.05$) affected by the high shear homogenization or high pressure homogenization.

In order to illustrate the morphological changes caused by homogenization, the microscopic photographs of 1% (w/w) tomato fiber suspension are shown in Figure 4 before and

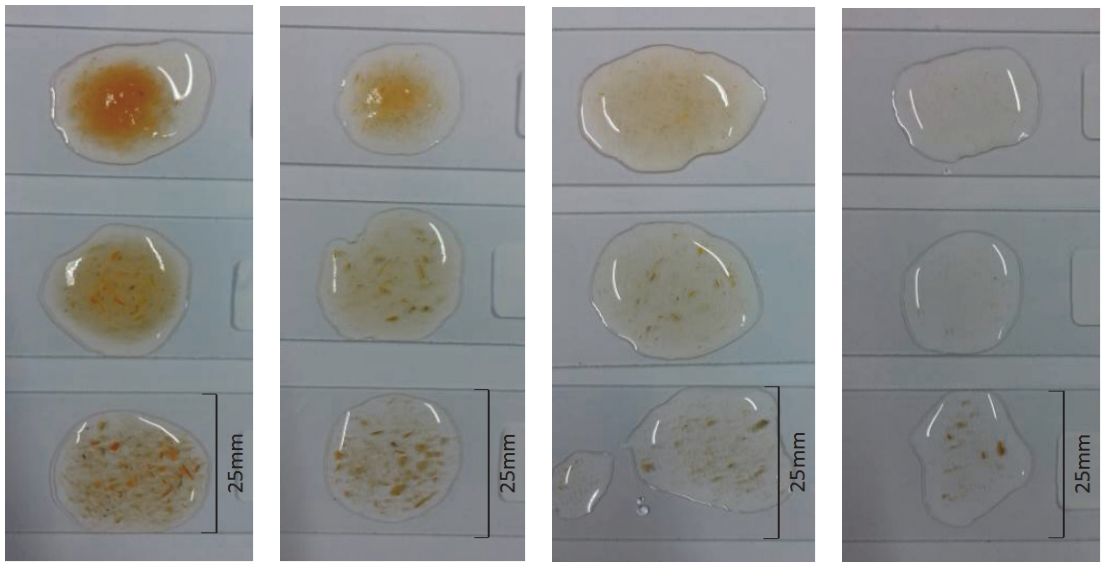

(a) 1%, w/w (b) 0.5%, w/w (c) 0.25%, w/w (d) 0.1%, w/w

Figure 2: Microscopic photographs of tomato fiber suspensions showing distribution of fiber solids at different concentration. In each photograph from bottom to top, untreated sample, shear homogenized sample, and high pressure homogenized sample.

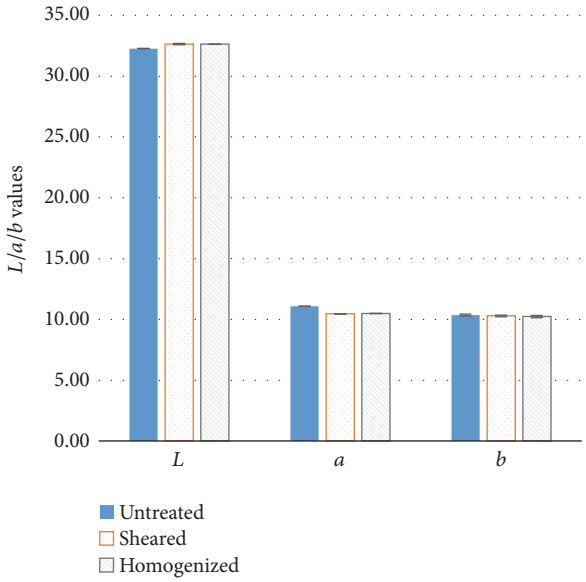

Figure 3: Effect of high shear and high pressure homogenization on the colorimetric parameters (L, a, and b) of 1% (w/w) tomato fiber suspension.

after homogenization. After high pressure homogenization, the solid tended to be evenly distributed at microscopic level (Figure 4(a)). The tomato fiber suspension showed a fibrous morphology with high degree of uniformity resembling a solution with negligibly very small amount of suspended solid after high pressure homogenization (shown in Figure 4(b)). The control samples showed unperturbed cells with intact membrane and the characteristic lycopene crystals. The homogenized samples showed a large number of small cell wall particles and internal cell constituents suspended in the juice serum which agreed with Kubo et al. observation [10]. It has been reported that no intact cells were observed in tomato pulp subjected to high pressure (479 bar) homogenization and the internal cell constituents were found to be uniformly distributed in the homogenized pulp [9].

3.2. Effect of Homogenization on Rheological Properties. As shown in preceding section, the texture of tomato fiber suspensions could be significantly modified by homogenization. The effect of high shear and high pressure homogenization on the apparent viscosity is shown in Figure 5. All the tomato fiber suspensions showed shear-thinning behavior regardless of the concentration before and after homogenization. The apparent viscosity of all the samples increased with the increase in fiber concentration. The high shear homogenization significantly ($p < 0.05$) increased the apparent viscosity compared to the untreated sample. The application of high pressure homogenization increased the apparent viscosity the most (Figures 5(a)–5(d)). Augusto et al. reported that the viscosity of tomato juice (4.5° Brix) increased when the homogenization pressure increased from 50 MPa to 150 MPa [12]. Similar effect of high pressure homogenization which was on tomato suspensions was reported in various studies [6, 7, 20]. The cell wall of tomato cells could be broken even at moderate shear and this rupture is linked with the increase in viscosity.

The power law model (see (1)) was used to predict the variation of apparent viscosity with shear rate of tomato fiber suspensions.

$$\mu_a = K\dot{\gamma}^{n-1}, \quad (1)$$

where μ_a is the apparent viscosity (Pa·s), $\dot{\gamma}$ is the shear rate (s^{-1}), K is consistency coefficient (Pa·s^n), and n is the flow behavior index (dimensionless). The values of K and n for all the test samples were determined by fitting (1)

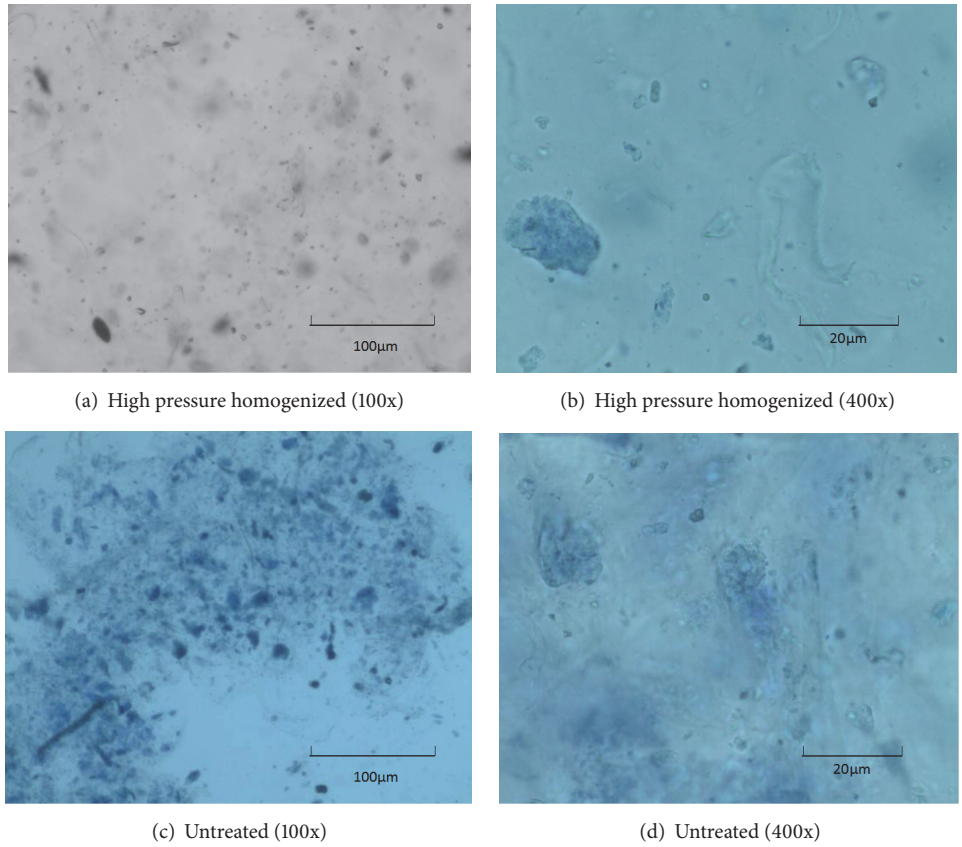

(a) High pressure homogenized (100x)

(b) High pressure homogenized (400x)

(c) Untreated (100x)

(d) Untreated (400x)

Figure 4: Microscopic photographs of 1% (w/w) tomato fiber suspension before and after mechanical treatment.

Table 3: Colorimetric parameters of unhomogenized tomato fiber suspensions at different concentration.

Conc.	L	a	b	a/b
0.25%	50.95 ± 1.79	4.63 ± 0.5	13.94 ± 0.27	0.33 ± 0.03
0.50%	40.35 ± 1.18	8.91 ± 0.25	14.80 ± 0.41	0.60 ± 0.033
1%	32.27 ± 0.02	11.08 ± 0.05	10.36 ± 0.01	1.07 ± 0.004
2%	32.23 ± 0.06	12.01 ± 0.02	10.39 ± 0.04	1.16 ± 0.004

to experimental apparent viscosity versus shear rate data presented in Figure 5 and are presented in Table 4. The flow behavior index (n) depends on the distribution of small and large particles and the rheology of the suspending fluid, while the consistency coefficient (K) depends on the maximum packing fraction (φ_m) and the distribution of small and large particles [21]. The K value increased very strongly with the increase of fiber concentration in all samples. The n value, which is indicator for shear-thinning behavior, was the lowest in pressure homogenized samples, the highest in the untreated samples, and intermediate in high shear homogenized samples at a given concentration. This means that the high pressure homogenized samples are most susceptible to shear thinning.

The values of storage modulus (G') of the homogenized and unhomogenized tomato fiber suspensions are shown in Figure 6. Both the homogenized and unhomogenized samples showed a slight increase of G' with the increase in angular frequency. At lower fiber concentrations (0.1%–1%), the G' value of the high shear homogenized suspension increased more strongly compared to the unhomogenized sample. The increase of the G' value was the strongest in high pressure homogenized suspension which is similar to the variation of apparent viscosity with shear rate. This observation agrees with the earlier report that the homogenization process increases both storage and loss modulus of tomato suspension [7, 19].

The loss modulus (G'') of tomato fiber suspensions are presented in Figure 7. The G'' values increased with the increase in tomato fiber concentration. Both high shear and high pressure homogenization processes significantly ($p < 0.05$) increased the G'' values. The high pressure homogenization appears to be more effective in increasing G'' values as a function of angular frequency. All suspensions exhibited solid-like behavior with G' being higher than G''. Augusto et al. studied the effect of high pressure homogenization (up to 150 MPa) on the viscoelastic properties of tomato juice and found both G' and G'' when the juice was homogenized [22].

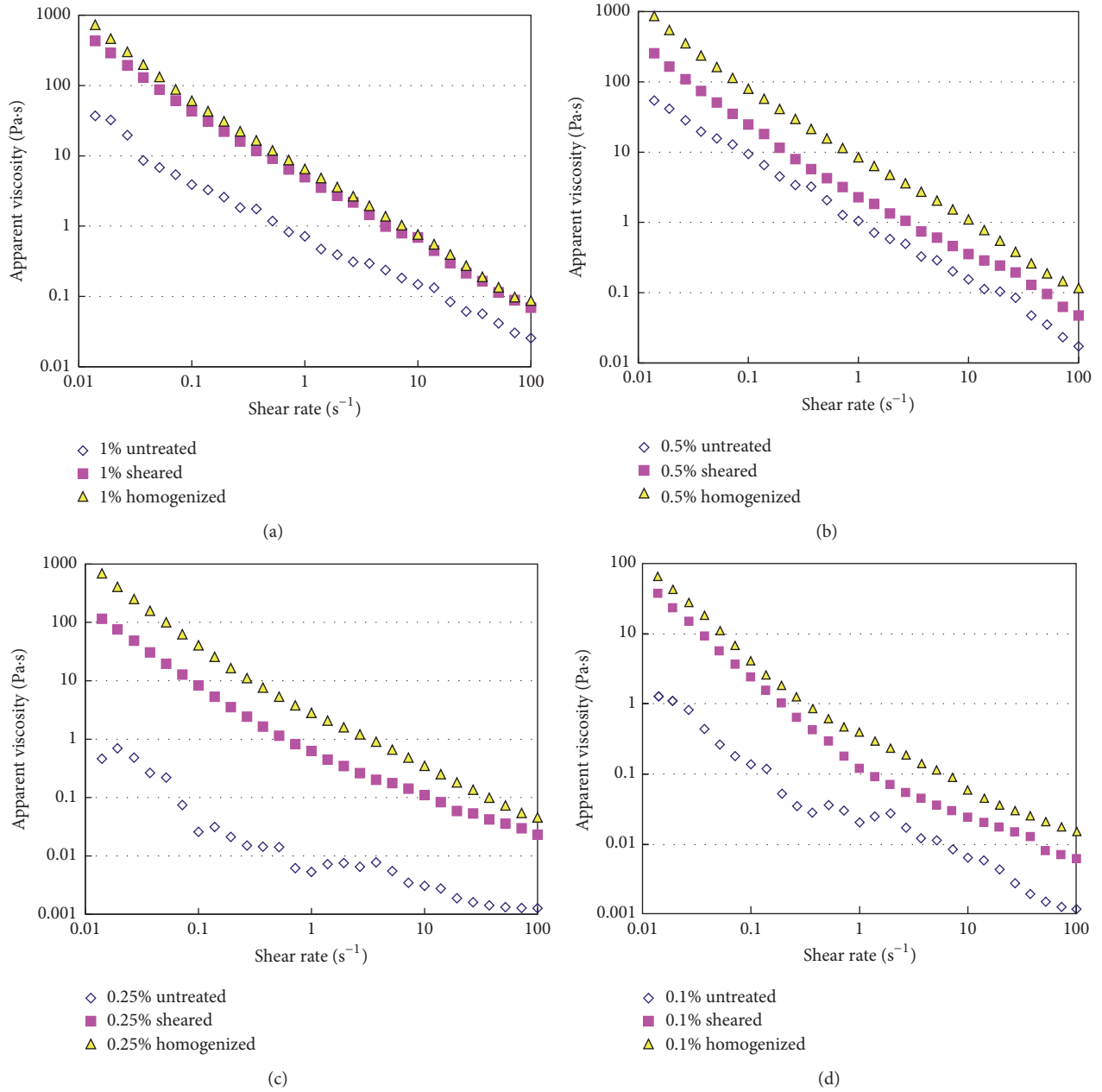

Figure 5: Flow behavior of tomato fiber suspensions before and after high shear or high pressure homogenization. Tomato fiber concentration: (a) 1%; (b) 0.5%; (c) 0.25%; (d) 0.1%; all in (w/w) basis.

The increase in homogenization pressure was also found to increase both G' (75.4 Pa to 212.2 Pa) and G'' (from 49.8 Pa to 80.9 Pa) in tomato suspensions [13].

The effect of homogenization on the creep behavior of tomato fiber suspensions is presented in Figure 8. At 1% (w/w) concentration, homogenized suspensions deformed less that the control sample under the same applied stress. The high pressure homogenized sample had the largest resistance to the applied stress among all the samples. This further indicates that homogenization helps build a stronger texture in the tomato fiber suspension, which could utilized to formulate food products with desirable texture. Figure 8 also shows that the slope of the creep curve is much smaller compared to that of the control sample. This indicates that high shear and high pressure homogenized suspensions achieve an equilibrium state to maintain their solid-like structure sooner compared to the unhomogenized suspension. At the same stress, the unhomogenized suspension would continue to deform. This observation is consistent with earlier publication which reported that the homogenized tomato juice reduced the compliance of tomato juice due to stronger internal structure [19].

Based on all the rheological data presented above, it could be concluded that the rheological properties of tomato fiber could be significantly altered by the application of high shear or high pressure homogenization. The homogenized

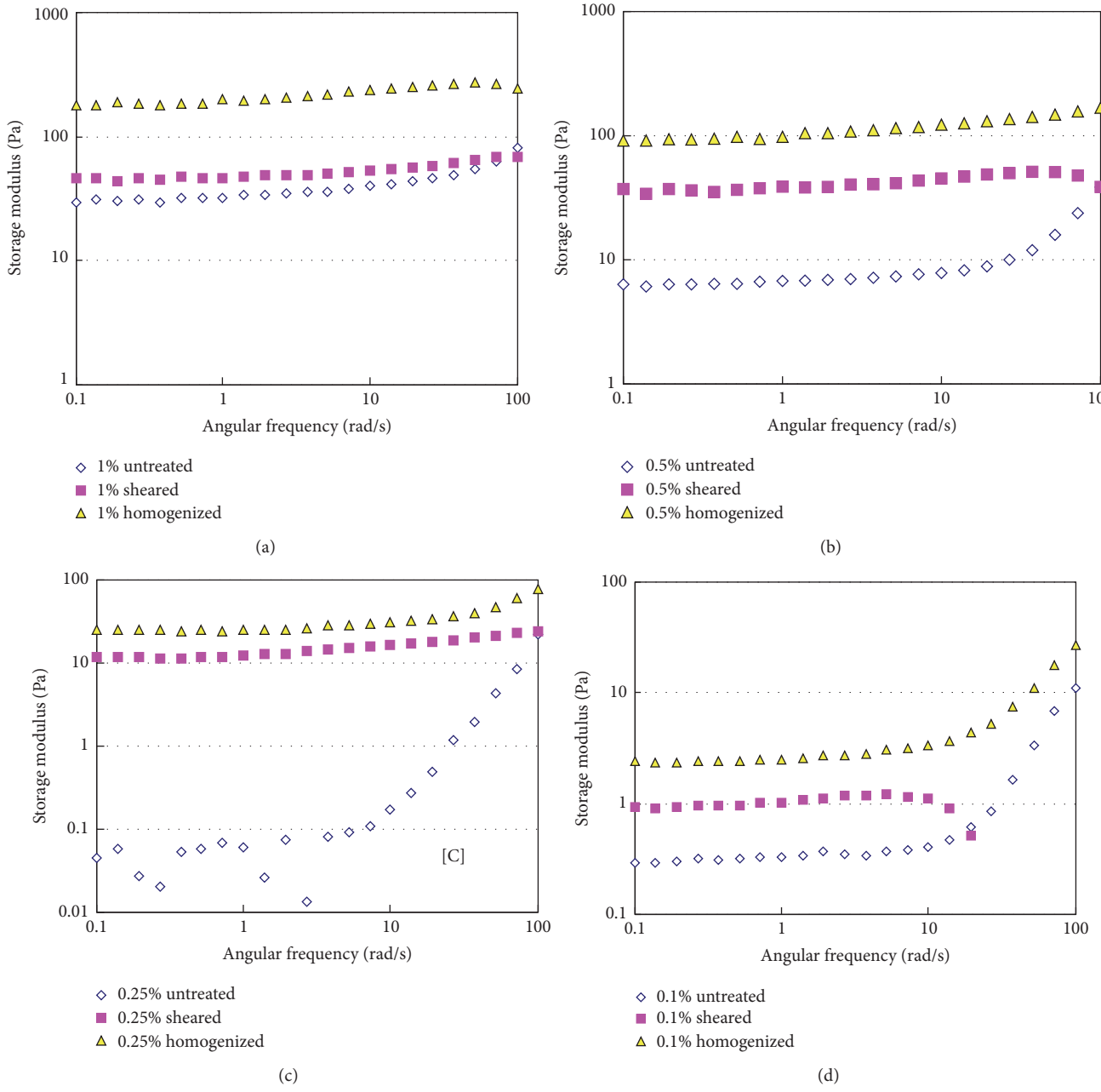

Figure 6: Storage modulus (G') of tomato fiber suspensions before and after homogenization. Tomato fiber concentration: (a) 1%; (b) 0.5%; (c) 0.25%; (d) 0.1% (w/w).

suspensions had higher apparent viscosity, higher G', and G'' and they could withstand larger external force and could maintain the solid-like structure better.

3.3. Comparison with Tomato Ketchup. Viscosity is a key indicator of quality of tomato paste and ketchup based on which consumers make their purchasing decision [23]. The apparent viscosity of high pressure homogenized tomato fiber suspension at 2.5% (w/w) fiber concentration was compared with that of tomato ketchup of 30° Brix (Figure 9). Despite the large difference in solid concentration between the two samples, they show similar shear-thinning behavior and comparable apparent viscosity. Thus, the tomato fiber can replace other thickeners which might have been used in tomato ketchup, for example, pectin or xanthan gum.

The G' and G'' versus angular frequency curves of high pressure homogenized tomato fiber suspension (2.5%, w/w) and tomato ketchup (30° Brix) are presented in Figure 10. The curves of G'' versus angular frequency of these two samples were almost identical. The G' versus angular frequency curves of these samples bear similar trend. The storage modulus of the homogenized fiber suspension was higher than that of the tomato ketchup within the entire angular frequency range. This indicated that the fiber suspension had stronger

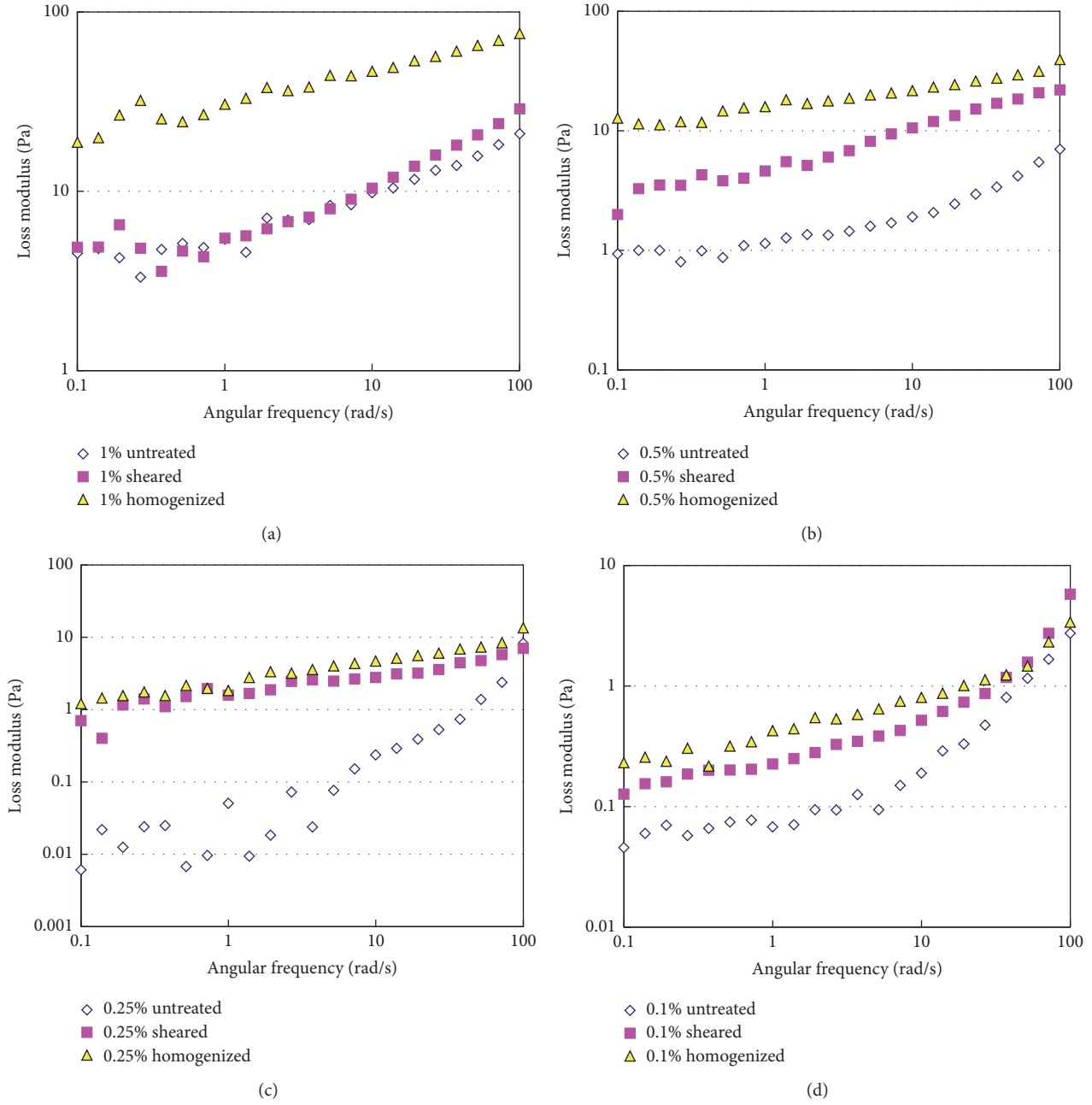

Figure 7: Loss modulus of tomato fiber suspension before and after homogenization. Tomato fiber concentration: (a) 1%; (b) 0.5%; (c) 0.25%; (d) 0.1% (w/w).

three-dimensional structure to resist external stress than the tomato ketchup. The viscoelastic characteristics of tomato sauce or ketchup are reported to depend on the diameter of the suspended particles water insoluble solids content [24]. The data presented in Figure 8 indicates that tomato fibers might be better choice if firmer or more solid-like texture is required.

The creep diagrams of high pressure homogenized tomato fiber suspension (2.5%, w/w) and tomato ketchup (30° Brix) are shown in Figure 11. The tomato fiber suspension deformed to a lesser extent than the tomato ketchup corroborating the fact that the tomato fibers provide firmer texture than the ketchup, although the texture is also affected by concentration. According to a sensory evaluation data reported in earlier study the tomato suspension homogenized at 90 bar had significantly better thicker and smoother texture and significantly weaker graininess compared with the untreated sample [13].

3.4. Application of Tomato Fiber in the Formulation of Tomato Sauce. Dietary fibers such as soybean fiber are frequently added to produce tomato sauce. Thus, the effect of addition of homogenized tomato fiber or soybean fiber was measured and is presented in Figure 12. Bostwick consistency is

Table 4: Power law tomato fiber suspension before and after mechanical treatment.

	Sample	K (Pa·s^n)	n	R^2
Untreated	1%	0.73 ± 0.017	0.27 ± 0.0024	0.97
	0.5%	1.13 ± 0.031	0.12 ± 0.0013	0.82
	0.25%	0.01 ± 0.001	0.55 ± 0.0045	0.87
	0.1%	0.02 ± 0.001	0.36 ± 0.0028	0.85
High shear homogenized	1%	4.91 ± 0.038	0.07 ± 0.0006	0.85
	0.5%	2.65 ± 0.016	0.14 ± 0.0018	0.85
	0.25%	0.76 ± 0.008	0.18 ± 0.0014	0.75
	0.1%	0.18 ± 0.002	0.17 ± 0.0019	0.75
High pressure homogenized	1%	6.54 ± 0.045	0.04 ± 0.0004	0.75
	0.5%	8.82 ± 0.076	0.06 ± 0.0009	0.78
	0.25%	3.21 ± 0.032	0.04 ± 0.0006	0.74
	0.1%	0.43 ± 0.003	0.20 ± 0.0022	0.87

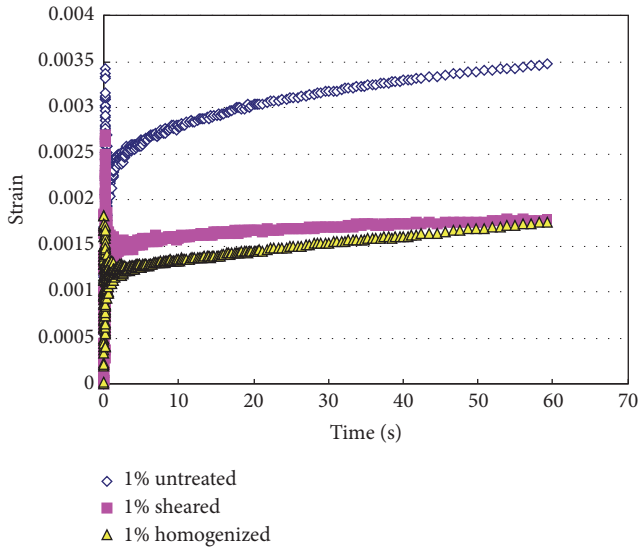

Figure 8: Creep diagrams of tomato fiber suspensions before and after homogenization. Tomato fiber concentration: 1% (w/w).

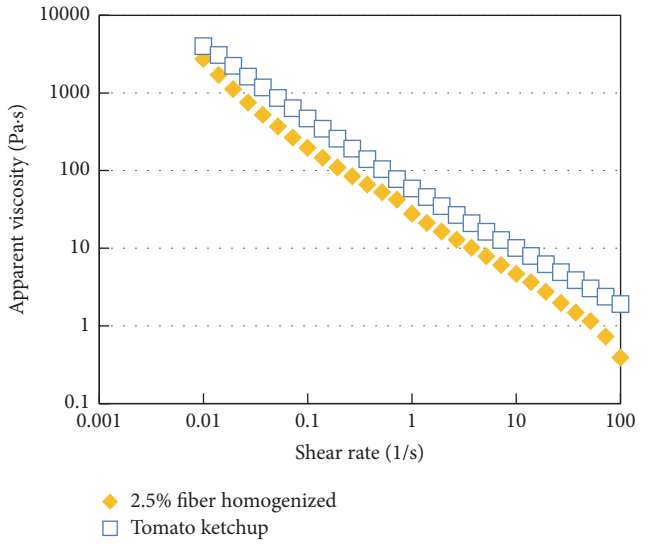

Figure 9: Apparent viscosity versus shear rate profiles of homogenized tomato fiber suspension and tomato ketchup (30° Brix).

employed in this section since it is more often used in the tomato industry than the rheological tests. A lower value of Bostwick consistency indicates a higher value of viscosity. As can be seen from this figure the addition of up to 0.5% (w/w) of tomato fiber could help the tomato sauce to achieve relatively high consistency. The amount of tomato fiber required would be one-third of the soybean fiber, to reach the same Bostwick consistency value. Typically, a tomato sauce with Bostwick consistency value of about 6–8 provides desirable texture or mouth feel of 0.2–0.5% dry fiber which is required.

A comparison of difference in color between the model tomato sauces prepared by using tomato fiber and soybean fiber is presented in Table 5. The Hunter color parameters (L, a, and b) and the ratio a/b are compared for these two formulations. A high value of a/b is desired in most tomato products. The a/b ratio containing tomato fiber is comparable but slightly higher compared to those containing soybean fiber. A slight decrease in total acidity was also observed in sauce samples containing tomato fiber.

4. Conclusions

The effects of high shear and high pressure homogenization on the morphological and rheological properties of tomato fiber were investigated. Both the high shear and high pressure homogenization processes made these suspensions much more homogeneous which enabled even distribution of fiber particles. Both the high shear and high pressure homogenization significantly ($p < 0.05$) increased the apparent viscosity of the tomato fiber suspensions. The apparent viscosity of the high pressure homogenized suspension was 10 times higher than that of unhomogenized one. The storage and loss modulus of the homogenized suspensions were higher than those of the unhomogenized one within the angular frequency range

Table 5: The color parameters, pH, and total tomato sauce formulations prepared using high pressure homogenized tomato fiber or soybean fiber.

Sample	2.5% tomato fiber homogenized (%)	Soybean fiber (%)	a/b	L	a	b	pH	Total acid (%)
P110	--	2.5	2.17	24.38	30.05	13.82	4.09	1.9
P111	13	--	2.23	23.32	29.63	13.30	4.07	1.86
P112	16	--	2.27	23.61	29.12	12.84	4.07	1.79
P113	19	--	2.22	23.38	29.11	13.12	4.05	1.69

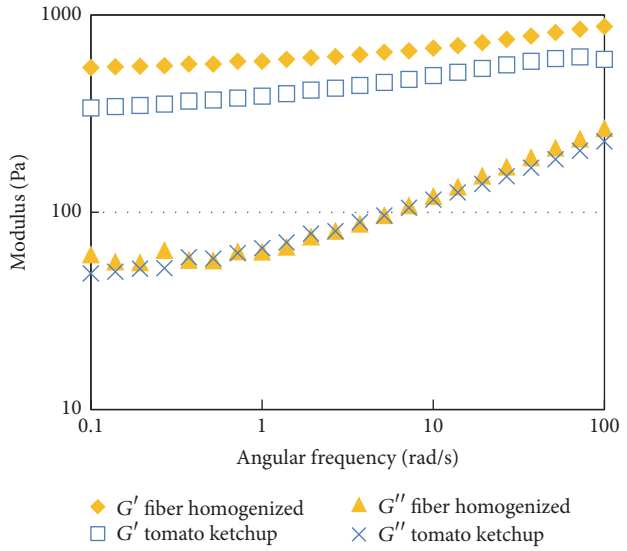

Figure 10: Storage and loss modulus of high pressure homogenized tomato fiber suspension (2.5%, w/w) and tomato ketchup (30° Brix).

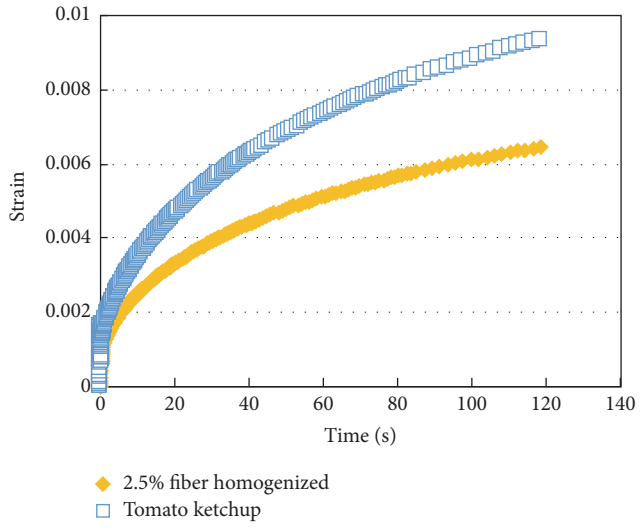

Figure 11: Creep diagram of high pressure homogenized tomato fiber suspension (2.5%, w/w) and tomato ketchup (30° Brix).

tested. The homogenized tomato fiber suspensions had more rigid structure compared to that of unhomogenized suspension and they resisted the deformation better (creep curve). The color and total acidity of model tomato sauce containing tomato fiber were more preferable than one containing soybean fiber at the same fiber content. The results presented

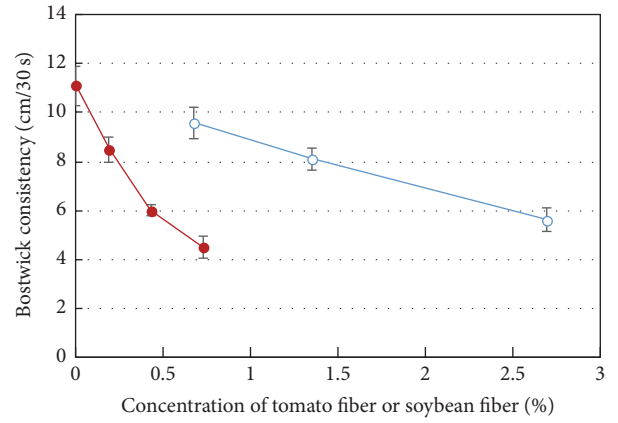

Figure 12: Bostwick consistency (cm/30 s) of tomato sauces prepared by using homogenized tomato fiber (0.19%–0.73%) or soybean fiber (0.67%–2.7%) using formula in Table 1. The red filled circles for tomato fiber; blue open circles for soybean fiber.

in this paper indicate that tomato fiber can be potentially used as food ingredient such as thickener or stablizer.

Conflicts of Interest

The authors declare that there are no conflicts of interest regarding the publication of this paper.

Acknowledgments

This research was supported by Beijing Advanced Innovation Center for Food Nutrition and Human Health Open Fund (20181043), China Postdoctoral Science Foundation Project (2012M520462), and Beijing Municipal Science and Technology Commission Project (D12110003112002). The authors wish to acknowledge COFCO Tunhe for kindly providing the test materials and access to the instruments. They also thank Mr. Jungang Zhao and Ms. Cheng Lv for their assistance in some of the experiments.

References

[1] J. L. Guil-Guerrero and M. M. Rebolloso-Fuentes, "Nutrient composition and antioxidant activity of eight tomato (Lycopersicon esculentum) varieties," *Journal of Food Composition and Analysis*, vol. 22, no. 2, pp. 123–129, 2009.

[2] A. K. Sankaran, J. Nijsse, L. Bialek, A. Shpigelman, M. E. Hendrickx, and A. M. Van Loey, "Enhanced electrostatic interactions in tomato cell suspensions," *Food Hydrocolloids*, vol. 43, pp. 442–450, 2015.

[3] S. K. Sharma, M. LeMaguer, A. Liptay, and V. Poysa, "Effect of composition on the rheological properties of tomato thin pulp," *Food Research International*, vol. 29, no. 2, pp. 175–179, 1996.

[4] N. Beresovsky, I. J. Kopelman, and S. Mizrahi, "The role of pulp interparticle interactions in determining tomato juice viscosity," *Journal of Food Processing and Preservation*, vol. 19, pp. 133–146, 1995.

[5] N. Takada and P. E. Nelson, "Pectineprotein interaction in tomato products," *Journal of Food Science*, vol. 48, pp. 1408–1411, 1983.

[6] E. Bayod, P. Månsson, F. Innings, B. Bergenståhl, and E. Tornberg, "Low shear rheology of concentrated tomato products. Effect of particle size and time," *Food Biophysics*, vol. 2, no. 4, pp. 146–157, 2007.

[7] E. Bayod and E. Tornberg, "Microstructure of highly concentrated tomato suspensions on homogenisation and subsequent shearing," *Food Research International*, vol. 44, no. 3, pp. 755–764, 2011.

[8] P. E. D. Augusto, A. Ibarz, and M. Cristianini, "Effect of high pressure homogenization (HPH) on the rheological properties of a fruit juice serum model," *Journal of Food Engineering*, vol. 111, no. 2, pp. 474–477, 2012.

[9] I. Colle, S. Van Buggenhout, A. Van Loey, and M. Hendrickx, "High pressure homogenization followed by thermal processing of tomato pulp: influence on microstructure and lycopene in vitro bioaccessibility," *Food Research International*, vol. 43, no. 8, pp. 2193–2200, 2010.

[10] M. T. K. Kubo, P. E. D. Augusto, and M. Cristianini, "Effect of high pressure homogenization (HPH) on the physical stability of tomato juice," *Food Research International*, vol. 51, no. 1, pp. 170–179, 2013.

[11] A. Panozzo, L. Lemmens, A. Van Loey, L. Manzocco, M. C. Nicoli, and M. Hendrickx, "Microstructure and bioaccessibility of different carotenoid species as affected by high pressure homogenisation: a case study on differently coloured tomatoes," *Food Chemistry*, vol. 141, no. 4, pp. 4094–4100, 2013.

[12] P. E. D. Augusto, A. Ibarz, and M. Cristianini, "Effect of high pressure homogenization (HPH) on the rheological properties of tomato juice: time-dependent and steady-state shear," *Journal of Food Engineering*, vol. 111, no. 4, pp. 570–579, 2012.

[13] H. Bengtsson, C. Hall, and E. Tornberg, "Effect of physicochemical properties on the sensory perception of the texture of homogenized fruit and vegetable fiber suspensions," *Journal of Texture Studies*, vol. 42, no. 4, pp. 291–299, 2011.

[14] F. Jiang and Y.-L. Hsieh, "Cellulose nanocrystal isolation from tomato peels and assembled nanofibers," *Carbohydrate Polymers*, vol. 122, pp. 60–68, 2015.

[15] P. García Herrera, M. C. Sánchez-Mata, and M. Cámara, "Nutritional characterization of tomato fiber as a useful ingredient for food industry," *Innovative Food Science and Emerging Technologies*, vol. 11, no. 4, pp. 707–711, 2010.

[16] I. Navarro-González, V. García-Valverde, J. García-Alonso, and M. J. Periago, "Chemical profile, functional and antioxidant properties of tomato peel fiber," *Food Research International*, vol. 44, no. 5, pp. 1528–1535, 2011.

[17] "AOAC Official Method 991.43 Total, Soluble, and Insoluble Dietary Fiber in Foods, AOAC International, Gaithersburg, Maryland, USA, 1994".

[18] "China National food safety standard GB 5009.5-2010 Determination of protein in foods, Ministry of Health of China, 2010".

[19] P. E. D. Augusto, A. Ibarz, and M. Cristianini, "Effect of high pressure homogenization (HPH) on the rheological properties of tomato juice: creep and recovery behaviours," *Food Research International*, vol. 54, no. 1, pp. 169–176, 2013.

[20] H. Bengtsson and E. Tornberg, "Physicochemical characterization of fruit and vegetable fiber suspensions. I: Effect of homogenization," *Journal of Texture Studies*, vol. 42, no. 4, pp. 268–280, 2011.

[21] C. Servais, R. Jones, and I. Roberts, "The influence of particle size distribution on the processing of food," *Journal of Food Engineering*, vol. 51, no. 3, pp. 201–208, 2002.

[22] P. E. D. Augusto, A. Ibarz, and M. Cristianini, "Effect of high pressure homogenization (HPH) on the rheological properties of tomato juice: viscoelastic properties and the Cox-Merz rule," *Journal of Food Engineering*, vol. 114, no. 1, pp. 57–63, 2013.

[23] E. Bayod, E. P. Willers, and E. Tornberg, "Rheological and structural characterization of tomato paste and its influence on the quality of ketchup," *LWT- Food Science and Technology*, vol. 41, no. 7, pp. 1289–1300, 2008.

[24] C. Valencia, M. C. Sánchez, A. Ciruelos, A. Latorre, J. M. Franco, and C. Gallegos, "Linear viscoelasticity of tomato sauce products: influence of previous tomato paste processing," *European Food Research and Technology*, vol. 214, no. 5, pp. 394–399, 2002.

Hindawi
International Journal of Analytical Chemistry
Volume 2018, Article ID 3013497, 8 pages
https://doi.org/10.1155/2018/3013497

Research Article

Optimum Extraction, Characterization, and Antioxidant Activities of Polysaccharides from Flowers of *Dendrobium devonianum*

Donghui Wang,[1] Bei Fan,[2] Yan Wang,[1] Lijing Zhang,[1] and Fengzhong Wang[1]

[1]*Institute of Food Science and Technology, Chinese Academy of Agricultural Sciences, Beijing 100193, China*
[2]*Laboratory of Quality & Safety Risk Assessment on Agro-Products Processing (Beijing), Ministry of Agriculture, Beijing, China*

Correspondence should be addressed to Fengzhong Wang; wangfengzhong@sina.com

Received 29 September 2017; Accepted 1 January 2018; Published 8 February 2018

Academic Editor: Jiajia Rao

Response surface methodology (RSM) was employed to optimize the conditions for the ultrasonic-assisted extraction (UAE) of polysaccharides from the flowers of *Dendrobium devonianum*. The optimal conditions for the maximum yields of DDFPs are as follows: an extraction temperature of 63.13°C, an extraction time of 53.10 min, and a water-to-raw material ratio of 22.11 mL/g. Furthermore, three fractions (DDFPs30, DDFPs50, and DDFPs70) were prepared from *Dendrobium devonianum* flowers polysaccharides (DDFPs) by the stepwise ethanol precipitation method. The DDFPs50 exhibited the highest antioxidant activity compared to the other fractions. The molecular weight, polydispersity, and conformation of these fractions were also characterized. In particular, the monosaccharide composition analysis of the DDFPs indicates that mannose and glucose are the primary components, similar to those of the *D. officinale* plant. This study provides a rapid extraction technology and essential information for the production of DDFPs, which could be potentially used as healthcare food.

1. Introduction

The genus *Dendrobium* belongs to the tribe Dendrobieae, the second largest genus in the family Orchidaceae with approximately 800–1500 species [1]. The *Dendrobium officinale* Kimura et Migo *(D. officinale)* plant, which is an important traditional Chinese herbal medicine, was officially included in the Chinese Pharmacopoeia (2005). The stems and leaves of *D. officinale* exhibit medicinal properties [2–4]. For example, they have been used to cure diabetes, obesity, and rheumatoid arthritis [5, 6]. However, because of overexploitation, the valuable *D. officinale* plant has been on the verge of extinction. Consequently, this herb is in high demand and has a high market value in China. In contrast to *D. officinale* species, *Dendrobium devonianum (D. devonianum)* has been mass-produced in China by tissue cultivation. The local people have the habit of drinking the extracts of the *D. devonianum* flowers (DDFs) as a tea beverage for health benefits. Several studies have demonstrated that polysaccharides are the major bioactive compounds in the *Dendrobium* species [6, 7]. Therefore, there is potential for the commercialization of the polysaccharides from DDFs.

Conventionally, hot-water-infusion technology has been successfully used for polysaccharide extraction [8]. Ultrasonic-assisted extraction (UAE) employs ultrasonic waves to effectively accelerate the release of the target compounds into the extraction solvent. Compared to the conventional extraction techniques, UAE has attracted much interest because of its inherent advantages such as simplified manipulation, significant reduction in energy consumption, lower temperature, and higher efficiency [9]. Response surface methodology (RSM) is a statistical technique for developing, improving, and optimizing processes. The main advantage of RSM is that it is an effective and accurate tool to evaluate multiple variables and their interactions [8].

However, thus far, there are limited studies on the optimization of the extraction process of DDF polysaccharides (DDFPs) as well as their characterization and antioxidant activities. In this study, both UAE and RSM were used to optimize the extraction conditions of DDFPs based on a

single-factor preliminary experiment. Three factors (temperature, time, and water-to-raw material ratio) affecting the extraction yield of the polysaccharides were investigated. Then, the *in vitro* antioxidant activities of three ethanol precipitation fractions of DDFPs were investigated. Finally, the aforementioned fractions were characterized by high-performance size-exclusion chromatography coupled with multiangle laser light scattering (HPSEC-MALLS) and high-performance anion-exchange chromatography coupled with pulsed amperometric detector (HPAEC-PAD) analysis.

2. Experimental

2.1. Materials and Chemicals. The flowers of *D. devonianum* were harvested in November 2013 in Baoshan city, Yunnan Province, China. The collected flowers were immediately dried at 60°C for 24 h. The samples were ground and sieved using a grinder and passed through a 40-mesh sieve. Standard monosaccharides, 1,3,5-tri(2-pyridyl)-2,4,6-triazine (TPTZ), and 1,1-diphenyl-2-picrylhydrazyl (DPPH) were purchased from Sigma Chemical Co. (Shanghai, China). Deionized water (18 MΩ cm) was obtained from an NW purified water system (Heal Force, Shanghai, China). All other chemical reagents were of analytical grade.

2.2. Extraction of Crude Polysaccharides. Extraction was performed according to a previously published method [10]. Each sample (2.0 g) was extracted using a KQ-600DV ultrasonic instrument (Kunshan Ultrasonic Machinery Co., Jiangsu, China) with distilled water as the solvent at designated temperatures from 30 to 80°C, extraction times at 10, 20, 30, 40, 50, 60, 70, and 80 min, respectively, and water-to-raw material at ratios from 10 to 35 mL/g. The extracts of each sample were cooled at room temperature and filtered, and then the polysaccharide concentration of the DDFPs was determined by the phenol–sulfuric acid method [11], with glucose solutions (50, 100, 150, and 200 μg/mL) as the standards.

The polysaccharide extraction yield (Y) was calculated as follows:

$$Y\ (\%) = \frac{(100 \times W_{\text{DDFPs}})}{W_{\text{sample}}}, \tag{1}$$

where W_{DDFPs} is the weight of the DDFPs and W_{sample} is the weight of the sample.

2.3. RSM Experimental Design. The conditions for the UAE of polysaccharides from DDFs were optimized by RSM. To investigate these conditions, the three variables for extraction—temperature, extraction time, and water-to-raw material ratio—were denoted as labels A, B, and C, respectively. Using RSM with a Box–Behnken design (BBD), the three independent variables were investigated in terms of the yield of DDFPs (denoted as Y), as shown in Table 1. The three independent variables (A, B, and C) were divided into three levels, coded +1, 0, and −1, for high, intermediate, and low values, respectively. The total experimental system was composed of 12 factorial experiments based on the BBD and five repeated tests at the center point.

2.4. Preparation of Three DDFP Fractions by the Stepwise Ethanol Precipitation Method. The DDFPs (1.0 g) were dissolved in 100 mL of deionized water. Then, the solution was adjusted to the final ethanol concentration of 30% using 95% ethanol and stored at 4°C overnight. The residue obtained after the precipitation was centrifuged at 10000 ×g and 25°C for 20 min and freeze-dried to obtain a dry fraction, denoted as DDFPs30. Similar cycles were performed to prepare the fractions of DDFPs50 and DDFPs70 by adjusting the final precipitation ethanol concentration to 50% and 70%, respectively.

2.5. Measurement of Antioxidant Activities

2.5.1. DPPH Radical-Scavenging Assay. The DPPH radical-scavenging capacity assay was based on a 96-well microplate method [12]. Briefly, 20 μL of three DDFP fractions (DDFPs30, DDFPs50, and DDFPs70) was mixed with 100 μL of a methanolic solution of DPPH (0.2 mM) and left for 30 min at room temperature before the absorbance was recorded at 517 nm using the microplate reader (MD190, Santa Barbara, CA, USA). The antioxidant activities of the radical scavengers in different polysaccharides were investigated. The radical-scavenging activities were calculated as percentages using the following equation:

$$\text{DPPH radical-scavenging activity (\%)} = \left[\frac{(A_{\text{DPPH}} - (A_1 - A_S))}{A_{\text{DPPH}}}\right] \times 100\%, \tag{2}$$

where A_{DPPH} is the absorbance of DPPH, A_1 is the absorbance of DPPH and the sample extract, and A_S is the absorbance of the sample extract. All the samples were tested in triplicate.

2.5.2. Ferric Reducing Antioxidant Power (FRAP) Assay. The FRAP assay was also conducted according to our previous method using 96-well microplates [12]. The samples (10 μL) were mixed with 300 μL of ferric-TPTZ reagent (prepared by mixing 300 mM acetate buffer, pH 3.6, 10 mM TPTZ in 40 mM HCl, and 20 mM $FeCl_3{\cdot}7H_2O$ in a ratio of 10 : 1 : 1 (v/v/v)). After 30 min of incubation at room temperature, the data were recorded at an absorbance of 593 nm against a blank (the FRAP reagent was previously prepared without the extracts). The data obtained with $FeSO_4{\cdot}7H_2O$ from the calibration curve were calculated using the following equation: average $R^2 = 0.9977$, $y = 0.005x + 0.0085$. The antioxidant activities were expressed as micromoles of $FeSO_4$ equivalent per gram dry weight (μmol Fe^{2+}E/g DW). All the samples were tested in triplicate.

2.6. Characterization of DDFPs

2.6.1. Molecular Weight and Size Distribution Analysis. Molecular weight and molecular size distribution were investigated using an HPSEC system coupled to an integrated detector array: a refractive index detector (Wyatt Technology, Santa Barbara, CA, USA), a UV L-2400 detector (Hitachi High Technologies America, Inc., Schaumburg,

Table 1: Response surface analysis program and results for the yield polysaccharides from *D. devonianum* flowers.

Run	Temperature *A*: temperature (°C)	Time *B*: extraction time (min)	Factor 3 *C*: water-to-material ratio	Yield of polysaccharides *Y*: (%)
1	50 (–1)	50 (0)	25 (1)	17.30
2	60 (0)	60 (1)	15 (–1)	16.11
3	60 (0)	40 (–1)	25 (1)	16.68
4	60 (0)	50 (0)	20 (0)	21.22
5	70 (1)	50 (0)	15 (–1)	16.22
6	50 (–1)	50 (0)	15 (–1)	15.66
7	60 (0)	40 (–1)	15 (–1)	15.41
8	60 (0)	60 (1)	25 (1)	19.57
9	60 (0)	50 (0)	20 (0)	19.4
10	50 (–1)	60 (1)	20 (0)	16.37
11	50 (–1)	40 (–1)	20 (0)	15.42
12	60 (0)	50 (0)	20 (0)	19.02
13	60 (0)	50 (0)	20 (0)	20.00
14	60 (0)	50 (0)	20 (0)	19.94
15	70 (1)	60 (1)	20 (0)	18.65
16	70 (1)	40 (–1)	20 (0)	17.90
17	70 (1)	50 (0)	25 (1)	18.58

Illinois, USA), and a MALLS detector (Wyatt Technology, Santa Barbara, CA, USA). The chromatographic system consisted of an L-2130 pump (Hitachi Scientific Instruments Inc., Columbia, Maryland, USA) and a TOSOH TSKgel G4000PWXL column (300 mm × 7.8 mm i.d., Tokyo, Japan). Each polysaccharide (2 mg mL^{-1}) of DDFPs30, DDFPs50, and DDFPs70 was subjected to the HPSEC system. The eluent consisted of a 0.1 mol L^{-1} $NaNO_2$ solution and 0.5 g L^{-1} NaN_3 at a flow rate of 0.5 mL min^{-1} with a run time of 25 min. The weight-average molecular weight (M_w), number-average molecular weight (M_n), and polydispersity index (M_w/M_n) were analyzed by the Astra software (version 4.73.04, Wyatt Technology, Santa Barbara, CA, USA).

2.6.2. Monosaccharide Composition Analysis. DDFPs30, DDFPs50, and DDFPs70 (5 mg each) were hydrolyzed in 2 mL of 2 M trifluoroacetic acid at 120°C for 6 h. Excess trifluoroacetic acid was removed by codistillation [13]. The monosaccharide compositions of DDFPs30, DDFPs50, and DDFPs70 were analyzed using a HPAEC-PAD (Dionex Technology, Sunnyvale, CA, USA) after acid hydrolysis. HPAEC was performed using a Dionex ICS-3000 system with a Carbo PAC™ PA10 analytical column (4.0 mm × 250 mm) and a PAC PA10 guard column (4.0 mm × 50 mm). The samples (10 μL) were injected into the column to analyze the monosaccharide and eluted with 9% NaOH and NaAC by decreasing the proportion of NaOH (0–20 min: 9% NaOH; 20–30 min: 9% NaOH + 5% NaAC; 35-36 min: 9% NaOH + 20% NaAC). The flow rate was adjusted to 1 mL min^{-1}, and the column temperature was set at 25°C. A standard curve was established with different concentrations (0.2, 0.5, 1, 5, and 10 mg/mL) of mixed standard solutions including glucose (Glu), mannose (Man), galactose (Gal), L-arabinose (Ara), α-L-rhamnose (Rha), fructose (Fru), galacturonic acid (Gal acid), and glucuronic acid (Glu acid).

3. Results and Discussion

3.1. Single-Factor Experiments. The RSM optimization of the UAE conditions was based on the maximum DDFP yield of the sample. All the parameters (*A*–*C*) were investigated by single-factor experiments in a wide range prior to the RSM optimization. This helped to narrow down the ranges of the parameters.

The effect of various temperatures (30, 40, 50, 60, 70, and 80°C) on the extraction efficiency of DDFPs was investigated by maintaining the other two factors (extraction time and water-to-raw material ratio) constant at 60 min and 30 mL/g, respectively. As shown in Figure 1(a), the DDFP yield significantly increased with the increase in temperature from 30 to 60°C. The yield was the highest at 60°C and then decreased with increasing temperature. At a higher temperature, the viscosity of the extracts decreased, thus increasing the solubility of the DDFPs, which in turn accelerated the release and dissolution of these compounds. A similar trend has been reported for polysaccharide extraction [14]. To prevent the yield loss and minimize the adverse effects of processing, 70°C was set as the highest temperature in this study. Therefore, the temperature range from 50 to 70°C was used as the optimal condition in the further design of the RSM experiment.

Extraction time is also one of the important variables affecting the extraction efficiency of polysaccharides from natural products [15]. The extraction time was set at 10, 20, 30, 40, 50, 60, 70, and 80 min while maintaining an extraction temperature of 60°C and water-to-raw material ratio at 30 mL/g. As shown in Figure 1(b), the extraction efficiency

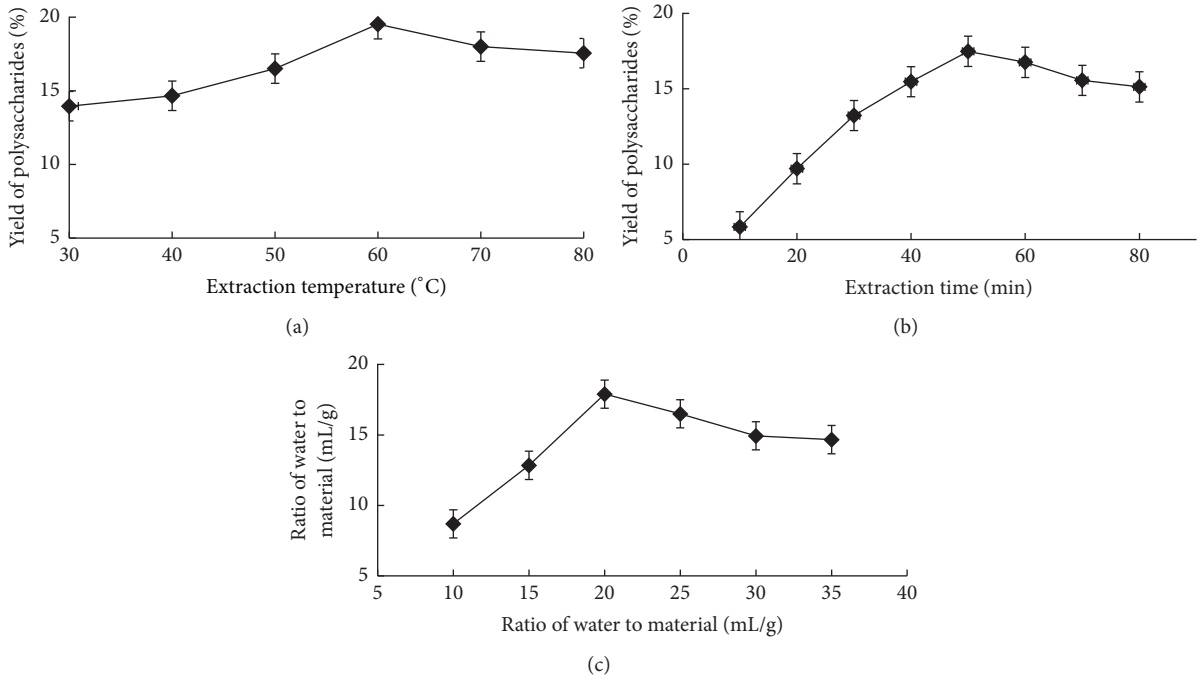

Figure 1: Effects of the extraction temperature (a), extraction time (b), and water-to-material ratio (c) on yield of DDFPs.

clearly increased as the extraction time increased from 10 to 50 min. After 50 min, the extraction efficiency slightly decreased with increasing extraction time, with continuous extraction to 80 min. It has also been reported that processing at a long extraction time may lead to the degradation, aggregation, and hydrolysis of polysaccharides [14]. Thus, an extraction time from 40 to 60 min was selected as the optimum condition.

The yields of the DDFPs extracted by different water-to-raw material ratios (10, 15, 20, 25, 30, and 35 mL/g) are shown in Figure 1(c) while maintaining an extraction temperature of 60°C and an extraction time of 60 min. The solvent volume in the studied range played an important role in the UAE extraction of the DDFPs. This may be caused by the fact that less amounts of polysaccharides can be extracted using a small quantity of an extraction solvent (water-to-raw material ratio = 10 mL/g). Increasing the water-to-raw material ratio to 20 mL/g increased the DDFP yield. Then, at the ratio 20 mL/g, all the polysaccharides could be extracted from DDF. Thus, the water-to-raw material ratio was set in the range 15–25 as the optimal condition.

Thus, the RSM experiments were conducted under the following conditions: an extraction temperature of 50–70°C, an extraction time of 40–60 min, and a water-to-raw material ratio of 15–25 mL/g.

3.2. Response Surface Model (Statistical Analysis). A total of 17 runs were designed to evaluate the three independent variables A, B, and C in the BBD, as shown in Table 1. The predicted model sufficiently explained the response. The independent and dependent variables are expressed by the following equation: $Y = 19.92 + 0.82A + 0.66B + 1.09C - 0.050AB + 0.18AC + 0.55BC - 1.42A^2 - 1.41B^2 - 1.56C^2$. Table 2 shows the model results of the independent variables on the extraction yield evaluated by the analysis of variance. The results indicate that the linear terms of A, B, and C were all significant ($P < 0.05$) to Y; in particular, C was very significant. Not all of the cross terms (AB, AC, and BC) were significant, and all the quadratic terms (A^2, B^2, and C^2) were very significant to Y ($P < 0.01$). The model used to fit the response variable was significant ($P < 0.05$) and adequate to represent the relationships between the response and independent variables. A "lack-of-fit F-value" of 0.758064 indicates that the lack-of-fit is not significantly relative to the pure error. There is a 57.31% chance that the lack-of-fit F-value is large, possibly because of noise. The total determination coefficient (R^2) and adjusted determination coefficient were 0.9200 and 0.8172, respectively, confirming that the model is reasonable and significant. The effects of the independent variables and their mutual interaction on the extraction yield were observed on the response surface and contour plots, as shown in Figure 2. The optimum conditions for the yield of the DDFPs are as follows: an extraction temperature of 63.13°C, an extraction time of 53.10 min, and a water-to-raw material ratio of 22.11 mL/g. Accordingly, the theoretical highest yield of DDFPs was predicted as 20.3779% by the developed model. Verification experiments were conducted by utilizing the modified conditions of an extraction temperature of 65°C, an extraction time of 55 min, and a water-to-raw material ratio of 22 mL/g for the three replicates. The average yield of the DDFPs was 20.25%. These experimental yields were in good agreement with those predicted by the model.

3.3. Evaluation of Antioxidant Activity of Three Fractions from DDFPs. To further select the polysaccharide fraction with the highest antioxidant activity, three fractions (DDFPs30,

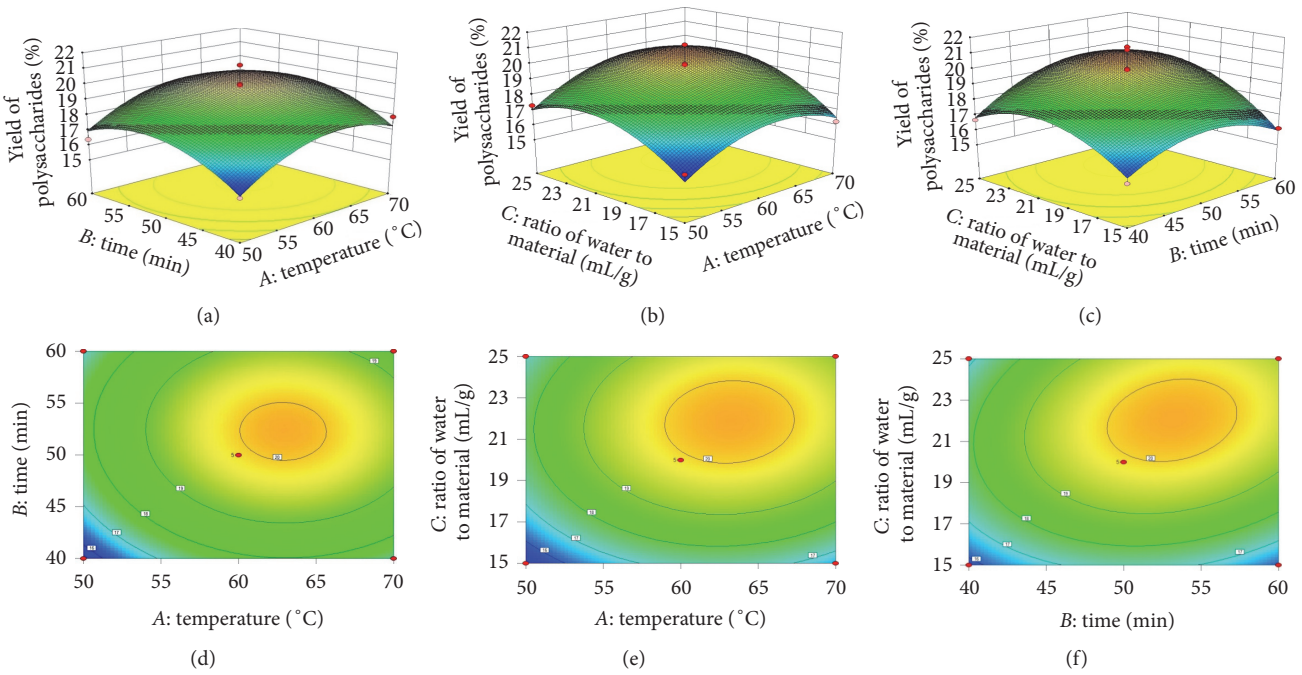

FIGURE 2: Response surface plots (a, b, and c) and contour plots (d, e, and f) showing the effect of time, temperature, and water-to-material ratio on yield of DDFPs.

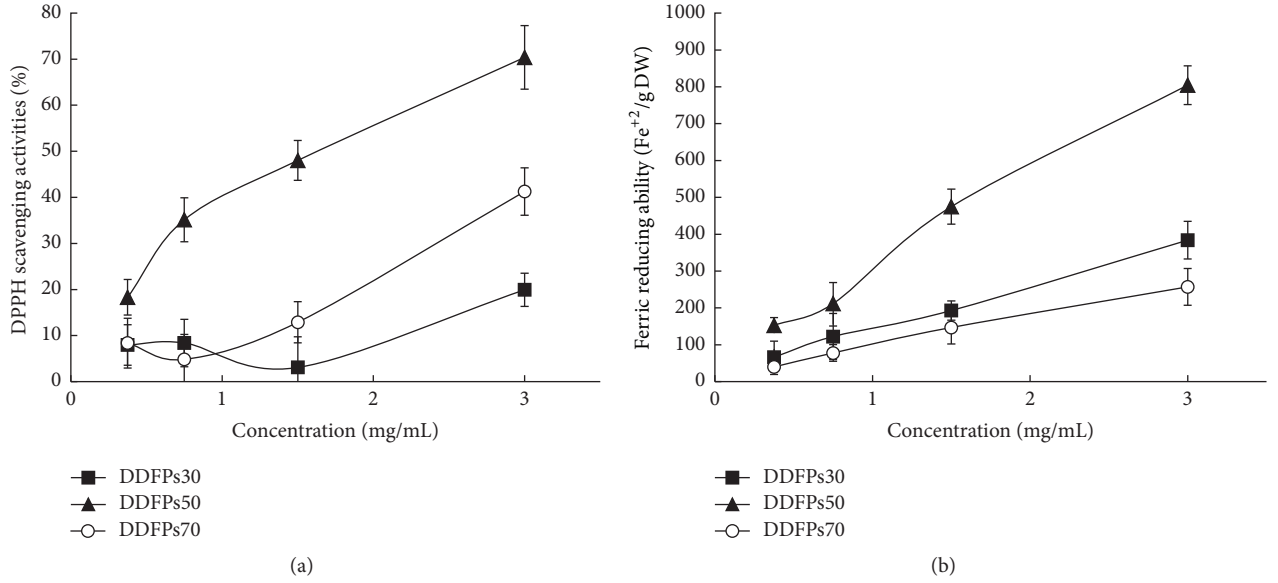

FIGURE 3: Antioxidant activity of three fractions from DDFPs. (a) Scavenging effect on DPPH radicals. (b) Reducing power evaluation.

DDFPs50, and DDFPs70) were prepared by the stepwise ethanol concentration precipitation method. Ethanol precipitation is an effective method for fractionation and purification of water-soluble DDFPs in aqueous solutions. In an aqueous solution, the DDFPs molecule exposes its charged and polar residues on the surface to maximize the contact with water molecules. Compared with other isolation methods for biopolymers such as chromatography and membrane, ethanol precipitation has the advantages of simple equipment and easy operation.

As shown in Figure 3(a), all three fractions exhibited scavenging effects, which almost correlated positively with increasing concentrations. The scavenging effect of three fractions increased in the order of DDFPs50 > DDFPs70 > DDFPs30, and their scavenging activities were 70.37 ± 6.89%, 41.26 ± 5.13%, and 19.93 ± 3.61%, respectively, at a concentration of 3 mg/mL.

The FRAP assay is a simple, reproducible, rapid, and inexpensive method to measure the reductive ability of an antiradical and is evaluated by the transformation of ferric

Table 2: ANOVA for response surface quadratic model: analysis of variance table (partial sum of squares). *A*: temperature (°C), *B*: extraction time (min), and *C*: water-to-material ratio.

Source	Sum of squares	DF	Mean square	*F* value	*P* value	Significant
Model	50.10	9	5.566395	8.944987	0.0043	*
A	5.45	1	5.445	8.74991	0.0212	*
B	3.50	1	3.498013	5.621174	0.0495	*
C	9.53	1	9.526613	15.30891	0.0058	**
A^2	0.01	1	0.01	0.01607	0.9027	
B^2	0.1296	1	0.1296	0.208262	0.6620	
C^2	1.199025	1	1.199025	1.926788	0.2077	
AB	8.451287	1	8.451287	13.5809	0.0078	**
AC	8.421487	1	8.421487	13.53301	0.0079	**
BC	10.23689	1	10.23689	16.45029	0.0048	**
Residual	4.356045	7	0.622292			
Lack-of-fit	1.578925	3	0.526308	0.758064	0.5731	
Pure error	2.77712	4	0.69428			
Cor. total	54.4536	16				

* $P < 0.05$ and ** $P < 0.01$.

Table 3: The physical properties of polysaccharides from *D. devonianum* flowers ($n = 3$).

Fractions	M_w/M_n (10^5 g/mol)	Polydispersity (M_w/M_n)	Slope
DDFPs30	5.41 ± 0.23	1.28 ± 0.15	0.33 ± 0.02
DDFPs50	3.78 ± 0.12	1.33 ± 0.09	0.35 ± 0.03
DDFPs70	5.63 ± 0.14	1.02 ± 0.05	0.32 ± 0.02

ion (Fe^{3+}) to ferrous ion (Fe^{2+}), as a measure of the total antioxidant capacity [16]. The concentration of three fractions increased the FRAP value in a dose-dependent manner (Figure 3(b)). Moreover, DDFPs50 also exhibited higher antioxidant activity (804.56 ± 52.70 μmol Fe^{2+}E/g DW) than DDFPs30 (383.89 ± 51.03 μmol Fe^{2+}E/g DW) and DDFPs70 (257.11 ± 50.02 μmol Fe^{2+}E/g DW).

3.4. Characterization of Three Fractions from DDFPs

3.4.1. Molecular Weight, Polydispersity, and Conformation. To better explore the structural difference between three fractions (DDFPs30, DDFPs50, and DDFPs70) from DDFPs, HPSEC-MALLS was used to determine the molecular weight (M_w), size distribution, root mean square (RMS), and slope exponent of a conformation plot (Table 3). The results indicate that M_w of DDFPs30, DDFPs50, and DDFPs70 ranged from 3.78×10^5 to 5.63×10^5. DDFPs70 had the highest M_w, followed by DDFPs30 and DDFPs50. The polydispersity indices of these fractions were 1.28, 1.33, and 1.02, respectively. The slope exponent of all these fractions ranged from 0.32 to 0.35. Theoretically, a slope of 0.33 indicates a sphere and slopes of 0.5–0.6 and close to 1.0 indicate a random coil and rigid rod, respectively [17]. The results indicate that all these fractions have more rod-like structures.

3.4.2. Monosaccharide Composition Analysis. The HPAEC-PAD analysis profiles and data of the monosaccharide compositions of the three polysaccharides from the flowers of *D. devonianum* are shown in Figure 4. The molar ratio of the monosaccharide compositions in DDFPs30 was as follows: Man : Glu : Gal : Rha : Ara : Fru : Gal acid = 4.77 : 5.18 : 1.00 : 0.46 : 0.64 : 0.50 : 1.39. DDFPs50 was composed of Man : Glu : Gal : Rha : Ara : Fru : Glu acid in a molar ratio of 8.45 : 2.93 : 1.00 : 0.06 : 0.37 : 0.04 : 0.2. DDFPs70 was composed of Man : Glu : Gal : Rha : Ara in a molar ratio of 9.00 : 1.43 : 1.00 : 0.28 : 0.59. The purified *O*-acetyl-glucomannan in *D. officinale* herbal materials was mainly composed of mannose and glucose in a molar ratio of 6.9 : 1 [5]. Our result showed that the DDFPs had similar monosaccharide composition.

4. Conclusions

In this study, RSM was applied for the first time to determine the optimal conditions for the extraction of DDFPs. The optimum conditions for the yield of DDFPs are as follows: an extraction temperature of 63.13°C, an extraction time of 53.10 min, and a water-to-raw material ratio of 22.11 mL/g. Furthermore, under the optimized conditions, the yield obtained from the verification experiments (20.25%) agreed well with the theoretical yield (20.38%), indicating that the regression model is efficient and successful for the extraction of DDFPs from DDFs. To further select the fraction with higher antioxidant activity, the stepwise ethanol precipitation method was used to separate the fractions from DDFPs as DDFPs30, DDFPs50, and DDFPs70. DDFPs50 exhibited the highest antioxidant activity in both the DPPH and FRAP assays. M_w of three fractions ranged from 3.78×10^5 to

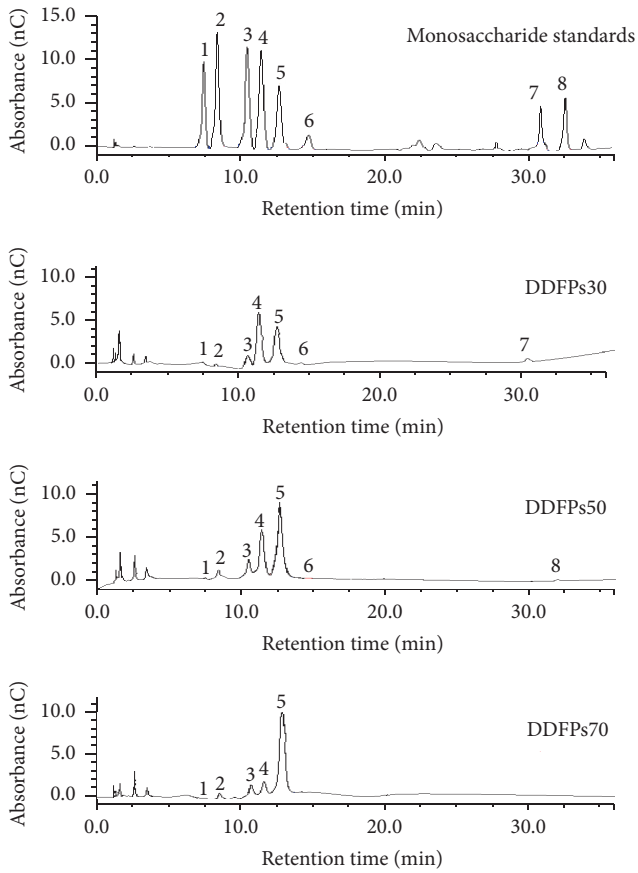

Figure 4: HPAEC-PAD analysis profiles of monosaccharide composition in three fractions from DDFPs. Each peak was separated as described as 1: α-L-rhamnose, 2: L-arabinose, 3: galactose, 4: glucose, 5: mannose, 6: fructose, 7: galacturonic acid, and 8: glucuronic acid.

5.63×10^5. The polydispersity indices of these fractions were 1.28, 1.33, and 1.02, respectively. The slope of the conformation plot indicated that all three fractions had rod-shaped structures. Interestingly, the results showed that the DDFPs had similar monosaccharide composition as the *D. officinale* plant, mainly composed of Man and Glu. Further research is required to study the accurate structure by methylation analysis and two-dimensional NMR spectroscopy. This study provides a rapid extraction technology for the production of DDFPs, which can be potentially used as a new type of antioxidant or a healthcare food.

Conflicts of Interest

The authors declare that they have no conflicts of interest.

Acknowledgments

This project was supported by the Agricultural Science and Technology Innovation Program (2014), China.

References

[1] X. G. Xiang, A. Schuiteman, D. Z. Li et al., "Molecular systematics of Dendrobium (Orchidaceae, Dendrobieae) from mainland Asia based on plastid and nuclear sequences," *Molecular Phylogenetics and Evolution*, vol. 69, no. 3, pp. 950–960, 2013.

[2] Z. Yuan, G. Cong, and J. Zhang, "Effects of exogenous salicylic acid on polysaccharides production of Dendrobium officinale," *South African Journal of Botany*, vol. 95, pp. 78–84, 2014.

[3] X. Lin, P.-C. Shaw, S. C.-W. Sze, Y. Tong, and Y. B. Zhang, "*Dendrobium* officinale polysaccharides ameliorate the abnormality of aquaporin 5, pro-inflammatory cytokines and inhibit apoptosis in the experimental Sjögren's syndrome mice," *International Immunopharmacology*, vol. 11, no. 12, pp. 2025–2032, 2011.

[4] Z. Chen, X. Sun, and K. Tang, "Cloning and expression of a novel cDNA encoding a mannose-binding lectin from Dendrobium officinale," *Toxicon*, vol. 45, no. 4, pp. 535–540, 2005.

[5] X. Xing, S. W. Cui, S. Nie, G. O. Phillips, H. D. Goff, and Q. Wang, "Study on Dendrobium officinale O-acetyl-glucomannan (Dendronan®): part I. Extraction, purification, and partial structural characterization," *Bioactive Carbohydrates and Dietary Fibre*, vol. 4, no. 1, pp. 74–83, 2014.

[6] X. Xing, S. W. Cui, S. Nie, G. O. Phillips, H. Douglas Goff, and Q. Wang, "A review of isolation process, structural characteristics, and bioactivities of water-soluble polysaccharides from *Dendrobium* plants," *Bioactive Carbohydrates and Dietary Fibre*, vol. 1, no. 2, pp. 131–147, 2013.

[7] A. Luo, X. He, S. Zhou, Y. Fan, A. Luo, and Z. Chun, "Purification, composition analysis and antioxidant activity of the

polysaccharides from Dendrobium nobile Lindl.," *Carbohydrate Polymers*, vol. 79, no. 4, pp. 1014–1019, 2010.

[8] Z. Wang, Y. Zhao, and T. Su, "Extraction and antioxidant activity of polysaccharides from Rana chensinensis skin," *Carbohydrate Polymers*, vol. 115, pp. 25–31, 2015.

[9] F. Chemat, Z.-E. Huma, and M. K. Khan, "Applications of ultrasound in food technology: processing, preservation and extraction," *Ultrasonics Sonochemistry*, vol. 18, no. 4, pp. 813–835, 2011.

[10] Z. Wu, H. Li, D. Tu, Y. Yang, and Y. Zhan, "Extraction optimization, preliminary characterization, and in vitro antioxidant activities of crude polysaccharides from finger citron," *Industrial Crops and Products*, vol. 44, pp. 145–151, 2013.

[11] M. Dubois, K. A. Gilles, J. K. Hamilton, P. A. Rebers, and F. Smith, "Colorimetric method for determination of sugars and related substances," *Analytical Chemistry*, vol. 28, no. 3, pp. 350–356, 1956.

[12] T. Wu, J. Yan, R. Liu, M. F. Marcone, H. A. Aisa, and R. Tsao, "Optimization of microwave-assisted extraction of phenolics from potato and its downstream waste using orthogonal array design," *Food Chemistry*, vol. 133, no. 4, pp. 1292–1298, 2012.

[13] Y. Jing, L. Huang, W. Lv et al., "Structural characterization of a novel polysaccharide from pulp tissues of litchi chinensis and its immunomodulatory activity," *Journal of Agricultural and Food Chemistry*, vol. 62, no. 4, pp. 902–911, 2014.

[14] S. Tahmouzi and M. Ghodsi, "Optimum extraction of polysaccharides from motherwort leaf and its antioxidant and antimicrobial activities," *Carbohydrate Polymers*, vol. 112, pp. 396–403, 2014.

[15] C. Zhu and X. Liu, "Optimization of extraction process of crude polysaccharides from Pomegranate peel by response surface methodology," *Carbohydrate Polymers*, vol. 92, no. 2, pp. 1197–1202, 2013.

[16] R. L. Prior and G. Cao, "In vivo total antioxidant capacity: comparison of different analytical methods," *Free Radical Biology & Medicine*, vol. 27, no. 11-12, pp. 1173–1181, 1999.

[17] E. Corroyer, M.-C. Brochier-Salon, D. Chaussy, S. Wery, and M. N. Belgacem, "Characterization of Commercial Polyvinylbutyrals," *International Journal of Polymer Analysis and Characterization*, vol. 18, no. 5, pp. 346–357, 2013.

Hindawi
International Journal of Analytical Chemistry
Volume 2018, Article ID 2416461, 5 pages
https://doi.org/10.1155/2018/2416461

Research Article

Multivariate Analysis of Fruit Antioxidant Activities of Blackberry Treated with 1-Methylcyclopropene or Vacuum Precooling

Jian Li, Guowei Ma, Lin Ma, Xiaolin Bao, Liping Li, Qian Zhao, and Yousheng Wang

Beijing Advanced Innovation Center for Food Nutrition and Human Health, Beijing Engineering and Technology Research Center of Food Additives, Beijing Technology and Business University, Beijing 100048, China

Correspondence should be addressed to Yousheng Wang; wangys@btbu.edu.cn

Received 29 September 2017; Accepted 31 December 2017; Published 1 February 2018

Academic Editor: Ying Yang

Effects of 1-methylcyclopropene (1-MCP) and vacuum precooling on quality and antioxidant properties of blackberries (*Rubus* spp.) were evaluated using one-way analysis of variance, principal component analysis (PCA), partial least squares (PLS), and path analysis. Results showed that the activities of antioxidant enzymes were enhanced by both 1-MCP treatment and vacuum precooling. PCA could discriminate 1-MCP treated fruit and the vacuum precooled fruit and showed that the radical-scavenging activities in vacuum precooled fruit were higher than those in 1-MCP treated fruit. The scores of PCA showed that H_2O_2 content was the most important variables of blackberry fruit. PLSR results showed that peroxidase (POD) activity negatively correlated with H_2O_2 content. The results of path coefficient analysis indicated that glutathione (GSH) also had an indirect effect on H_2O_2 content.

1. Introduction

Blackberries (*Rubus* spp.) are notable for their antioxidant activities, particularly due to their high contents of polyphenolic compounds, such as ellagic acid, quercetin, gallic acid, anthocyanins, and cyanidins, plus excellent contents of the antioxidant vitamins A and C [1–3]. However, blackberries have a short market life and the fruit quality is rapidly reduced after harvesting [4, 5].

Reactive oxygen species (ROS), like hydrogen peroxide (H_2O_2) and superoxide $O^{\bullet-}$, could promote the oxidation of proteins and lipids and thus lead to fruit senescence and a decrease of fruit quality [6, 7]. The antioxidant enzymes, including catalase (CAT), ascorbate peroxidase (APX), peroxidase (POD), and polyphenol oxidase (PPO), can prevent the accumulation of ROS and repair oxidative damage [8]. The antioxidants, such as polyphenolic compounds, also play an important role in scavenging excess ROS [9]. There are many correlated factors affecting the fruit quality. Hence, application of a multivariate technique to characterize the relationship among the antioxidant enzymes' activities, ROS levels, and antioxidant activities seems to be appropriate.

Principal component analysis (PCA) is a multivariate technique used to extract the important information from multivariate data [10]. Partial least squares (PLS) and path analysis can be especially useful to find the correlations between intercorrelated quantitative dependent variables. PLS has been used to predict the changes of quality of pasteurized pineapple juice during storage [11].

In this study, the quality and antioxidant parameters were collected from 1-MCP treated, vacuum precooled, and control fruit. Principal component analysis (PCA) was applied to evaluate the effect of 1-MCP and vacuum precooling on physiological properties of fruit. Correlations between quality and antioxidant parameters were studied through partial least squares (PLS) and path analysis.

2. Materials and Methods

2.1. Plant Material and Treatment. Blackberry fruit (*Rubus* spp. cv. Triple Crown) at the commercially mature stage was harvested from an orchard near Beijing. Fruit was sorted to eliminate damaged and diseased fruit and selected for uniformity in size and color. Fruit was randomized and

divided into 3 lots for the following treatments: (1) untreated and referred to as the control and (2) treated with 5 μg/L 1-methylcyclopropene (1-MCP). Fruits were placed in sealed 250 L plastic chambers with 1-MCP powdered formulation (1250 μg 1-MCP release) at room temperature for 24 h and (3) precooled in vacuum cooler at 10°C for 1 h.

After the treatments, all the fruits were placed in 60 cm × 37 cm × 20 cm plastic containers and then stored at 0°C with 85–95% RH.

2.2. Fruit Quality Measurement. Flesh firmness of the fruit was measured using a texture analyzer (LFRA, Brookfield Ltd., USA). Fifteen fruits were measured at each sampling time.

Fruit of each treatment was distributed into three groups (30 fruit per group), and each group represented one replicate. The number of decayed fruits in each plastic container was counted and decay rate was calculated as percentage of decayed fruit versus total fruit.

2.3. Enzymatic Activity Analysis. For the ascorbate peroxidase (APX), peroxidase (POD), and polyphenol oxidase (PPO) activities assay, 10.0 g samples were thoroughly homogenized with 20 mL extracting buffer (pH 7.8 100 mM phosphate buffer containing 0.2 g polyvinylpolypyrrolidone) and centrifuged at 10,000 ×g at 4°C for 20 min, and the supernatant was collected and stored at −80°C for further analysis.

APX activity was determined spectrophotometrically by monitoring the decline in absorbance at 290 nm as ascorbate was oxidized [12]. APX activity was expressed as $U \cdot g^{-1}$ FW.

POD activity was measured as the oxidation of guaiacol in the presence of H_2O_2 by measuring the absorbance at 460 nm [13]. The POD activity was expressed as $U \cdot g^{-1}$ FW.

PPO activity was measured according to the method of Jiang et al. and expressed as $U \cdot g^{-1}$ FW [13].

2.4. GSH Assays. Glutathione (GSH) was extracted from 10.0 g of the flesh tissue with 20 mL of ice-cold 5% trichloroacetic acid containing 5 mM Ethylenediaminetetraacetic Acid (EDTA) and then centrifuged at 4°C for 10 min at 10,000 ×g. The supernatant was assayed for GSH according to the method of Guri, and the GSH content was expressed as $mg \cdot 100\ g^{-1}$ FW [14].

2.5. H_2O_2 Assays. H_2O_2 was extracted by homogenizing 10.0 g of fruit tissue in 20 ml of cold acetone and was measured according to the method of Brennan and Frenkel [15]. The H_2O_2 content was expressed as $mg \cdot 100\ g^{-1}$ FW.

2.6. Antioxidant Activities Assay. For antioxidant activities assay, 10.0 g samples were thoroughly homogenized with 20 mL methyl alcohol and centrifuged at 10,000 ×g at 4°C for 20 min. The supernatant was used for antioxidant activities, total phenol, and total flavonoid concentration assays.

Total antioxidant activity was measured using ferric reducing antioxidant potential assay (FARP) [16]. The values were expressed as the concentration of antioxidants having a ferric reducing ability equivalent to that of 1 mmol/L $FeSO_4$.

Trolox equivalent antioxidant capacity (TEAC) was determined according to the method of Arts et al. [17]. 50% of the 2,2′-Azinobis-(3-ethylbenzothiazoline-6-sulphonate) (ABTS) radical-scavenging activity is defined as one activity unit. TEAC activity was expressed as $U \cdot g^{-1}$ FW.

The 2,2-diphenylpicrylhydrazyl (DPPH) radical-scavenging activity was assayed by the method of Shon et al. [18]. 50% of the DPPH radical-scavenging activity is defined as an activity unit and the DPPH radical-scavenging activity was expressed as $U \cdot g^{-1}$ FW.

Superoxide anion scavenging activity was measured by Nitrotetrazolium Blue chloride (NBT) reduction method [19]. 50% of the superoxide anion scavenging activity is defined as an activity unit. Superoxide anion scavenging activity was expressed as $U \cdot g^{-1}$ FW.

Hydroxyl radical-scavenging activity is determined by the method of Shon et al. [18]. 50% of the hydroxyl radical-scavenging activity is defined as an activity unit. Hydroxyl radical-scavenging activity was expressed as $U \cdot g^{-1}$ FW.

The total phenolic concentration of flesh extracts was measured using a modified Folin–Ciocalteu colorimetric method [20]. Absorbance was measured at 760 nm after 60 min at room temperature. The results were expressed as micrograms of gallic acid equivalents per gram of fresh weight.

The total flavonoid concentration of flesh extracts was determined using a colorimetric assay [20]. The absorbance of the solution versus a blank at 510 nm was measured after 60 min. The results were expressed as micrograms of catechin equivalents per gram of fresh weight.

2.7. Statistical Analysis. All data were analyzed by one-way analysis of variance (ANOVA) with SPSS 11.0 statistical software. Significant differences were performed by a least significant difference method (LSD test, $P \leq 0.05$) for all treatments at different sampling times.

For multivariate analysis, data were centered and weighted by the inverse of the standard deviation of each variable in order to avoid dependence on measured units. Principal component analysis (PCA) and partial least squares (PLS) in this study were performed using Unscrambler 9.7 statistical software. Path analysis model was developed by DPS (v.8.01) software.

3. Results and Discussion

3.1. One-Way Analysis of Variance. 1-Methylcyclopropene (1-MCP) has been proved to slow down the ripening of some fruits [21, 22]. In this work, the decay rate of blackberry fruit was reduced significantly ($P < 0.05$) by 1-MCP treatment (Table 1). The antioxidant enzymes, polyphenol oxidase (PPO), in 1-MCP treated fruit were also higher than control. On the other hand, a higher firmness was observed with vacuum precooling compared to control after 38 days of storage. The PPO activities were also enhanced by vacuum precooling after storage at 0°C for 38 days. Our finding suggested that both 1-MCP and vacuum precooling treatment had a potential value in delaying the senescence of blackberries.

Table 1: Changes of quality and reactive oxygen metabolism indexes in blackberries during postharvest storage with different treatments.

	Days of storage						
		Control		1-MCP		Vacuum precooling	
	Harvest	21 d	38 d	21 d	38 d	21 d	38 d
Firmness	21.38^{d}	12.33^{b}	6.09^{a}	15.00^{bc}	5.84^{a}	17.76^{bcd}	18.31^{cd}
Decay rate (%)	0.00^{a}	0.00^{a}	21.67^{c}	0.00^{a}	11.67^{b}	0.00^{a}	18.34^{c}
H_2O_2 (mg/100 g fw)	6.28^{a}	16.76^{b}	23.52^{d}	18.92^{c}	31.76^{f}	16.99^{b}	26.22^{e}
GSH (mg/100 g fw)	61.55^{d}	65.89^{e}	26.62^{a}	80.80^{f}	39.43^{c}	97.02^{g}	35.22^{b}
APX (U/g fw)	0.02^{a}	0.03^{a}	0.09^{c}	0.05^{ab}	0.08^{bc}	0.02^{a}	0.04^{a}
POD (U/g fw)	105.71^{b}	5.58^{a}	1.32^{a}	5.41^{a}	4.17^{a}	5.09^{a}	4.96^{a}
PPO (U/g fw)	1.54^{f}	0.75^{b}	0.59^{a}	0.92^{c}	0.91^{c}	1.2^{e}	1.1^{d}
FRAP (U/g fw)	45.43^{e}	30.04^{b}	36.30^{c}	28.03^{a}	42.50^{d}	36.86^{c}	48.96^{f}
TEAC (U/g fw)	0.2232^{b}	0.1980^{a}	0.2172^{b}	0.2609^{c}	0.3192^{f}	0.2937^{e}	0.2824^{d}
DPPH (U/g fw)	31.74^{c}	30.51^{a}	31.24^{b}	31.73^{c}	38.30^{e}	31.22^{b}	36.61^{d}
NBT (U/g fw)	7.80^{a}	33.18^{e}	26.18^{c}	35.69^{f}	24.25^{b}	36.96^{g}	30.77^{d}
Hydroxyl radical-scavenging activity (U/g fw)	42.51^{f}	38.17^{a}	40.75^{e}	38.90^{b}	39.33^{c}	39.97^{d}	38.05^{a}
Total phenol (μg/g)	6.15^{a}	8.43^{c}	7.68^{b}	9.02^{d}	9.43^{f}	9.18^{e}	9.37^{f}
Total flavonoid (μg/g)	9.93^{f}	8.15^{b}	7.28^{a}	9.18^{d}	9.37^{e}	8.57^{c}	9.01^{d}

The different superscript letters in the same row indicated significant difference ($P < 0.05$).

The antioxidant activities can be characterized by TEAC, DPPH, FARP, and NBT radical-scavenging activities. Compared with vacuum precooling, at the end of storage, 1-MCP treated fruit had higher TEAC and DPPH radical-scavenging activities but lower FARP and NBT radical-scavenging activities. So, it was difficult to compare the effect between 1-MCP and vacuum precooling. For this reason, the PCA model was performed.

3.2. Principal Component Analysis. The parameters in Table 1 were used to develop the PCA model. The first three PCs explained 89% of the variance in the data, which was high enough to represent all the variables. The score plot for PC1 versus PC2 (Figure 1(a)) clearly distinguished three groups defined by length of storage, indicating that storage time had a major influence on the quality and reactive oxygen metabolism parameters of blackberry fruit.

Following PC3, the 1-MCP treated fruit and the vacuum precooled fruit were discriminated (Figure 1(b)). The loading plot of the variables showed that the TEAC and DPPH radical-scavenging activities had a heavy load on the positive coordinate of PC3. So, PC3 could be defined by antioxidant activities. The vacuum precooled fruit had higher positive scores for PC3 than 1-MCP treated fruit. These results suggested that precooled fruit might have values larger than the mean of the antioxidant activities, while 1-MCP treated fruit had relatively lower values.

3.3. Partial Least Squares. H_2O_2 as signal molecule plays an important role inside plant bodies [23]. From the PCA study (Figure 1(a)), H_2O_2 content had a heavy load on the negative coordinate of PC1, suggesting that H_2O_2 content was the most important variable of blackberry fruit. We chose H_2O_2 content as X variable and the other parameters as Y variable to develop the PLS model to obtain a closer understanding of the relation between them. 64% of X variables explained 88% of the variability of Y variables. Many studies have showed that the production of H_2O_2 increased when plants were exposed to various biotic and abiotic stresses [23]. Peroxidase (POD) can decompose H_2O_2 by oxidation of cosubstrates, such as phenolic compounds and antioxidants [24], which could explain why a strongly negative correlation between POD activity and H_2O_2 content was found in the present study (Figure 2). It also showed that TEAC, FRAP, and NBT radical-scavenging activities slightly correlated with H_2O_2 (Figure 2), which indicated that they had little influence on H_2O_2 content.

Table 2: The result of path analysis taking H_2O_2 as dependent variable.

	GSH	APX	POD	DPPH	Total flavonoid
Direct	0.0441	0.2559	−0.4243	0.6499	−0.1618
→GSH		−0.0307	0.0037	−0.0231	0.0101
→APX	−0.178		−0.116	0.0959	−0.1044
→POD	−0.0359	0.1923		0.0792	−0.2541
→DPPH	−0.3397	0.2436	−0.1213		0.2654
→Total flavonoid	−0.0371	0.066	−0.0969	−0.0661	

3.4. Path Analysis. The direct effect of physiological parameters on H_2O_2 content was analyzed by PLS model. To find the indirect factors, the path analysis model was developed. As shown in Table 2, the indirect path coefficient of GSH based on DPPH was −0.3397, which suggested that GSH was also a factor affecting H_2O_2 content.

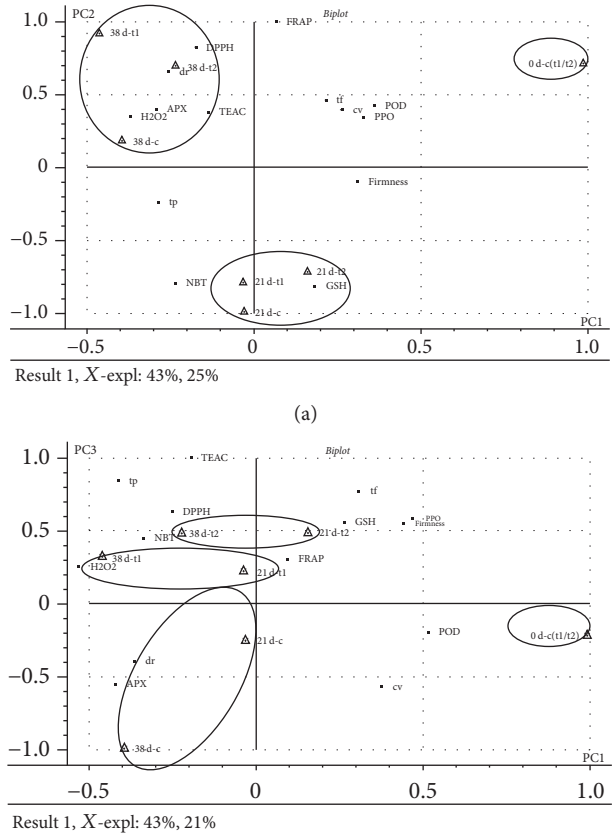

Figure 1: Loadings and scores from PCA of blackberries. "c": the control group; "t1": treatment of 1-MCP; "t2": treatment of vacuum precooling; "dr": decay rate; "cv": hydroxyl radical-scavenging activity; "tp": total phenol; "tf": total flavonoids.

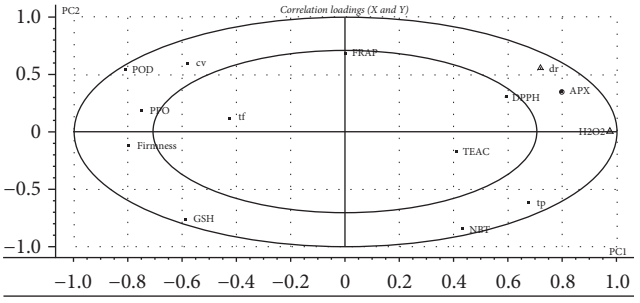

Figure 2: Correlation loading plot from a PLSR model. The inner and outer ellipses represent 50% and 100% of explained variance, respectively. "dr": decay rate; "cv": hydroxyl radical-scavenging activity; "tp": total phenol; "tf": total flavonoids.

4. Conclusion

Based on the results of PCA, vacuum precooling treatment could play a stronger role in keeping the antioxidant activities of blackberry fruit than did the 1-MCP treatment. The score of PCA also revealed that H_2O_2 was the most important variable of blackberry fruit. Results from partial least squares regression and path analysis showed that POD activity had a direct effect and GSH content had an indirect effect on H_2O_2 content, while TEAC, FRAP, and NBT radical-scavenging activities had little effect on H_2O_2 content.

Conflicts of Interest

The authors declare that there are no conflicts of interest regarding the publication of this article.

Acknowledgments

This research was supported by the National Natural Science Foundation of China (31471626), the National Science & Technology Support Program of China (2015BAD16B06), and the Importation and Development of High-Caliber Talents Project of Beijing Municipal Institutions (CIT&TCD201504008).

References

[1] J. Gudej and M. Tomczyk, "Determination of flavonoids, tannins and ellagic acid in leaves from *Rubus*L. species," *Archives of Pharmacal Research*, vol. 27, no. 11, pp. 1114–1119, 2004.

[2] S. Y. Wang and H. Lin, "Antioxidant activity in fruits and leaves of blackberry, raspberry, and strawberry varies with cultivar and developmental stage," *Journal of Agricultural and Food Chemistry*, vol. 48, no. 2, pp. 140–146, 2000.

[3] I. Koca and B. Karadeniz, "Antioxidant properties of blackberry and blueberry fruits grown in the black sea region of Turkey," *Scientia Horticulturae*, vol. 121, no. 4, pp. 447–450, 2009.

[4] M. Joo, N. Lewandowski, R. Auras, J. Harte, and E. Almenar, "Comparative shelf life study of blackberry fruit in bio-based and petroleum-based containers under retail storage conditions," *Food Chemistry*, vol. 126, no. 4, pp. 1734–1740, 2011.

[5] G. A. Manganaris, I. F. Ilias, M. Vasilakakis, and I. Mignani, "The effect of hydrocooling on ripening related quality attributes and cell wall physicochemical properties of sweet cherry fruit (Prunus avium L.)," *International Journal of Refrigeration*, vol. 30, no. 8, pp. 1386–1392, 2007.

[6] G. Cheng, X. Duan, J. Shi et al., "Effects of reactive oxygen species on cellular wall disassembly of banana fruit during ripening," *Food Chemistry*, vol. 109, no. 2, pp. 319–324, 2008.

[7] Y. Imahori, M. Takemura, and J. Bai, "Chilling-induced oxidative stress and antioxidant responses in mume (Prunus mume) fruit during low temperature storage," *Postharvest Biology and Technology*, vol. 49, no. 1, pp. 54–60, 2008.

[8] D. Inzé and M. V. Montagu, "Oxidative stress in plants," *Current Opinion in Biotechnology*, vol. 6, no. 2, pp. 153–158, 1995.

[9] U. Imeh and S. Khokhar, "Distribution of conjugated and free phenols in fruits: antioxidant activity and cultivar variations," *Journal of Agricultural and Food Chemistry*, vol. 50, no. 22, pp. 6301–6306, 2002.

[10] Y. Y. Voon, N. Sheikh Abdul Hamid, G. Rusul, A. Osman, and S. Y. Quek, "Volatile flavour compounds and sensory properties of minimally processed durian (Durio zibethinus cv. D24) fruit during storage at 4∘C," *Postharvest Biology and Technology*, vol. 46, no. 1, pp. 76–85, 2007.

[11] H. Zheng and H. Lu, "Use of kinetic, Weibull and PLSR models to predict the retention of ascorbic acid, total phenols and antioxidant activity during storage of pasteurized pineapple juice," *LWT- Food Science and Technology*, vol. 44, no. 5, pp. 1273–1281, 2011.

[12] A. Jiménez, J. A. Hernández, L. A. del Río, and F. Sevilla, "Evidence for the presence of the ascorbate-glutathione cycle in mitochondria and peroxisomes of pea leaves," *Plant Physiology*, vol. 114, no. 1, pp. 275–284, 1997.

[13] A. Jiang, S. P. Tian, and Y. Xu, "Effects of controlled atmospheres with high-O2 or high CO2 concentrations on postharvest physiology and storability of "Napoleon" sweet cherry," *Acta Botanica Sinica*, vol. 44, pp. 925–930, 2002.

[14] A. Guri, "Variation in glutathione and ascorbic acid content among selected cultivars of phaseolus vulgaris prior to and afer exposure to ozone," *Canadian Journal of Plant Science*, vol. 63, no. 3, pp. 733–737, 1983.

[15] T. Brennan and C. Frenkel, "Involvement of Hydrogen Peroxide in the Regulation of Senescence in Pear," *Plant Physiology*, vol. 59, no. 3, pp. 411–416, 1977.

[16] I. F. F. Benzie and J. J. Strain, "The ferric reducing ability of plasma (FRAP) as a measure of "antioxidant power": the FRAP assay," *Analytical Biochemistry*, vol. 239, no. 1, pp. 70–76, 1996.

[17] M. J. T. J. Arts, J. S. Dallinga, H.-P. Voss, G. R. M. M. Haenen, and A. Bast, "A critical appraisal of the use of the antioxidant capacity (TEAC) assay in defining optimal antioxidant structures," *Food Chemistry*, vol. 80, no. 3, pp. 409–414, 2003.

[18] M.-Y. Shon, T.-H. Kim, and N.-J. Sung, "Antioxidants and free radical scavenging activity of *Phellinus baumii* (Phellinus of Hymenochaetaceae) extracts," *Food Chemistry*, vol. 82, no. 4, pp. 593–597, 2003.

[19] C. Larrigaudière, A. P. Candan, D. Ubach, and J. Graell, "Physiological response of "Larry Ann" plums to cold storage and 1-MCP treatment," *Postharvest Biology and Technology*, vol. 51, no. 1, pp. 56–61, 2009.

[20] F. Bamdad, M. Kadivar, and J. Keramat, "Evaluation of phenolic content and antioxidant activity of Iranian caraway in comparison with clove and BHT using model systems and vegetable oil," *International Journal of Food Science & Technology*, vol. 41, no. 1, pp. 20–27, 2006.

[21] R. A. Spotts, P. L. Sholberg, P. Randall, M. Serdani, and P. M. Chen, "Effects of 1-MCP and hexanal on decay of d'Anjou pear fruit in long-term cold storage," *Postharvest Biology and Technology*, vol. 44, no. 2, pp. 101–106, 2007.

[22] R. Zhou, Y. Li, L. Yan, and J. Xie, "Effect of edible coatings on enzymes, cell-membrane integrity, and cell-wall constituents in relation to brittleness and firmness of Huanghua pears (*Pyrus pyrifolia* Nakai, cv. Huanghua) during storage," *Food Chemistry*, vol. 124, no. 2, pp. 569–575, 2011.

[23] S. Navabpour, K. Morris, R. Allen, E. Harrison, S. A-H-Mackerness, and V. Buchanan-Wollaston, "Expression of senescence-enhanced genes in response to oxidative stress," *Journal of Experimental Botany*, vol. 54, no. 391, pp. 2285–2292, 2003.

[24] Y. F. Xue and Z. P. Liu, "Antioxidant enzymes and physiological characteristics in two Jerusalem artichoke cultivars under salt stress," *Russian Journal of Plant Physiology*, vol. 55, no. 6, pp. 776–781, 2008.

Hindawi
International Journal of Analytical Chemistry
Volume 2018, Article ID 1273907, 8 pages
https://doi.org/10.1155/2018/1273907

Research Article

The Effects of Storage Conditions on Lycopene Content and Color of Tomato Hot Pot Sauce

He Li,[1] **Jian Zhang**,[1] **Yong Wang**,[2] **Jian Li**,[1] **Yihe Yang**,[2] **and Xinqi Liu**[1]

[1]*Beijing Advanced Innovation Center for Food Nutrition and Human Health, Beijing Technology & Business University, Beijing 100048, China*
[2]*Nutrition & Health Research Institute, COFCO Corporation, Beijing Key Laboratory of Nutrition & Health and Food Safety, Beijing 102209, China*

Correspondence should be addressed to Yong Wang; wang-yong@cofco.com and Xinqi Liu; liuxinqi@btbu.edu.cn

Received 29 September 2017; Accepted 26 December 2017; Published 31 January 2018

Academic Editor: Ying Yang

Tomato hot pot sauce (THPS) at different storage temperatures (0, 25, and 37°C) and with two kinds of packaging for 120 days was investigated in this study. High performance liquid chromatography was employed for detecting lycopene and 5-hydroxymethylfurfural (HMF). The changes of lycopene and HMF during storage were regressed with kinetic equation of both zero-order and first-order models, and the latter fitted better. The kinetic equation constant (k value) of lycopene or HMF at 37°C was higher than that at 25°C. The k value of lycopene of PET/PE (P1) packaged THPS was 1.60 times of that of PET/Al/EAA/PE (P2) packaged at 37°C, while it was 2.12 times at 25°C. The k value of HMF of P1 packaged THPS was 1.69 times of that of P2 packaged at 37°C, while it was 1.01 times at 25°C. Significant correlations between color index of L^*, a^*, and a^*/b^* and lycopene or HMF were found at storage temperature. Browning color was attributed to both Maillard reaction and degradation of lycopene. In conclusion, lower storage temperature and stronger oxygen barrier property of package could maintain color stability and extend shelf life.

1. Introduction

Hot pot is one of the most popular Chinese foods in China and has spread all over the world since it is very easy to keep its authentic taste. The core of hot pot taste is the hot pot sauce, which is used to prepare the base soup of hot pot. In the last decade, hot pot sauce has been upgraded from handmade in small kitchen to industrialized central kitchens which are equipped with large sauce cooking bowl up to 1000 kg/batch. This upgrade not only benefits the hot pot restaurants to uniform the recipe and increase the kitchen efficiency, but also provides consumers with alternative choice to cook top-taste hot pot in their own home. Tomato hot pot sauce (THPS) is made from tomato paste, soybean oil, tomato, onion, ginger, and other seasonings and could be classified as vegetable-based semisolid seasoning. Because of its unique soup color, sour taste, and nutritional value, THPS is growing popular among consumers. The sales of THPS also increase rapidly in supermarkets and wholesale market place; thus it becomes a favored product category by food companies and chain restaurant with central kitchen. But the long time storage on shelf (usually 6–12 months) could lead to unfavorable quality changes such as nutrients degradation or browning color, which might be taken as unsuitable for consumption [1].

There are many studies on the color changes of tomato paste [1], tomato juice [2], tomato powder [3], and tomato sauce [4] during processing and storage. But the color change of THPS during processing and storage remains unclear, and the mechanism behind the color change needs further investigation. Maillard reaction and the ascorbic acid oxidation might be two reasons that contribute to the color change of tomato product during the long-term storage [3]. Lycopene is not only an important characteristic component, but also the major coloring ingredient of tomato and tomato products. Thus lycopene has been a hot topic among the researches on the color changes of tomato products [5], although the changes of amino acid content or reducing sugar are also related to the quality change in storage.

In this study, the quality of THPS was investigated to explore the mechanism of color change during storage. The contents changes of lycopene and 5-hydroxymethylfurfural (HMF) were tracked under different packaging and storage conditions. It is helpful to guide the optimization of packaging and storage conditions of THPS, so as to improve the shelf life of the products and meet the market demand.

2. Materials and Methods

2.1. Chemicals. Standard lycopene and 5-hydroxymethylfurfural (HMF) were purchased from Sigma-Aldrich Chemical Co. (United States). Ethanol and acetonitrile of HPLC grade were purchased from Fluka Chemical Co. (Germany). Pyrogallic acid, potassium ferrocyanide, zinc sulphate, and other reagents were of analytical grade.

2.2. Tomato Hot Pot Sauce and Preparation. Tomato paste (cold break) was purchased from COFCO Tunhe Co., Ltd. (China). Other food materials were purchased from local market.

The THPS was prepared according to the following procedures. Firstly, the samples were weighed and waited for further cooking, including tomato paste (cold break, 28.5 Brix°) 40%, soybean oil 25%, sucrose 14%, fresh onion 10%, pickle ginger 4%, chicken essence 3%, salt 2.5%, soy sauce 1%, citric acid 0.25%, and dry spice mixture (cinnamon, amomum tsao-ko, clove, aniseed, fennel, white cardamom, bay leaf, dried orange peel, and Chinese red pepper, with equal weight) 0.25%. Secondly, as shown in Figure 1, the soybean oil was heated up to 160°C, followed by adding compound spice, pickle ginger, and onion and stirring for 3 min. Thirdly, the tomato paste was added and the sample was kept at the intermittent boiling state for 20 min by gentle heat. Fourthly, sucrose, citric acid, and salt were added and stirred for 6 min. Fifthly, soy sauce was added together with chicken essence with one-minute stirring. Finally the samples were cooled down to 80°C and packaged into 200 g per bag.

Storage Conditions. There were packaging P1 (polyethylene terephthalate/polyethylene), with oxygen permeability 60.00 $cm^3/(m^2 \cdot 24\,h \cdot 0.1\,MPa)$, and packaging P2 (polyethylene terephthalate/aluminum/ethylene acrylic acid copolymer/polyethylene), with oxygen permeability 0.23 $cm^3/(m^2 \cdot 24\,h \cdot 0.1\,MPa)$. The storage temperature was 0°C, 25°C, or 37°C, respectively, and they were stored for 0, 30, 60, 90, or 120 days.

2.3. Color Analyses. The color of THPS was measured using a colorimeter of Labscan XE (HunterLab, Hunter Associates Laboratory Inc., United States). A whole package of THPS 200 g was transferred into a beaker. After mixed for 2 minutes at 3000 r/min by a blender, the samples were placed in Petri dishes and filled to the top. Color was recorded as L^* (lightness), a^* (green-red tonality), and b^* (blue-yellow tonality). The Hue value (a^*/b^*) was calculated based on measured, a^* and b^*, values [1].

2.4. Lycopene Analysis. Briefly, a whole package of THPS 200 g was transferred into a beaker. After mixed for 2 minutes at 3000 r/min by a blender, 2.000 g THPS was weighed in a 250 mL flask and wrapped with aluminum foil to prevent exposure to light. The procedure of extraction and HPLC detection was in accordance with previous study [6]. 50 mL of solvent (50 : 25 : 25 hexane/acetone/ethanol containing 2.5% pyrogallic acid) was added with nitrogen protection. After shaken for 10 min, 10 mL of distilled water was added for a further shaking. The hexane phase was filtered through a 0.2 μm nylon filter. One injection volume of filtrate 10 μL was injected into a liquid chromatography equipped with diode array detector (LC-Prominence-20AT and SPD-M20A, Shimadzu Co., Japan). An analytical column C_{18} (Shim–pack VP-ODS 15 cm × 4.6 mm ID, 5 μm) was employed and kept at 30°C. An isocratic elution of mobile phase with 50 : 50 methanol/acetonitrile was delivered at a flow rate 1 mL/min. Lycopene was detected at 472 nm, and its calibration curves ($R^2 = 0.984$) had previously been established by the standard lycopene. The limit of detection was 2.6×10^{-6} μg/mL, the recovery rate was 92%, and coefficient of variation was 3.44%. The peaks and areas were calculated with LC solution software.

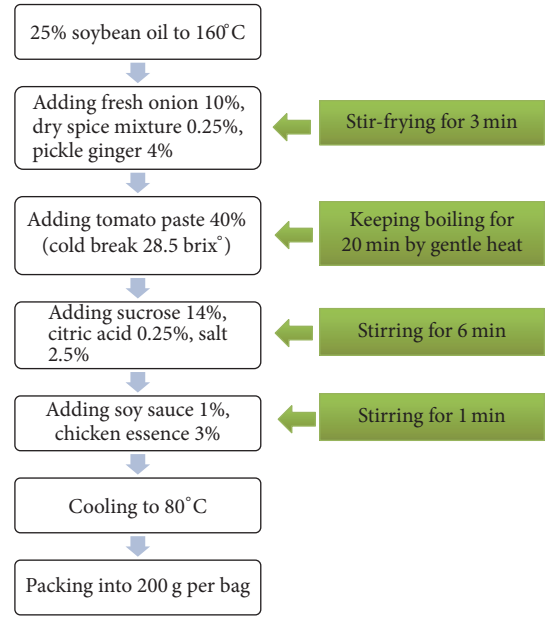

Figure 1: Tomato hot pot sauce making procedures.

2.5. 5-Hydroxymethylfurfural Analysis. After homogenization of the sample, 5-hydroxymethylfurfural concentration was determined by HPLC [6, 7]. 5.000 g of THPS was placed in a 50 mL centrifuge tube, and 2 mL of 15% (w/v) potassium ferrocyanide and 2 mL of 30% (w/v) zinc sulphate were added with slow stirring and the volume made up with distilled water. After standing for 30 min, the mixture was centrifuged for 1 h at 12,000 r/min. Then 2 mL supernatant was filtered through a 0.2 μm cellulose acetate filter. HPLC apparatus, column, injection volume of sample, and software of chromatograms analysis were the same as lycopene employed in the above part. The column was kept in a stabilizer at 40°C, and an isocratic elution of mobile phase with 90 : 10

water/methanol was delivered at a flow rate 1 mL/min. HMF was detected at 285 nm, and its calibration curves ($R^2 = 0.992$) had previously been established by the standard HMF. The limit of detection was 1.9×10^{-4} μg/mL, the recovery rate was 91%, and coefficient of variation was 4.22%.

2.6. Ascorbic Acid Analysis. Ascorbic acid concentration was determined by HPLC [8].

2.7. Statistical Analysis. All experiments were performed in triplicate. Statistical analyses were performed with SPSS 11.5. The results were expressed as the means ± standard deviation (SD) of triplicate. The data were subjected to one-way analysis of variance (ANOVA) and the significance of difference between samples means was calculated by Duncans' multiple range test. $P < 0.05$ indicates the significant difference. Pearson correlation test was used to analyze the correlation between lycopene, HMF, and color index.

The reaction model of the relationship between the content change and the time was analyzed by the zero-order equation [9, 10] (1) or the first-order equation [11–14] (2), and the correlation coefficient R^2.

$$y = C - kt \quad (1)$$

$$y = C * \exp(-kt), \quad (2)$$

where "y" is the dependent variable of lycopene, HMF, or color index; "t" is the time; "k" is the kinetic equation constant; and "C" is the starting value.

3. Results and Discussion

3.1. Changes of Lycopene Content. Lycopene is an important characteristic nutrient substance in tomato, and it is also the main coloring material of tomato. Thus it is of practical significance to study the changes of lycopene content during storage period. As shown in Figure 2, the content of lycopene did not change significantly during the storage of the two types of packaging (P1 and P2) under the storage conditions of 0°C ($P > 0.05$). At 25°C and 37°C, the contents of lycopene in the two types of packaging (P1 and P2) decreased with the prolongation of storage. After storage for 30 days, the content of lycopene at 37°C was significantly lower than that of the same packaging at 25°C ($P < 0.05$). Tamburini et al. [15] found that there was no change in lycopene content of tomato purée during one year's storage. A similar result was found, and no change was observed in lycopene content of tomato ketchup during 8 months of storage at 30°C [6]. The stability of lycopene might be attributed to the thermal inactivation of enzymes that might expose lycopene to oxidants by destroying the cell wall.

In this study, the moisture content of THPS was low and the oil content was close to 20%. During the high temperature frying process, the tomato lycopene was dissolved from the cell wall and transferred to the oil and exposed to the oxidizing environment. During the storage period it could further extend the lycopene degradation [16–18]. Oxygen permeability rate of P2 packaging was much lower than that

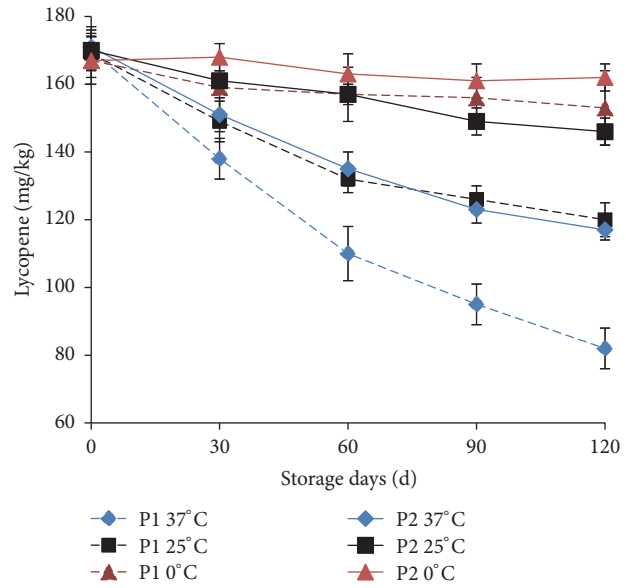

Figure 2: Changes of lycopene in THPS during storage. The experiments were performed in triplicate, and results were expressed as the means ± standard deviation (SD).

of P1, thus reducing the lycopene oxidation loss. As shown in Figure 2, the content of lycopene in the P2 packaged THPS was significantly higher than that of the same storage time in P1 packaged sample ($P < 0.05$) at 25°C or 37°C for 30 days.

The fitting results of the zero-order kinetic model and the first-order kinetic model were shown in Table 1. The lycopene loss rate of the two types of packaged THPS under the conditions of 25 and 37°C storage was well fitted with the zero-order kinetic and the first-order kinetic model equation, where R^2 of the first-order equation was higher than that of the zero-order equation. The relationship between lycopene and the time-dependent change in THPS was more consistent with the first-order kinetic model equation. The degradation of free lycopene and encapsulated lycopene in the storage model system also showed that lycopene degradation was accorded with the first-order kinetic model, and the kinetic constants increased with raising storage temperature [12]. It has also been reported that the degradation of free lycopene content was at a lower rate in oil media comparing with water media [13].

As shown in Table 1, k value of first-order kinetic model at 37°C was 1.86 times of the k value at 25°C for P1 packaged THPS, while it was 2.46 times for P2 packaged THPS. Because of the lower oxygen permeability, packaging P2 showed a greater effect on suppressing degradation of lycopene than packaging P1. When THPS was stored at 37°C or 25°C, the k value of P1 packaged THPS was 1.60 or 2.12 times of the k value of P2 packaged THPS, respectively. It could be seen that the storage temperature and the oxygen permeability of the packaging had great influence on the degradation of lycopene in THPS.

3.2. Changes of HMF Content. HMF is a product of the Maillard reaction at early stage, and the HMF content can be

Table 1: Kinetic equation of lycopene in THPS during storage.

Storage temperature	Packaging		Kinetic equation	Correlation coefficient R^2
37°C	P1	First-order	$y_1 = 166\exp(-0.00512t)$	0.956
		Zero-order	$y_1 = -0.729t + 163$	0.936
	P2	First-order	$y_1 = 167\exp(-0.00320t)$	0.942
		Zero-order	$y_1 = -0.453t + 167$	0.926
25°C	P1	First-order	$y_1 = 164\exp(-0.00276t)$	0.900
		Zero-order	$y_1 = -0.463t + 164$	0.885
	P2	First-order	$y_1 = 169\exp(-0.00130t)$	0.862
		Zero-order	$y_1 = -0.199t + 169$	0.859

Note. "y_1" is the dependent variable of lycopene (mg/kg); "t" is storage time (day).

Table 2: Kinetic equation of HMF in THPS during storage.

Storage temperature	Packaging		Kinetic equation	Correlation coefficient R^2
37°C	P1	First-order	$y_2 = 7.66\exp(0.00741t)$	0.962
		Zero-order	$y_2 = 0.0957t + 6.88$	0.908
	P2	First-order	$y_2 = 7.72\exp(0.00438t)$	0.939
		Zero-order	$y_2 = 0.0455t + 7.50$	0.914
25°C	P1	First-order	$y_2 = 7.74\exp(0.00359t)$	0.938
		Zero-order	$y_2 = 0.0359t + 7.57$	0.902
	P2	First-order	$y_2 = 7.55\exp(0.00354t)$	0.867
		Zero-order	$y_2 = 0.0346t + 7.38$	0.846

Note. "y_2" is the dependent variable of HMF (mg/kg); "t" is storage time (day).

used as a measure of the extent of the Maillard reaction [19]. HMF is promoted to produce brown nitrogen-containing polymers, making the product color deterioration for a longer storage time. As shown in Figure 3, the content of HMF in the THPS of P1 and P2 package was not significantly changed ($P > 0.05$) at 0°C within the storage period. At 25°C and 37°C, the contents of HMF in the THPS of P1 and P2 package increased with the storage time.

Storage temperature was an important factor in affecting the reaction speed of Maillard reaction. The HMF content of THPS with P1 package was significantly higher if stored at 37°C than that stored at 25°C, when both samples were stored for more than 30 days. The same rule of HMF content of THPS with P2 package was found, when samples were stored for more than 60 days. Packaging could affect the amount of HMF in THPS during whole storage period. But in this study, it was found that the HMF content in THPS was significantly different ($P < 0.05$) between P1 package and P2 package, when THPS was stored at a high temperature (37°C) and more than 60 days.

The fitting results of HMF content and storage time by using zero-order kinetic model and first-order kinetic model were shown in Table 2. The results showed that the growth of HMF content was in accordance with the zero-order kinetics and the first-order kinetic model equation. And the coefficient of determination (R^2) of first-order kinetic equation was higher than that of the zero-order kinetic model at 25°C and 37°C storage. Thus the first-order kinetic model equation was used to analyze the relationship between the content of HMF in THPS and storage time. Similarly, in a kheer mix powder storage model, the formation of HMF followed a first-order reaction at 37 or 45°C also and showed a good correlation [14].

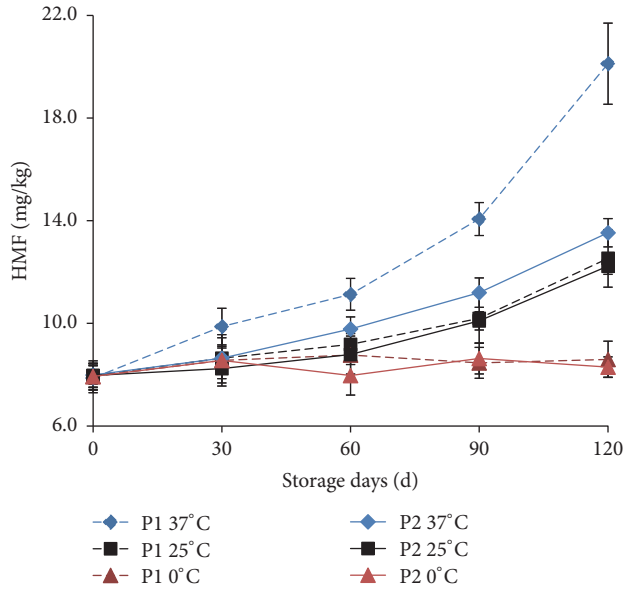

Figure 3: Changes of HMF in THPS during storage. The experiments were performed in triplicate, and results were expressed as the means ± standard deviation (SD).

As shown in Table 2, the kinetic equation constant (k value) of HMF at 37°C was higher than that at 25°C. The k

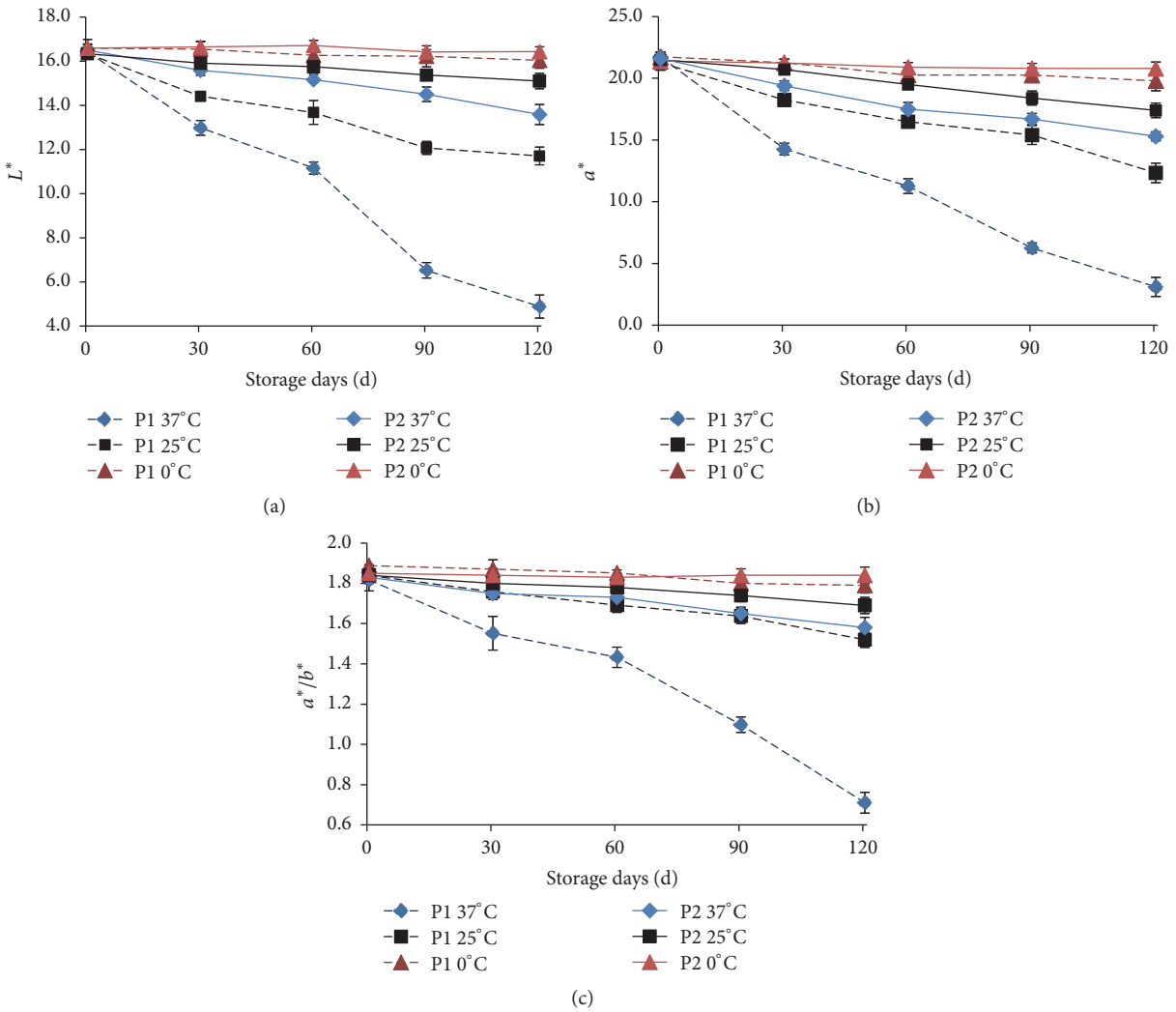

Figure 4: Changes of L^* (a), a^* (b), a^*/b^* (c) in THPS during storage. The experiments were performed in triplicate, and results were expressed as the means ± standard deviation (SD).

value of HMF of P1 packaged THPS was 1.69 times of that by P2 packaged at 37°C, while it was 1.01 times at 25°C. It could be seen that there was no significant difference in the content of HMF in P1 and P2 package at 25°C ($P > 0.05$). But when the storage temperature was high (37°C), the P2 package was better than P1 package to inhibit the increase of HMF content.

3.3. Changes of Ascorbic Acid Contents. Ascorbic acid oxidation can also cause nonenzymatic browning. During storage, the ascorbic acid oxidation degradation is often dependent on the processing method and the storage conditions. Ascorbic acid degradation followed first-order kinetic equation in strawberry jam during storage, and the rate constant (k) increased with an increase in the temperature [20]. As the TPHS is usually subjected to a long period of boiling, ascorbic acid oxidation degradation is promoted and will cause the sample color to become brown. The content of ascorbic acid before storage was less than 1.0 mg/kg, and there was no significant change at 0, 25, and 37°C during storage ($P > 0.05$). It showed that the ascorbic acid was almost all destroyed during the thermal processing.

3.4. Changes of Color Index. The change in color can be used to evaluate the shelf life of the THPS, which is one of the most important indicators of the THPS quality or other tomato products [21, 22]. In order to highlight the change of the redness of THPS, the color constant a^*/b^* value is introduced to better evaluate the color [1]. Both a^*/b^* value and a^* value are used as an important index of international trade in tomato products. The higher the L^*, a^*, and a^*/b^* value of the tomato products, the more acceptable the color [3, 6]. In Figures 4(a), 4(b), and 4(c), it could be seen that there was no significant difference in L^*, a^*, a^*/b^* between P1 and P2 at 0°C ($P > 0.05$). At 25°C or 37°C, the values of L^*, a^*, or a^*/b^* in the TPHS were decreased with the storage time prolonged. This was consistent with the decrease of lycopene content and the increase of HMF content.

Table 3: Correlation analysis of L^*, a^*, a^*/b^* with lycopene and HMF in THPS during storage.

Color index	Packaging	Storage temperature	Pearson correlation coefficient (r)	
			Lycopene	HMF
L^*	P1	37°C	0.963**	−0.934*
		25°C	0.976**	−0.881*
	P2	37°C	0.967**	−0.967**
		25°C	0.995**	−0.926*
a^*	P1	37°C	0.992**	−0.916*
		25°C	0.962**	−0.951*
	P2	37°C	0.994**	−0.931*
		25°C	0.981**	−0.942*
a^*/b^*	P1	37°C	0.929*	−0.988**
		25°C	0.943*	−0.974**
	P2	37°C	0.958*	−0.975**
		25°C	0.974**	−0.966**

Note. ∗∗ indicates an extremely significant correlation with $P < 0.01$; ∗ indicates a significant correlation with $P < 0.05$.

When the THPS in P1 package was stored at 37°C after 30 days, the L^* value was significantly lower than that at 25°C ($P < 0.05$). But a significantly different L^* value of P2 package at 37°C and 25°C was found after 60 days of storage ($P < 0.05$). It was also found that the L^* value of the P2 packaged TPHS at 37°C was still higher than the L^* value of the same storage period at 25°C with P1 package (Figure 4(a)). When the THPS in P1 package or P2 package was stored at 37°C for more than 30 days, the a^* value was significantly lower than that at 25°C ($P < 0.05$). The values of a^* of P2 package THPS storage at 37°C were significantly higher than those of the P1 packaged THPS at 25°C (Figure 4(b)). The value of a^*/b^* of P1 packaged THPS storage at 37°C after 30 days was significantly lower ($P < 0.05$) than that at 25°C. But a significantly different a^*/b^* value of P2 package at 37°C and 25°C was found after 60 days of storage ($P < 0.05$). There was no significant difference in the a^*/b^* value between THPS stored at 37°C in P2 package and at 25°C in P1 package for 60 or 90 days ($P > 0.05$). When the THPS was stored for 120 days, it was found that the a^*/b^* value of the P2 packaged TPHS stored at 37°C was significantly higher ($P < 0.05$) than that of the P1 packaged TPHS stored at 25°C (Figure 4(c)). As a result, the P2 package reduced the deterioration of the color index compared to the P1 package. Even if the storage temperature rose to 37°C, the color index of P2 sample has equal degree of reduction to the P1 sample at 25°C.

HMF content can reflect the browning of processed fruit and vegetable products during storage, thus affecting the L^*, a^*, and a^*/b^* of the THPS. As shown in Table 3, the Pearson correlation coefficients of HMF and L^*, a^*, a^*/b^* were significantly negatively correlated ($r = -0.881 \sim -0.988$) under different storage temperatures and packaging types. Thus the loss of L^*, a^*, and a^*/b^* was mainly caused by Millard reaction, which is consistent with the changes HMF presented above [3]. The degradation of lycopene mainly produces ketones, aldehydes, alcohols, furan, olefins, aromatics, and a small amount of acids and esters [23]. There was a significant positive correlation (indicated by Pearson correlation coefficient) between lycopene and L^*, a^*, a^*/b^* under different storage temperature and packaging ($r = 0.929$–0.995). Differently, it was not found that the change of lycopene was significant during 8-month storage in tomato ketchup [6] and 5-month storage in tomato powder [3]. The stability of lycopene might be attributed to the thermal inactivation of enzymes that might expose lycopene to oxidants by destroying the cell wall [24]. However, it is known that THPS is processed by high temperature soybean oil, and part of lycopene is extracted from cell wall and dissolved in oil. In this study, lycopene of THPS shows a poor stability unless placed in oxygen resistance packaging and kept in low temperature storage. Therefore, the HMF content which could be used as index of the Maillard reaction and the content of lycopene had significant effect on the color change of THPS during storage. During the storage period, the control of lycopene content decrease and the HMF content increase can effectively maintain the color of THPS.

4. Conclusions

When the storage temperature was 25°C and 37°C, the lycopene and color index (L^*, a^*, a^*/b^*) of the two kinds of packaged THPS were significantly decreased ($P < 0.05$), while the HMF content was increased ($P < 0.05$). The changes of the above parameters were not significant at 0°C ($P > 0.05$). The changes of lycopene and HMF during the storage of THPS can be fitted with the first-order equation. At 25°C and 37°C, the degradation of color index (L^*, a^*, a^*/b^*), the decrease of lycopene content, and the increase of HMF content all showed similar trends, indicated by Pearson correlation coefficient.

Low temperature and high oxygen resistance packaging can reduce the increase in HMF and lycopene reduction, slow down the storage process of browning, protect lycopene, and improve the color of THPS at the end of the storage

period. The L^*, a^*, a^*/b^* of oxygen resistance packaging is also approximately the same as or better than that of the composite film at 25°C. The effect of oxygen resistance packaging on extending shelf life can be more obvious than that of composite film if THPS is stored under unfavorable high temperature. 30 kinds of polyphenols in tomato [25], which may transfer into tomato paste and THPS, will play a role in inhibition of lycopene oxidation. The effects of antioxidant polyphenols on lycopene protection should be investigated in further studies. These pieces of information could be used to guide the processing and storage of THPS.

Conflicts of Interest

The authors declare that there are no conflicts of interest regarding the publication of this paper.

Acknowledgments

This study was supported by grants from National Natural Science Foundation of China (no. 31772038), Support Project of High-Level Teachers in Beijing Municipal Universities in the Period of 13th Five-Year Plan (CIT&TCD201704037), and National Key R&D Program of China (2016YFD0400400).

References

[1] M. Ganje, S. M. Jafari, A. Dusti, D. Dehnad, M. Amanjani, and V. Ghanbari, "Modeling quality changes in tomato paste containing microencapsulated olive leaf extract by accelerated shelf life testing," *Food and Bioproducts Processing*, vol. 97, pp. 12–19, 2016.

[2] K. G. L. R. Jayathunge, I. R. Grant, M. Linton, M. F. Patterson, and A. Koidis, "Impact of long-term storage at ambient temperatures on the total quality and stability of high-pressure processed tomato juice," *Innovative Food Science & Emerging Technologies*, vol. 32, pp. 1–8, 2015.

[3] F. Liu, X. Cao, H. Wang, and X. Liao, "Changes of tomato powder qualities during storage," *Powder Technology*, vol. 204, no. 1, pp. 159–166, 2010.

[4] A. Rajchl, M. Voldřich, H. Čížková et al., "Stability of nutritionally important compounds and shelf life prediction of tomato ketchup," *Journal of Food Engineering*, vol. 99, no. 4, pp. 465–470, 2010.

[5] M. Anese, F. Bot, A. Panozzo, G. Mirolo, and G. Lippe, "Effect of ultrasound treatment, oil addition and storage time on lycopene stability and in vitro bioaccessibility of tomato pulp," *Food Chemistry*, vol. 172, pp. 685–691, 2015.

[6] H. Li, X. Liu, L. Yang, D. Chen, and H. Cui, "The effects of adding soybean fiber on the quality of tomato ketchup," *Acta Horticulturae*, vol. 971, pp. 211–216, 2013.

[7] E. Korbel, E. H. Attal, J. Grabulos et al., "Impact of temperature and water activity on enzymatic and non-enzymatic reactions in reconstituted dried mango model system," *European Food Research and Technology*, vol. 237, no. 1, pp. 39–46, 2013.

[8] C. Chanforan, M. Loonis, N. Mora, C. Caris-Veyrat, and C. Dufour, "The impact of industrial processing on health-beneficial tomato microconstituents," *Food Chemistry*, vol. 134, no. 4, pp. 1786–1795, 2012.

[9] S. Wibowo, T. Grauwet, G. B. Gedefa, M. Hendrickx, and A. Van Loey, "Quality changes of pasteurised mango juice during storage. Part II: Kinetic modelling of the shelf-life markers," *Food Research International*, vol. 78, pp. 410–423, 2015.

[10] M. Dak, V. R. Sagar, and S. K. Jha, "Shelf-life and kinetics of quality change of dried pomegranate arils in flexible packaging," *Food Packaging and Shelf Life*, vol. 2, no. 1, pp. 1–6, 2014.

[11] Y. Chen and A. Martynenko, "Storage stability of cranberry puree products processed with hydrothermodynamic (HTD) technology," *LWT- Food Science and Technology*, vol. 79, pp. 543–553, 2017.

[12] C. F. Pu and W. T. Tang, "Encapsulation of lycopene in Chlorella pyrenoidosa: Loading properties and stability improvement," *Food Chemistry*, vol. 235, pp. 283–289, 2017.

[13] J. Chen, J. Shi, S. J. Xue, and Y. Ma, "Comparison of lycopene stability in water- and oil-based food model systems under thermal- and light-irradiation treatments," *LWT- Food Science and Technology*, vol. 42, no. 3, pp. 740–747, 2009.

[14] A. Jha and A. A. Patel, "Kinetics of HMF formation during storage of instant kheer mix powder and development of a shelf-life prediction model," *Journal of Food Processing and Preservation*, vol. 38, no. 1, pp. 125–135, 2014.

[15] R. Tamburini, L. Sandei, A. Aldini, F. Sio, and C. Leoni, "Effect of storage conditions on lycopene content in tomato purees obtained with different processing techniques," *Industria Conserve*, vol. 74, no. 4, pp. 341–357, 1999.

[16] E. Demiray, Y. Tulek, and Y. Yilmaz, "Degradation kinetics of lycopene, β-carotene and ascorbic acid in tomatoes during hot air drying," *LWT- Food Science and Technology*, vol. 50, no. 1, pp. 172–176, 2013.

[17] I. J. P. Colle, L. Lemmens, G. N. Tolesa et al., "Lycopene degradation and isomerization kinetics during thermal processing of an olive oil/tomato emulsion," *Journal of Agricultural and Food Chemistry*, vol. 58, no. 24, pp. 12784–12789, 2010.

[18] G. Knockaert, S. K. Pulissery, I. Colle, S. Van Buggenhout, M. Hendrickx, and A. V. Loey, "Lycopene degradation, isomerization and in vitro bioaccessibility in high pressure homogenized tomato puree containing oil: effect of additional thermal and high pressure processing," *Food Chemistry*, vol. 135, no. 3, pp. 1290–1297, 2012.

[19] M. G. Davoodi, P. Vijayanand, S. G. Kulkarni, and K. V. R. Ramana, "Effect of different pre-treatments and dehydration methods on quality characteristics and storage stability of tomato powder," *LWT - Food Science and Technology*, vol. 40, no. 10, pp. 1832–1840, 2007.

[20] A. Patras, N. P. Brunton, B. K. Tiwari, and F. Butler, "Stability and Degradation Kinetics of Bioactive Compounds and Colour in Strawberry Jam during Storage," *Food and Bioprocess Technology*, vol. 4, no. 7, pp. 1245–1252, 2011.

[21] M. N. Safdar, A. Mumtaz, M. Amjad, N. Siddiqui, and T. Hameed, "Development and quality characteristics studies of tomato paste stored at different temperatures," *Pakistan Journal of Nutrition*, vol. 9, no. 3, pp. 265–268, 2010.

[22] H. M. Velioğlu, S. H. Boyaci, and Ş. Kurultay, "Determination of visual quality of tomato paste using computerized inspection system and artificial neural networks," *Computers and Electronics in Agriculture*, vol. 77, no. 2, pp. 147–154, 2011.

[23] M. Uenojo, M. R. Marostica, and G. M. Pastore, "Carotenoids: Properties, applications and biotransformation in flavor compounds," *Quimica Nova*, vol. 30, no. 3, pp. 616–622, 2007.

[24] R. Tamburini, L. Sandei, A. Aldini, F. de Sio, and C. Leoni, "Effect of storage conditions on lycopene content in tomato

purees obtained with different processing techniques," *Industria Conserve*, vol. 74, no. 4, pp. 341–357, 1999.

[25] D. Anton, I. Bender, T. Kaart et al., "Changes in Polyphenols Contents and Antioxidant Capacities of Organically and Conventionally Cultivated Tomato (*Solanum lycopersicum* L.) Fruits during Ripening," *International Journal of Analytical Chemistry*, vol. 2017, pp. 1–10, 2017.

Hindawi
International Journal of Analytical Chemistry
Volume 2017, Article ID 6254793, 11 pages
https://doi.org/10.1155/2017/6254793

Research Article

Infrared Drying as a Quick Preparation Method for Dried Tangerine Peel

Mingyue Xu,[1] Guifang Tian,[1] Chengying Zhao,[1] Aftab Ahmad,[2] Huijuan Zhang,[1] Jinfeng Bi,[1] Hang Xiao,[3,4] and Jinkai Zheng[1]

[1]*Institute of Food Science and Technology, Chinese Academy of Agricultural Sciences, Beijing 100193, China*
[2]*State Key Laboratory of Chemical Resource Engineering, Beijing University of Chemical Technology, Beijing 100029, China*
[3]*Department of Food Science, University of Massachusetts, Amherst, MA 01003, USA*
[4]*College of Bioscience and Biotechnology, Hunan Agricultural University, Changsha, Hunan 410128, China*

Correspondence should be addressed to Jinfeng Bi; bijinfeng2010@163.com and Jinkai Zheng; zhengjinkai@caas.cn

Received 4 July 2017; Accepted 11 September 2017; Published 19 November 2017

Academic Editor: Changmou Xu

To establish the most convenient and effective method to dry tangerine peels, different methods (sun drying, hot-air drying, freeze drying, vacuum drying, and medium- and short-wave infrared drying) were exploited. Our results indicated that medium- and short-wave infrared drying was the best method to preserve nutraceutical components; for example, vitamin C was raised to 6.77 mg/g (D.W.) from 3.39 mg/g (sun drying). Moreover, the drying time can be shortened above 96% compared with sun drying. Importantly, the efficiency of DPPH radical scavenging was enhanced from 26.66% to 55.92%. These findings would provide a reliable and time-saving methodology to produce high-quality dried tangerine peels.

1. Introduction

Tangerine (mandarin) is the second most important citrus genera, whose specific species is *Citrus reticulata* [1]. The data from the Food and Agriculture Organization (FAO) of the United Nations showed that China is the largest producer of tangerines in the world that produced 15.17 million tons of tangerines in 2013. Tangerine is usually consumed as a fresh fruit in China because of its delicious taste and high nutritional components. In addition, tangerines were mostly processed to produce juice and canned tangerines [2]. Tangerine peels are usually treated as agroindustrial waste. However, they are rich in various nutraceutical components, including essential oils, flavonoids, pectin, and carotenes [2, 3]. Currently, the applications of these functional components are mainly focused on cosmetics, foods, dyes, and medicines [3–5].

It is also well known that tangerine peels are the main raw material to produce dried tangerine peel that can be used as an ingredient in traditional Chinese medicine as well as functional foods. Dried tangerine peel could be produced by drying fresh peels of *Citrus reticulata* Blanco or its cultivars collected between September and December in sun or at low temperatures [6]. It has been reported to alleviate indigestion, improve cardiac circulation, and suppress inflammatory syndromes of the respiratory tract such as bronchitis and asthma [7, 8]. Fresh tangerine peels were reported to have less biological functions than dried tangerine peels. The relatively lower biological importance of fresh tangerine peels is correlated to its high water content [9] and the low concentration of the function compounds, such as hesperidin. The Chinese pharmacopoeia explicitly stipulated that moisture content in Pericarpium Citri Reticulatae must be no more than 13% and that hesperidin content in Pericarpium Citri Reticulatae must be more than 3.5%. Hesperidin, an abundant and medicinally important bioflavonoid in tangerine peels, which determines the quality of dried tangerine peel, plays a vital role in preventing tumors, diminishing inflammation, performing bacteriostasis, and lowering cholesterol levels [10]. Literature survey indicates that phenolic compounds, especially flavonoids, are an important class of bioactive phytochemicals that provides many health benefits, such

as hypocholesterolemic, hypoglycaemic, antioxidant, anti-inflammatory, anticancer, and antiatherogenic activities [7]. Synephrine, another essentially functional component in dried tangerine peel, is used to dilate blood vessels, decrease blood pressure, and expand trachea and bronchus [5]. Similarly, vitamin C, a vital nutrient found in citrus, can promote body growth and enhance its resistance to disease. It also plays an important role in preventing and curing scurvy, especially in the early stages [11]. With all these beneficial bioactive compounds found in Pericarpium Citri Reticulatae, it is important to investigate the variation of these functional components during the drying of tangerine peels.

The main preparation method of dried tangerine peel, sun drying, has the advantages of low cost and simple operations. However, the quality of tangerine peels dried in the sun was inhomogeneous and unstable because it was very susceptible to weather and environments variations, such as natural disasters, insects, and dust [12]. Moreover, the sun drying method is very time-consuming to produce dried tangerine peel, making it vital to seek new drying methods for production. Nowadays, many drying methods had been used to dry fruits and vegetables, such as hot-air drying for grape leather, freezing drying for button mushroom, vacuum drying for carrot slices, and infrared drying for potato slices [13–15].

In spite of previous studies on drying processes of tangerine peels [12, 16, 17], there is no detailed report on the influence of different drying methods on the nutraceutical components in tangerine peels, which are important indexes for assessing the quality of dried tangerine peel. This study systematically investigated the influence of different drying methods (sun drying, hot-air drying, freeze drying, vacuum drying, and medium- and short-wave infrared drying) on the main compositions of tangerine peels (moisture, soluble solid, reducing sugars, total sugar, crude fiber, titratable acid, ash content, and minerals), major functional components (total phenolic compounds, total flavonoids, hesperidin, synephrine, and vitamin C), and the antioxidant activity of the dried tangerine peels.

2. Materials and Methods

2.1. Chemicals. Folin & Ciocalteu's phenol reagent, 1,1-diphenyl-2-picrylhydrazyl radical (DPPH), 2,4,6-tripyri-dyl-1,3,5-triazine (TPTZ), 2,2′-azinobis-(3-ethylbenzthiazoline-6-sulfonic acid) (ABTS), 6-hydroxy-2,5,7,8-tetramethylchroman-2-carboxylic acid (Trolox), gallic acid monohydrate, 2,6-dichloroindophenol, (+)-catechin hydrate, and vitamin C were purchased from Sigma-Aldrich (Shanghai, China). The hesperidin was purchased by Chengdu Institute of Biology, Chinese Academy of Sciences (Chengdu, China). The synephrine was purchased from National Institute for the Control of Pharmaceutical and Biological Products (NICPBP, Beijing, China). All other reagents of HPLC-grade and analytical grade were purchased from Sinopharm Chemical Reagent Co., Ltd. (Beijing, China).

2.2. Material Pretreatment. Fresh tangerines (*Citrus reticulata* v. tangerine) were grown in Jiangmen city (Guangdong Province, China) and purchased (November 2014) from a local market in Beijing. The ripe tangerines, with an average weight of 151.83 ± 4.65 g, were washed, dried, cut into eight pieces, and peeled carefully by hand without destroying their shape. The initial moisture content of tangerine peels was 2.50 ± 0.10 g water/g dry material and the thickness of tangerine peels was 2.68 ± 0.11 mm measured with Vernier caliper.

2.3. Drying Processes and Conditions. The tangerine peels were dried by 5 methods, which were sun drying (SD), freeze drying (FD), hot-air drying (HAD), vacuum drying (VD), and medium- and short-wave infrared drying (IRD). The weight loss was recorded by a CPA-125 digital electronic balance purchased from Sartorius Instrument System Co., Ltd. (Beijng, China), with the precision of 0.1 mg. Tangerine peels were dried until the moisture content was less than 0.05 g water/g dry material. Thirty grams of tangerine peels was placed in a sample steel tray ($30 \times 50\ cm^2$) with 60 holes whose diameter was 5 cm to form a layer of 0.5 cm before being dried. The process of each drying method was briefly described as follows.

(1) SD. The sample tray was exposed to sunlight from 9 am to 4 pm at the ambient temperature (15~20°C) with relative humidity within 30%–40%. The sample was taken out every 5 hours and weighed.

(2) FD. It was carried out in a freeze dryer (Alphal-4 Lplus, Marin Christ, Germany) at −30°C under 10^{-3} Mpa. The sample was taken out every 2 hours and weighed.

(3) HAD. HAD was performed in an oven (DHG-9070, Shanghai Yiheng Scientific Instruments Co., Ltd., China) at 60, 70, 80, and 90°C with a fixed air velocity of 2.1 m/s. Hot air was supplied in vertical model. The samples were taken out every 10 minutes and weighed.

(4) VD. The drying was carried out in vacuum dryer (D2F6090, Shanghai Jinghong Laboratory Instrument Co., Ltd., Shanghai, China) at 60, 70, 80, and 90°C with a fixed vacuum degree of 3×10^{-3} Mpa. The samples were taken out every 20 minutes and analyzed for weight loss.

(5) IRD. IR was conducted in a medium- and short-wave infrared radiation dryer (Senttech, Shengtaike Infrared Technology Instrument Co., Ltd., China). The drying was performed at different temperatures (60, 70, 80, and 90°C) with a power consumption of 1350 w and fixed air velocity of 2.1 m/s. The samples were taken out every 5 minutes and weighed.

2.4. Drying Kinetics. The drying kinetics of tangerine peels were based on weight loss, which was represented by drying curve and drying rate curve. Drying curve was presented as moisture ratio versus drying time and drying rate curve was presented as drying rate versus moisture content [17].

The initial water content is associated with a reduction in weight of tangerine peels before and after drying. The initial moisture content of tangerine peels was obtained by

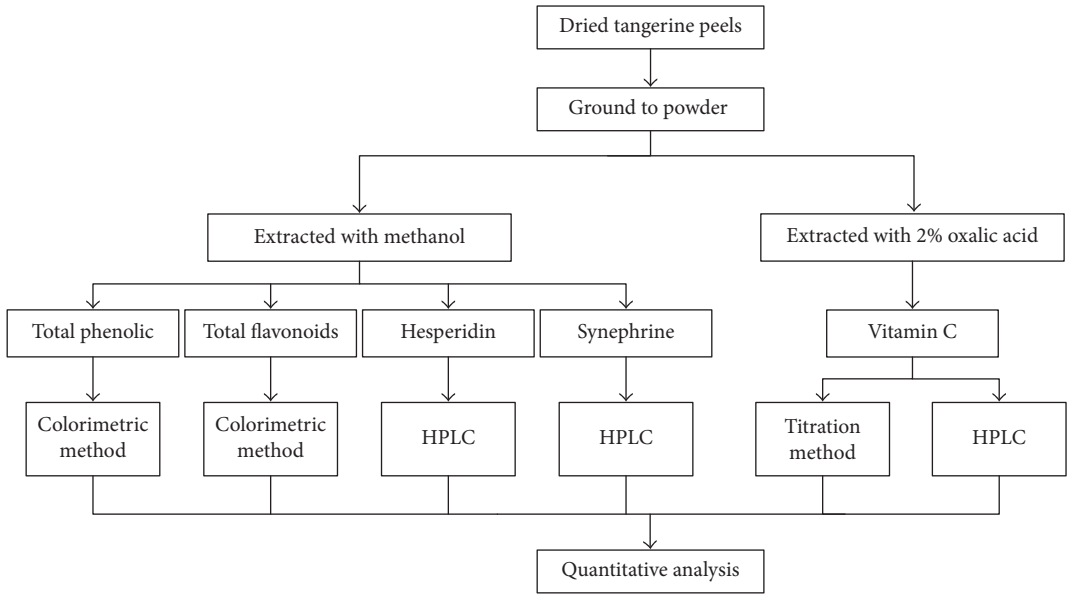

Figure 1: Flowchart of extracting of total phenolics, total flavonoids, hesperidin, synephrine, and vitamin C.

comparing the amount of evaporated water with drying samples at 105 ± 1°C until the weight was not changed. The moisture content at any time (X_t) was shown in the following [12]:

$$X_t = \frac{W_t - W_0}{W_0}, \quad (1)$$

where W_0 is the dry weight of sample and W_t is the weight at any time.

The moisture ration (MR) was obtained by the following [12]:

$$\mathrm{MR} = \frac{X_t - X_f}{X_0 - X_f}, \quad (2)$$

where X_0 is the initial moisture content, X_f is the final moisture content (0.05 g water/g dry weight), and X_t is the moisture content at any time.

The drying rate (R_i) was obtained by the following [17]:

$$R_i = \left(\frac{dX}{dt}\right)_i. \quad (3)$$

2.5. Main Components of Dried Tangerine Peels. The soluble solid was measured by using a digital-display refractometer (WZB 45, Shanghai Precision Scientific Instrument Co., Ltd., Shanghai, China) and the results were obtained by refractive index multiplied by the dilution ratio [18]. Total sugars, reducing sugars, crude fiber, ash content, and titratable acids were determined by the phenol-sulphuric acid method [19], DNS method [20], the gravimetric method using a fiber tester, the muffle furnace (Lindberg/Blue, Thermo Fisher, USA) at 550°C [17], and the potentiometric titration method [18], respectively.

2.6. Extraction. As shown in Figure 1, dried tangerine peels were grinded with a pestle in liquid nitrogen. One gram of sample was homogenized with 10 mL methanol for ultrasonic-assisted extraction for 1 h. Then, the mixture was centrifuged at 10,000 rpm for 10 min. The extraction procedure was repeated again. The supernatants were combined to detect total phenolic compounds, total flavonoids [21], hesperidin [22], and synephrine contents [5]. In order to analyze the vitamin C content, 1 g powder samples were extracted with 10 mL 2% oxalic acid and the mixture was centrifuged at 7600 rpm for 20 min to collect the supernatant [23]. Pure ethanol and 50% methanol were also used to optimize solvents for the extraction of hesperidin and synephrine.

2.7. Determination of Functional Components

2.7.1. Total Phenolics Content and Total Flavonoids Content. Folin-Ciocalteu method and colorimetric assay were used to determine the total phenolic content and total flavonoids content of tangerine peels with some modification, respectively [21]. When the total phenolic content was measured, the optical density was measured at 765 nm using a UV spectrophotometer (UV-1800, Shimadzu, China). Gallic acid was used as a reference standard. The value of total phenolic content was expressed as mg gallic acid equivalents (GAE) per g dried sample (mg GAE g^{-1} d.w.). While the total flavonoids content was measured, the absorbance was 510 nm. The detection of total flavonoids content was based on the standard curve of (+)-catechin hydrate, which was expressed as mg (+)-catechin hydrate equivalents (CHE) per g dried sample weight (mg GHE g^{-1} d.w.).

2.7.2. Hesperidin Content and Synephrine Content. HPLC was used to determine hesperidin and synephrine as previously designed methods with some modifications [5, 22]. The

absorbance was 278 nm, the injection volume was 10 μL and flow rate was maintained at 1 mL/min. The mobile phase system was comprised of methanol as mobile phase A and 0.1% (v/v) formic acid in deionized water as mobile phase B. The linear solvent gradient was composed of 30% A from the beginning to 5 min, 5% A at 15 min, 7% A at 20 min, and 30% A from 25 min to 30 min.

2.7.3. Vitamin C Content. The vitamin C content was determined by two methods, namely, 2,6-dichloroindophenol titration method [24] and HPLC method [23]. 10 mL diluted supernatant was titrated against 2,6-dichloroindophenol solution. The process of titration was terminated when a pink color appeared and lasted for at least 15 s (end point). The blank experiment was performed with 10 mL 2% oxalic acid solution. The HPLC method for vitamin C determination was performed as follows. The mobile phase was composed of methanol as mobile phase A and phosphate buffer with 2% methanol as mobile phase B. The injection volume was 10 μL, the flow rate was maintained at 1 mL/min, and absorbance was set up at 245 nm. The linear solvent gradient was composed of 100% B at the beginning, 20% B at 9 min, 20% B at 9.1 min, and 100% B from 14.1 min to 20 min.

2.8. Antioxidant Capacity Assays. One gram of dried tangerine peels was mixed with 20 mL MeOH and sonicated for 2 h. After being centrifuged for 10 min at 10000 r/min, the supernatant was obtained. This process is repeated and the supernatant was combined and stored in 4°C. Before determination, the supernatant was diluted 40 times with MeOH. Antioxidant capacity was evaluated by three assays: free radical scavenging activity by DPPH method, total antioxidant capacity by ABTS method, and ferric reducing ability by FRAP method [25]. The detection wavelengths were 517, 734, and 593 nm for DPPH, ABTS, and FRAP assays, respectively. Trolox was used as a standard. The results were expressed as the percentage of DPPH radical scavenged, the percentage of $ABTS^{\bullet+}$ radical scavenged, and μmol Trolox equivalent antioxidant capacity per 100 mg dried sample weight (μmol TE/100 mg dw) for DPPH, ABTS, and FRAP assays, respectively.

2.9. Statistical Analysis. All measurements were performed in triplicate. The experimental data were analyzed by the SPSS 19.0. Differences between quality indexes affected by different treatments were determined by ANOVA procedure ($P < 0.05$) and least significant difference (LSD) method. The figures were plotted by the origin 8.0.

3. Results and Discussion

It is generally known that the dried tangerine peels have more potential for storage and application than the fresh ones. Moisture content was one of the major differences between the dehydrated and the fresh tangerine peels. But the drying process not only reduced the moisture content but also had great effect on the nutraceutical components, including main compositions and functional components of tangerine peels.

3.1. Effect of Drying Conditions on Drying Kinetics of Tangerine Peels. The tangerine peels were dried by sun drying (SD), hot-air drying (HAD), freeze drying (FD), vacuum drying (VD), and infrared drying (IRD), respectively. The drying time with respect to moisture ratio and moisture content with respect to drying rate were investigated to evaluate the effect of different drying methods, respectively.

The results of FD and SD were not shown in Figure 2 because samples dried by freeze drying and sunlight needed about 1320 min and 3000 min to reach the final moisture content, respectively. Figures 2(a), 2(b), and 2(c) showed that the drying times of tangerine peels at 60, 70, 80, and 90°C in HAD, VD, and IRD ranged from 150 to 200 min, 280 to 400 min, and 75 to 110 min, respectively. The drying time decreased with the increase of temperature. Among the tested drying methods, the SD was the most time-consuming method followed by FD, VD, and HAD. IRD was the fastest method to dry tangerine peels among all the methods. The longer drying time during the SD method may be related to a low and unstable temperature and the sample susceptibility to air humidity [26, 27]. Because the processes of freezing and sublimation are also time-consuming, FD takes longer time to dry a sample. The heat of HAD could be delivered by thermal convection in vertical supply model from outside into the tangerine peels. However, the radiant heat of the IRD might be directly generated deep inside the samples, which led to an efficient inside-out heat transfer. The moisture in VD remained for a longer time than HAD, so the drying time of VD was longer. In a vacuum oven, the moisture on the surface of samples evaporates quickly but the inside moisture cannot migrate to the surface in time; hence, a film is formed on the surface of samples, which impeded the inside moisture migration and prolonged drying time [14].

Figures 2(d), 2(e), and 2(f) illustrated that the falling-rate of drying period was the main drying process of tangerine peels, which was similar to the drying processes of sweet potato [28]. These results suggested that the drying rate was increased with the increase of temperatures. For example, when the moisture ratio of samples in hot-air dryer was decreased from 1 to 0.2, the drying times at 60, 70, 80, and 90°C were about 80, 70, 55, and 40 min, respectively. The phenomena were the same as VD and IRD. The decrease in drying time at elevated temperatures and low moisture content may be attributed to the increase in the temperature difference between the drying air and the product, which accelerated the speed of water diffusion [29].

3.2. Effect of Different Drying Methods on Main Compositions of Tangerine Peels. Table 1 showed the main components of tangerine peels dried at different methods, including soluble solid, reducing sugar, total sugar, crude fiber, titratable acid, ash content, and mineral content (Na, Mg, K, Ca, Fe, Mn, Cu, Zn, and Se). The contents of these components have a close relationship with the functions of dried tangerine peels. 80°C was set as the dried temperature of HAD, IRD, and VD because the main components of tangerine peels were high at 80°C of different drying methods and the dried time was long at low temperature.

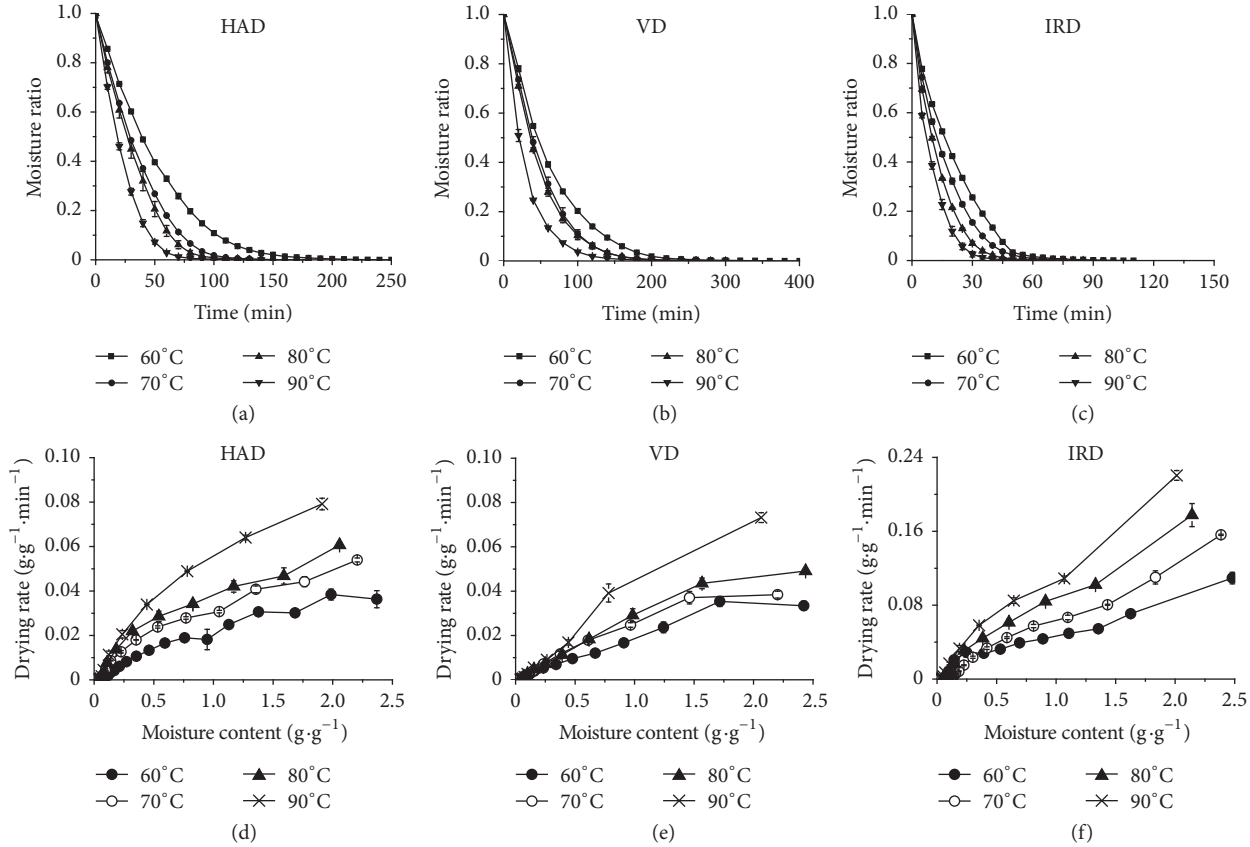

Figure 2: Drying curves and drying rate curves of tangerine peels dried by hot-air drying (a, d), vacuum drying (b, e), and medium- and short-wave infrared radiation drying (c, f).

Soluble solids in different dried tangerine peels were in the range of 41%~54%, while those in fresh tangerine peels were 14%. It is known that dried samples had higher soluble solids than the fresh ones. The tangerine peels had the most soluble solids after IRD and FD treatment, while the peels had the least soluble solids after SD treatment. The soluble solids are a relatively important index because dried peels were always soaked in water to drink. So IRD and FD were suitable ways to store soluble solids.

The sugar in tangerine peels might be the substrate of other compounds, such as vitamin C and glycoside. The investigation of sugar content is beneficial in providing the change mechanism of the other compounds. The reducing sugar content of tangerine peels after different drying processes was in the range of 489.43~545.59 mg/g dw, and the total sugar content of tangerine peels after different drying processes was in the range of 325.86~553.45 mg/g dw. The reducing sugar and total sugar content of the dried peels were both lower than those of fresh ones (725.41 mg/g dw, 753.50 mg/g dw). The sugars might be degraded while heating the samples for a long time during SD treatment. The samples dried by SD had the lowest total sugar content, while samples after FD had the highest one (553.45 mg/g dw).

The crude fiber was the major ingredient of cell walls. The change of its content could reflect the cell's membrane damage degree. The crude fiber content in fresh samples was 12.8%, while that in dried samples was lower in the range of 10.5%~11.1%, in line with previous report [21]. The results showed that the drying process had a slight effect on the cell wall damage.

The titratable acid content had a great effect on the flavor quality of dried tangerine peels. Compared with 0.875% in fresh peels, the titratable acid content in dried samples was in the range of 0.355%~0.835%. Of all drying methods, the titratable acid content was the highest after IRD and HAD treatment and was the lowest after SD treatment. The organic acids degrade much more rapidly during sun drying.

The storage and flavor quality of tangerine peels was also affected by the mineral content. When 80°C was set as the dried temperature of HAD, IRD and VD, the amounts of Na, Mg, Ca, Mn and Zn in fresh samples were higher than those in dried samples. Moreover, the amounts of Fe and Se in fresh ones were higher than those in dried samples except ones dried by SD while the amounts of K and Cu in fresh samples were lower than those in dried samples. The contents of Na and Cu were the highest in dried samples after IRD. The contents of Mg, Ca, Fe and Se were the highest after SD treatment. The contents of K and Zn were the highest after FD, while the level of Mn was higher in samples dried by VD treatment than others. So it can be seen that the mineral contents were influenced by the treatments.

Table 1: Effect of different drying methods on main compositions of tangerine peels.

Drying conditions	Soluble solid (%)	Reducing sugar (mg/g dw)	Total sugar (mg/g dw)	Crude fiber (%)	Titratable acid (%)	Ash content (%)	Minerals (ppm)								
							Na	Mg	K	Ca	Fe	Mn	Cu	Zn	Se
F	14.0 ± 0.28^{d}	725 ± 4.10^{a}	753 ± 41.04^{a}	12.8 ± 0.6^{a}	0.875 ± 0.064^{a}	2.88 ± 0.016^{a}	250	1904	6713	11016	22.8	20.2	1.23	14.3	0.014
SD	41.1 ± 1.41^{c}	489 ± 8.96^{b}	325 ± 26.01^{d}	10.8 ± 0.1^{b}	0.355 ± 0.049^{c}	2.74 ± 0.000^{c}	59.3	996	7204	5418	30.2	15.9	1.81	6.10	0.016
FD	51.1 ± 1.41^{a}	542 ± 47.84^{b}	553 ± 9.92^{b}	11.1 ± 0.1^{b}	0.670 ± 0.028^{b}	2.79 ± 0.001^{b}	58.4	805	9605	3934	14.1	6.09	2.07	8.77	0.009
HAD, 80°C	45.3 ± 0.94^{bc}	489 ± 94.63^{b}	474 ± 4.87^{c}	11.0 ± 0.0^{b}	0.820 ± 0.028^{a}	2.57 ± 0.012^{d}	53.4	908	8325	3602	15.3	7.11	1.95	7.32	0.000
VD, 80°C	45.9 ± 2.83^{b}	497 ± 85.36^{b}	454 ± 8.60^{c}	10.5 ± 0.0^{b}	0.695 ± 0.049^{b}	2.87 ± 0.017^{a}	73.2	973	8076	4913	15.5	16.7	1.82	6.55	0.010
IRD, 80°C	54.2 ± 2.83^{a}	545 ± 51.44^{b}	496 ± 14.26^{c}	11.1 ± 0.5^{b}	0.835 ± 0.021^{a}	2.82 ± 0.033^{b}	91.6	795	9452	3936	15.9	13.5	2.09	6.57	0.000

Results are mean ± SD. Different letters in the same column indicate that values are significantly different ($P < 0.05$).

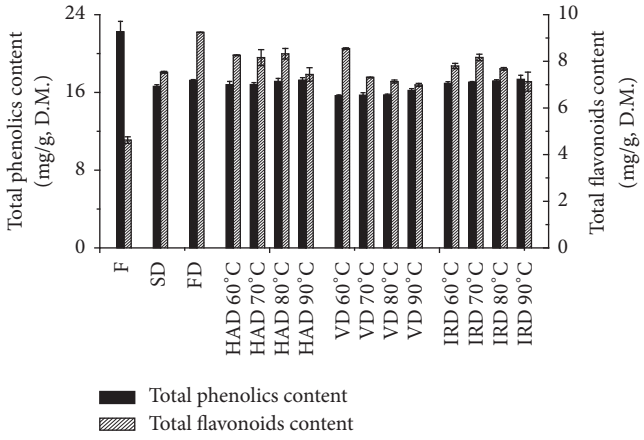

Figure 3: The content variation of total flavonoids content and total phenolics content in tangerine peels dried by different drying methods.

The ash content is an important index of inorganic substances in food. The ash contents in dried samples were in the range of 2.574%~2.874% in comparison with 2.881% in fresh ones. The tangerine peel had high ash content after VD, whereas it had low ash content after HAD. The ash content consistently decreased after drying. Ash content represents the total content of minerals [30]. Similar results were obtained in mineral determination.

Overall all, FD and IRD were the best to preserve soluble solid, reducing sugar, total sugar, crude fiber, and titratable acid for tangerine peels, while SD is better at preserving the minerals in tangerine peel, which is in agreement with previous report on strawberry [31]. However, FD is the most expensive process. The above research findings of this study could provide an empirical proof for quality evaluation and industrialization.

3.3. Effect of Different Drying Methods on Total Phenolics Content and Total Flavonoids Content of Tangerine Peels. Among the natural functional components, phenolic compounds have attracted wide attention for their promising antioxidant activity and potential roles in the treatment of chronic and degenerative diseases. It was revealed that tangerine peels after drying with different methods presented variable total phenolic contents ranging within 15.66~17.24 mg GAE/g dw (Figure 3), which is lower than the fresh ones (22.24 mg GAE/g dw) ($P < 0.01$). The contents of total phenolic compounds after drying ranked from most to least are IRD/FD/HAD > SD > VD ($P < 0.05$), respectively. With the increase in drying temperatures, a slightly increase in the total phenolics content of tangerine peels was observed in IRD, HAD, and VD. When the plants were dried, the phenolic compounds stored in the plant vacuole are more freely released [32]. IRD could break down the covalent bond of phenolic compounds and liberate low-molecular-weight antioxidants, such as flavonoids and polyphenols. Other heat treatments might destroy the other type of bonds and increased the phenolic content [33, 34].

Flavonoids in tangerine peels (such as hesperidin, naringin, and neohesperidin) are used to treat various physical symptoms such as high cholesterol level, cardiovascular disease, and gastrointestinal function. The total flavonoids contents of tangerine peels dried by 5 drying methods were shown in Figure 3. The total flavonoids content of tangerine peels dried by FD and IRD at 70°C, which was twice of fresh ones, was higher than those dried by the other methods ($P < 0.05$), whereas the lowest content was achieved in tangerine peels after VD at 90°C (6.99 mg GHE/g dw). A considerable amount of total flavonoids contents was also achieved by HAD but was lower than those of FD and IRD at 70°C ($P < 0.05$). Compared with those of fresh ones, the total flavonoids contents of tangerine peels were increased after drying at different temperatures. It was reported that heating and radiation could break down certain types of bonds and release antioxidants such as flavonoids and polyphenols from polymers [33]. Figure 3 also declared that the total flavonoids contents of samples in HAD and IRD were almost not affected by temperature (≤80°C) but were decreased with further raising temperatures (>80°C). Too high temperature was confirmed to be harmful to preserve flavanone glycosides [35, 36]. It might be related to the fact that naturally occurring antioxidants such as flavonoids might be destroyed by the too high temperature. Therefore, the FD, HAD, and IRD were beneficial in preserving the total flavonoids at low temperatures (<80°C). However, less total flavonoids was liberated with IRD since the drying time was shorter than FD and HAD. In conclusion, the effect of IRD was relatively much better than the other methods used.

3.4. Effect of Different Drying Methods on Hesperidin, Synephrine, and Vitamin C Contents of Tangerine Peels. Hesperidin was the main flavonoid while synephrine was the most important alkaloid in citrus. So the effect of different drying methods was studied on hesperidin and synephrine. As shown in Figure 4(a), the hesperidin content of tangerine peels obtained by FD method was 1.77 times higher than that of fresh ones. In addition, the hesperidin content achieved by this method was also higher than other drying methods. Of all the drying methods, the lowest hesperidin content of samples was obtained by SD. Food processing helps destroy the cell wall and allows phenolic compounds to be released from the insoluble portion of the tangerine peel, which can lead to increased levels of hesperidin content [36]. The HAD was a better drying method to preserve hesperidin than VD and IRD after statistical analysis ($P < 0.05$). FD, HAD, and IRD were all beneficial in preserving hesperidin.

Like hesperidin, the synephrine content in tangerine peels after drying was significantly higher than that in fresh ones ($P < 0.05$) as shown in Figure 4(b). Similarly, it was largely related to the content of essential oils. In fresh peels, the contents of essential oils were high, so the synephrine content was relatively low. After being dried, essential oils in the samples were significantly reduced, and, hence, the proportion of synephrine increased. At high temperatures for VD, the film formed on the surface, which hindered the essential oils' volatilization. In summary, FD, HAD, and IRD were the most suitable to retain synephrine at high

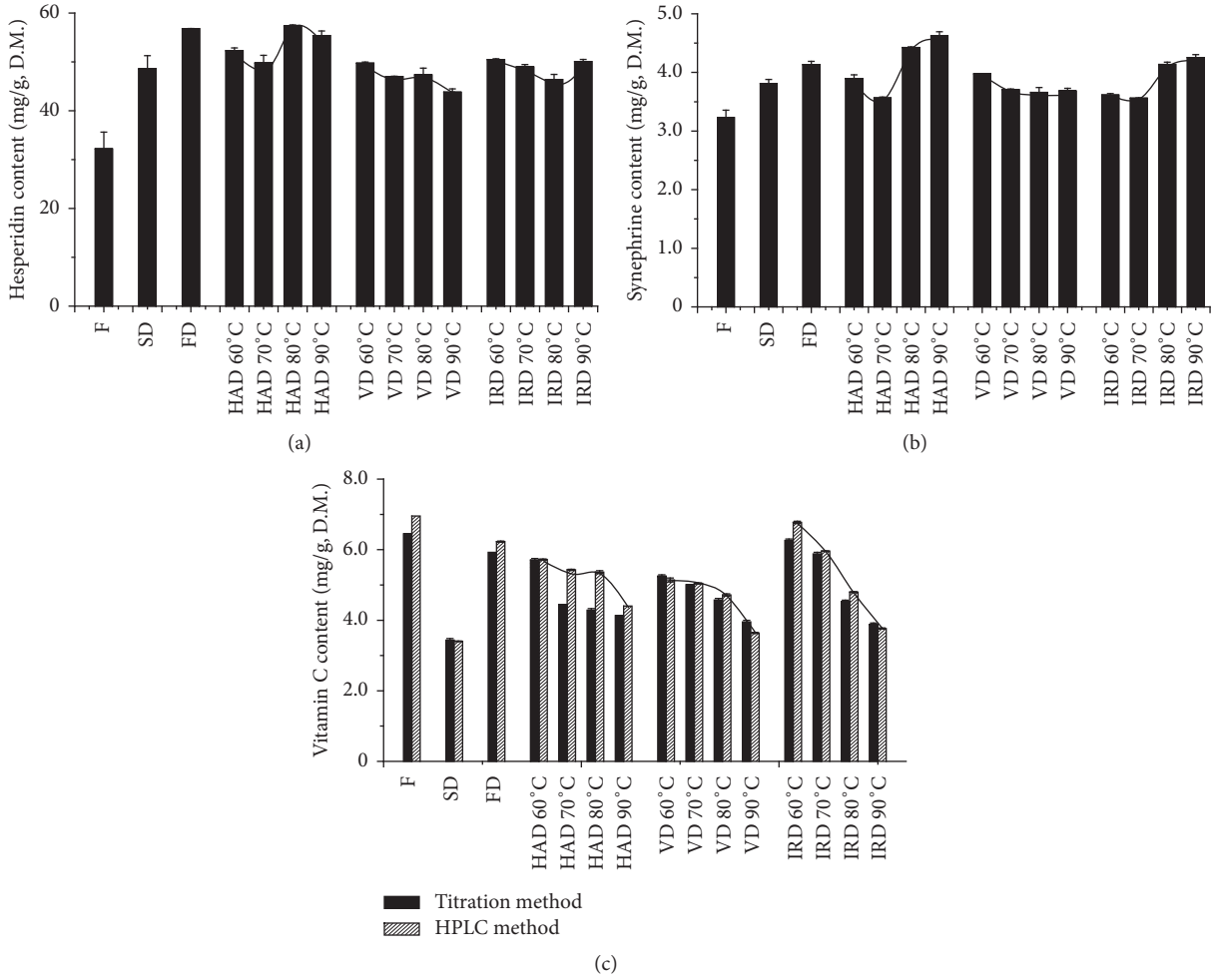

Figure 4: The content variation of hesperidin (a), synephrine (b), and vitamin C (c) in tangerine peels dried by different drying methods.

temperatures (80°C and 90°C) and dried tangerine peels had much more functions than fresh peels.

The vitamin C content of peels was determined by 2,6-dichloroindophenol titration and HPLC methods (Figure 4(c)). The trends in the results tested by two methods were similar. However, the data obtained by HPLC method was higher than that obtained by titration method. It may be because that 2,6-dichloroindophenol titration method was easily affected by the environment, artificial operation, and the identification of the final point of titration. HPLC method was chosen because of its high accuracy and sensitivity. The vitamin C content of fresh tangerine peels was significantly higher than those of the dried ones ($P < 0.05$). As it is generally known that vitamin C is susceptible to heat and oxygen. Heating and oxidation might accelerate the degradation of vitamin C during the drying process. Therefore, the content of vitamin C decreased gradually along with the increase of temperature [21, 37]. The reason for the low vitamin C content obtained by SD may be the result of samples exposure to air at inconsistent temperatures for a long period. On the other hand, drying at relatively lower temperature and oxygen tension had less effect on the vitamin C content as obtained by FD method compared to other tested methods. Because the samples were dried under short time at low temperature, the peels dried by IRD had significantly higher vitamin C content than those dried by HAD, VD, and SD ($P < 0.05$). Among the drying methods, the IRD was an economical and effective way to preserve vitamin C.

3.5. Effect of Different Drying Methods on Antioxidant Activity of Tangerine Peels. The antioxidant activities of fresh and dried tangerine peels were evaluated by ABTS, DPPH and FRAP assays (Figure 5). The antioxidant activities of the peels after SD were the lowest of the dried peels, which were also lower than the fresh ones ($P < 0.001$). This result was inconsistent with the low contents of vitamin C and phenolic compounds in the peels dried by sunlight. It means the antioxidant activities of dried tangerine peels obtained by traditional methods (SD) had been greatly reduced. The total antioxidant capacity evaluated by ABTS of the peels after VD at 90°C was stronger than others ($P < 0.05$). The peels after IRD had stronger total antioxidant capacity than FD ($P < 0.05$). Similarly, the peels dried by SD and FD had

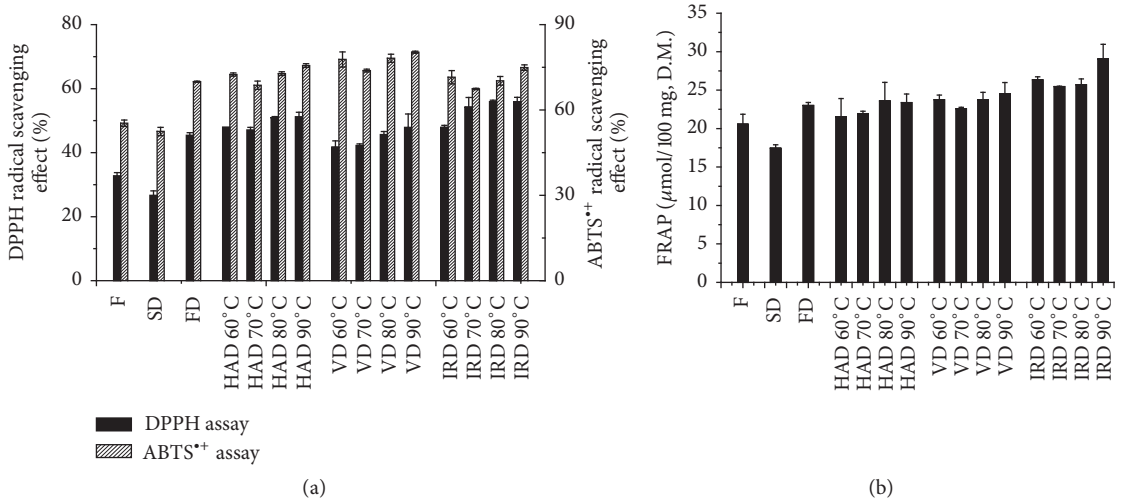

Figure 5: Effect of different methods on the antioxidant activity of tangerine peels: ABTS, DPPH (a), and FRAP (b).

the lowest ability on free radical scavenging ($P < 0.001$) evaluated by DPPH. The ability on free radical scavenging of peels after IRD was stronger than HAD and VD ($P < 0.05$). On reducing ferric, the peels after SD were markedly inferior to other drying methods ($P < 0.001$). Hence, our findings suggested that IRD was a suitable drying method to obtain the high antioxidant activities due to the lower temperatures and shorter drying time necessary for the desired moisture content compared to the other drying methods.

4. Conclusions

The impact of the 5 drying methods on nutraceutical components and antioxidant activity of tangerine peels were studied. In general, IRD was an appropriate choice for drying tangerine peels. Compared with the traditional drying method (SD), IRD not only was beneficial in preserving the nutraceutical components of tangerine peels but also shortened the drying time to a greater extent. Altogether, different drying methods may have different advantages to maintain optimal concentrations of the desired components in the dried peels, but the IRD method was found as the most efficient and convenient drying method in preserving main compositions, nutraceutical compositions, and antioxidant activity for tangerine peels. Overall, this study would provide useful information for the preparation method of dried tangerine peel and its industrial applications.

Conflicts of Interest

The authors declare that they have no conflicts of interest.

Authors' Contributions

Mingyue Xu and Guifang Tian have contributed equally to this work.

Acknowledgments

The authors would like to acknowledge the financial support of the National Natural Science Foundation of China (nos. 31401581 and 31428017). This work was also supported by the Program of Introducing International Advanced Agricultural Science and Technology of the Ministry of Agriculture of China (948 Program, no. 2016-X31).

References

[1] P. García-Salas, A. M. Gómez-Caravaca, D. Arráez-Román et al., "Influence of technological processes on phenolic compounds, organic acids, furanic derivatives, and antioxidant activity of whole-lemon powder," *Food Chemistry*, vol. 141, no. 2, pp. 869–878, 2013.

[2] M.-L. Chen, D.-J. Yang, and S.-C. Liu, "Effects of drying temperature on the flavonoid, phenolic acid and antioxidative capacities of the methanol extract of citrus fruit (*Citrus sinensis* (L.) Osbeck) peels," *International Journal of Food Science & Technology*, vol. 46, no. 6, pp. 1179–1185, 2011.

[3] G. M. Kamal, F. Anwar, A. I. Hussain, N. Sarri, and M. Y. Ashraf, "Yield and chemical composition of *Citrus* essential oils as affected by drying pretreatment of peels," *International Food Research Journal*, vol. 18, no. 4, pp. 1275–1282, 2011.

[4] M. Kratchanova, E. Pavlova, and I. Panchev, "The effect of microwave heating of fresh orange peels on the fruit tissue and quality of extracted pectin," *Carbohydrate Polymers*, vol. 56, no. 2, pp. 181–185, 2004.

[5] S. Inafuku-Teramoto, R. Suwa, Y. Fukuzawa, and Y. Kawamitsu, "Polymethoxyflavones, synephrine and volatile constitution of peels of citrus fruit grown in Okinawa," *Journal of the Japanese Society for Horticultural Science*, vol. 80, no. 2, pp. 214–224, 2011.

[6] L. Yi, N. Dong, S. Liu, Z. Yi, and Y. Zhang, "Chemical features of Pericarpium Citri Reticulatae and Pericarpium Citri Reticulatae Viride revealed by GC-MS metabolomics analysis," *Food Chemistry*, vol. 186, pp. 192–199, 2015.

[7] M.-Y. Choi, C. Chai, J. H. Park, J. Lim, J. Lee, and S. W. Kwon, "Effects of storage period and heat treatment on phenolic compound composition in dried Citrus peels (Chenpi) and discrimination of Chenpi with different storage periods through targeted metabolomic study using HPLC-DAD analysis," *Journal of Pharmaceutical and Biomedical Analysis*, vol. 54, no. 4, pp. 638–645, 2011.

[8] S.-C. Ho and C.-T. Kuo, "Hesperidin, nobiletin, and tangeretin are collectively responsible for the anti-neuroinflammatory capacity of tangerine peel (*Citri reticulatae* pericarpium)," *Food and Chemical Toxicology*, vol. 71, pp. 176–182, 2014.

[9] A. Kammoun Bejar, N. Boudhrioua Mihoubi, and N. Kechaou, "Moisture sorption isotherms - Experimental and mathematical investigations of orange (Citrus sinensis) peel and leaves," *Food Chemistry*, vol. 132, no. 4, pp. 1728–1735, 2012.

[10] T. Inoue, S. Tsubaki, K. Ogawa, K. Onishi, and J.-I. Azuma, "Isolation of hesperidin from peels of thinned *Citrus unshiu* fruits by microwave-assisted extraction," *Food Chemistry*, vol. 123, no. 2, pp. 542–547, 2010.

[11] M. A. Esteban, T. Wang, B. Qin et al., "Vitamin C enhances the generation of mouse and human induced pluripotent stem cells," *Cell Stem Cell*, vol. 6, no. 1, pp. 71–79, 2010.

[12] S. M. Tasirin, I. Puspasari, A. Z. Sahalan, M. Mokhtar, M. K. A. Ghani, and Z. Yaakob, "Drying of Citrus sinensis Peels in an Inert Fluidized Bed: Kinetics, Microbiological Activity, Vitamin C, and Limonene Determination," *Drying Technology*, vol. 32, no. 5, pp. 497–508, 2014.

[13] A. Maskan, S. Kaya, and M. Maskan, "Hot air and sun drying of grape leather (pestil)," *Journal of Food Engineering*, vol. 54, no. 1, pp. 81–88, 2002.

[14] F. Pei, W.-J. Yang, Y. Shi et al., "Comparison of Freeze-Drying with Three Different Combinations of Drying Methods and Their Influence on Colour, Texture, Microstructure and Nutrient Retention of Button Mushroom (Agaricus bisporus) Slices," *Food and Bioprocess Technology*, vol. 7, no. 3, pp. 702–710, 2014.

[15] G. Musielak and A. Kieca, "Influence of Varying Microwave Power during Microwave-Vacuum Drying on the Drying Time and Quality of Beetroot and Carrot Slices," *Drying Technology*, vol. 32, no. 11, pp. 1326–1333, 2014.

[16] A. K. Bejar, "Effect of microwave treatment on physical and functional properties of orange (Citrus sinensis) peel and leaves," *Food Processing & Technology*, vol. 2, no. 2, pp. 109–128, 2011.

[17] N. Ghanem, D. Mihoubi, N. Kechaou, and N. B. Mihoubi, "Microwave dehydration of three citrus peel cultivars: Effect on water and oil retention capacities, color, shrinkage and total phenols content," *Industrial Crops and Products*, vol. 40, no. 1, pp. 167–177, 2012.

[18] C.-W. Lee, H.-J. Oh, S.-H. Han, and S.-B. Lim, "Effects of hot air and freeze drying methods on physicochemical properties of citrus 'hallabong' powders," *Food Science and Biotechnology*, vol. 21, no. 6, pp. 1633–1639, 2012.

[19] F. Hajji, B. Kunz, and J. Weissbrodt, "Polymer incompatibility as a potential tool for polyphenol recovery from olive mill wastewater," *Food Chemistry*, vol. 156, pp. 23–28, 2014.

[20] R. Hu, L. Lin, T. Liu, P. Ouyang, B. He, and S. Liu, "Reducing sugar content in hemicellulose hydrolysate by DNS method: A revisit," *Journal of Biobased Materials and Bioenergy*, vol. 2, no. 2, pp. 156–161, 2008.

[21] R. Lemus-Mondaca, K. Ah-Hen, A. Vega-Gálvez, C. Honores, and N. O. Moraga, " Stevia rebaudiana Leaves: Effect of Drying Process Temperature on Bioactive Components, Antioxidant Capacity and Natural Sweeteners," *Plant Foods for Human Nutrition*, vol. 71, no. 1, pp. 49–56, 2016.

[22] J.-T. Lin, S.-C. Liu, G. J. Tsay, and D.-J. Yang, "Composition of flavonoids and phenolic acids in Glycin tomentella Hayata cultivated in various soils," *Food Chemistry*, vol. 121, no. 3, pp. 659–665, 2010.

[23] J. Vanamala, G. Cobb, N. D. Turner et al., "Bioactive compounds of grapefruit (*Citrus paradisi* cv. rio red) respond differently to postharvest irradiation, storage, and freeze drying," *Journal of Agricultural and Food Chemistry*, vol. 53, no. 10, pp. 3980–3985, 2005.

[24] J. Z. Hua, X. X. Liu, W. Wu, and C. Y. Wei, "Determination of vitamin C and its content changes in clover," *Food Research and Development*, vol. 37, no. 1, pp. 45–47, 2016.

[25] J. C. Danilewicz, "Folin-Ciocalteu, FRAP, and DPPH assays for measuring polyphenol concentration in white wine," *American Journal of Enology and Viticulture*, vol. 66, no. 4, pp. 463–471, 2015.

[26] M. Chaijan, W. Panpipat, and M. Nisoa, "Chemical deterioration and discoloration of semi-dried tilapia processed by sun drying and microwave drying," *Drying Technology*, vol. 35, no. 5, pp. 642–649, 2017.

[27] M. C. Villalobos, M. J. Serradilla, A. Martín, C. Pereira, M. López-Corrales, and M. G. Córdoba, "Evaluation of different drying systems as an alternative to sun drying for figs (Ficus carica L)," *Innovative Food Science and Emerging Technologies*, vol. 36, pp. 156–165, 2016.

[28] I. Doymaz, "Infrared drying of sweet potato (Ipomoea batatas L.) slices," *Journal of Food Science and Technology*, vol. 49, no. 6, pp. 760–766, 2012.

[29] P. K. Wankhade, R. S. Sapkal, and V. S. Sapkal, "Drying characteristics of okra slices on drying in hot air dryer," in *Proceedings of the 3rd Nirma University International Conference on Engineering, NUiCONE 2012*, pp. 371–374, ind, December 2012.

[30] N. F. A. Rahman, R. Shamsudin, A. Ismail, and N. N. A. Karim Shah, "Effects of post-drying methods on pomelo fruit peels," *Food Science and Biotechnology*, vol. 25, pp. 85–90, 2016.

[31] N. Adak, N. Heybeli, and C. Ertekin, "Infrared drying of strawberry," *Food Chemistry*, vol. 219, pp. 109–116, 2017.

[32] P. Raksakantong, S. Siriamornpun, and N. Meeso, "Effect of drying methods on volatile compounds, fatty acids and antioxidant property of Thai kaffir lime (Citrus hystrix D.C.)," *International Journal of Food Science & Technology*, vol. 47, no. 3, pp. 603–612, 2012.

[33] S. Jeong, S. Kim, D. Kim et al., "Effect of heat treatment on the antioxidant activity of extracts from citrus peels," *Journal of Agricultural and Food Chemistry*, vol. 52, no. 11, pp. 3389–3393, 2004.

[34] I. Hamrouni-Sellami, F. Z. Rahali, I. B. Rebey, S. Bourgou, F. Limam, and B. Marzouk, "Total Phenolics, Flavonoids, and Antioxidant Activity of Sage (Salvia officinalis L.) Plants as Affected by Different Drying Methods," *Food and Bioprocess Technology*, vol. 6, no. 3, pp. 806–817, 2013.

[35] S.-C. Ho and C.-C. Lin, "Investigation of heat treating conditions for enhancing the anti-inflammatory activity of citrus fruit (*Citrus reticulata*) peels," *Journal of Agricultural and Food Chemistry*, vol. 56, no. 17, pp. 7976–7982, 2008.

[36] G. Xu, X. Ye, J. Chen, and D. Liu, "Effect of heat treatment on the phenolic compounds and antioxidant capacity of citrus peel extract," *Journal of Agricultural and Food Chemistry*, vol. 55, no. 2, pp. 330–335, 2007.

[37] S. M. Oliveira, T. R. S. Brandão, and C. L. M. Silva, "Influence of Drying Processes and Pretreatments on Nutritional and Bioactive Characteristics of Dried Vegetables: A Review," *Food Engineering Reviews*, vol. 8, no. 2, pp. 134–163, 2016.